Republic of Iraq
Ministry of Higher Education
and Scientific Research
University of Kerbala
College of Science

Biosynthesis, Characterization, Antioxidant Activity, and Clinical Application of Silver Nanoparticles Synthesized from *Dodonaea viscosa* Leaves Extract

A Thesis

Submitted to the council of the College of Science-University of Kerbala as a Partial Fulfillment of the Requirement for the Degree of Master in Chemistry Science/ Biochemistry.

By

Zainab Faisal Habeeb
B.Sc. Chemistry/College of Science /University of Kerbala (2017)

Supervised by
Prof. Dr. Narjis Hadi Al-Saadi
Ph. D. Biochemistry

2021A.D 1443 A.H

Certification of Supervisor

I certify that this thesis "**Biosynthesis, Characterization, Antioxidant Activity, and Clinical Application of Silver Nanoparticles Synthesized from *Dodonaea viscosa* Leaves Extract**" was prepared under my supervision at the Department of Chemistry, College of Science, University of Kerbela, as a partial fulfillment of the requirements for the degree of Master of Chemistry.

Signature:

Name: **Dr. Narjis Hadi Al-Saadi**

Title: **Professor**

Address: University of Kerbala /College of Science / Department of Chemistry

Date: / / 2021

Report of the Head of Chemistry Department

According to the recommendations presented by the Supervisor and the Postgraduate Studies Director, I forward this thesis "**Biosynthesis, Characterization, Antioxidant Activity, and Clinical Application of Silver Nanoparticles Synthesized from *Dodonaea viscosa* Leaves Extract**" for examination.

Signature:

Name**: Assist. Prof. Dr. Adnan Ibrahim Mohammed**

Head of Chemistry Department

Address: University of Kerbala /College of Science / Department of Chemistry.

Date: / /2021

Examination Committee Certification

We, the examining committee, certify that we have read this thesis and examined the student (**Zainab Faisal Habeeb**) in its contents and that in our opinion; it is adequate as a thesis for the degree of Master of Science in Chemistry.

Signature:
Name: **Dr. Mohammed Talat Abbas**
Title: Professor
Address: University of Kirkuk - College of Pharmacy.
Date: / / 2021
(Chairman)

Signature:
Name: **Dr. Amer Hasan Abdullah**
Title: Assistant Professor
Address: University of Mustansiriyah, College of Science, Department of Chemistry.
Date: / / 2021
(Member)

Signature:
Name: **Dr. Rehab jasim Mohammad**
Title: Assistant Professor
Address: University of Kerbala, College of Education for Pure Science, Department of Chemistry.
Date: / / 2021
(Member)

Signature:
Name: **Dr. Narjis Hadi Al-Saadi**
Title: Professor
Address: University of Kerbala, College of Science, Department of Chemistry.
Date: / /2021
(Member & Supervisor)

Approved by the council of the College of Science

Signature:
Name: **Dr. Jasem Hanoon Hashim Al-Awadi**
Title: Assistant Professor
Address: **Dean of College of Science, University of Kerbala.**
Date: / /2021

Dedication

To the source of my pride and strength, to the secret of my existence …. My dears parents May God grant me success to achieve their satisfaction. To the one who inhabits my heart and fills my life with knowledge and dedication. To one who supported me and stood by me and the secret of my success in every step and bearing the difficulties of my studies….. My dear husband. To the shining stars in the sky of our life …. My dears brothers and my beloved sister. To the pure and kind hearts and the innocent souls, and the winds of my life and my heart and happiness…. ….. My dear children. To all of you are dedicated my humble efforts.

Zainab Faisal

Acknowledgements

Praise be to Allah, the Lord of the worlds, and the prayer and peace upon the messenger, mercy to the worlds, our prophet Mohammad, and to his family of the good. At the beginning, I would like to thank the dean of the College of Science, University of Kerbala. Also, I want to thank to the head of department of Chemistry (Dr. Adnan Mohammed), and the staff in the Department of Chemistry for their help.

Words cannot express my sincere gratitude and appreciation to the supervisor Professor Dr. Narjis Hadi Al-Saadi for her assistance, great interest, kindness and supportive advice in this work. I am very grateful to her for her continuous encouragement and support during the completion of the work. Calling on God Almighty to give her a long health and wellness and more scientific prosperity.

My angel in life, to the meaning of love, compassion and dedication to the smile of life. To the secret of existence and to those whose pray were the secret of my success (My dear parents, my husband, and my children).

I would like to thank those who have a great credit in encouraging me and their presence acquired strength. My thanks go to all the professors and staff of the Department of Chemistry.

Grateful thanks to those who were fraternity and distinguished by loyalty. Also special thanks to Miss Hanin for her assistant in sample analysis by FT-IR.

Zainab Faisal

Summary

Biosynthesis of silver nanoparticles (AgNPs) from plant extracts is considered one of the green chemistry methods, as this method is characterized by ease, fast and low cost. Interestingly, AgNPs have an important role, especially in nano-medicine. In this study, silver nanoparticles were biosynthesized using *Dodonaea viscosa* leaves extract. The first evidence for the formation of these particles was proven through the color change.

Gas chromatography and mass spectroscopy analysis was used to indicate the constituents found in the aqueous leaves extract of *D. viscosa*, which involved the reduction of silver ion into silver nanoparticles. The biosynthesized AgNPs were characterized using different techniques. UV.-visible spectrophotometry that indicated the formation of AgNPs at the wavelength of 463 nm. and Fourier Transform Infra-Red (FT-IR) spectroscopy which revealed the effective functional groups that have ability to bio-reduction Ag^{+}. In addition, X-ray diffraction (XRD) determined the crystal structure of AgNPs, as shown by the peaks at 2θ values of 38.1874, 46.2491, 57.5409 and76. 8313^{o}.The atomic force microscopy (AFM) analysis showed the size and the surface properties of biosynthesized nanoparticles, and the silver nanoparticles had an average size of 60.22 nm. Finally, scanning electron microscopy (SEM) showed spherical shape of AgNPs and having different average diameter D1 (21.10), D2 (21.39) and D3 (11.86) nm.

In vitro study, the synthesized AgNPs exhibited potential anti-tumor activities against human lung cancer (A549) carcinoma cell line in a dose-dependent manner. The efficacy of AgNPs against bacteria and its potential as an antioxidant was tested. AgNPs inhibited some

bacterial growth and their biofilm such as, gram-positive bacteria (*Staphylococcus aureus* and *Streptococcus pneumonia.*) and gram-negative bacteria (*E. coli* and *Pseudomonas aeruginosa*). AgNPs showed antioxidant activity and can be used as a potential radical scavenger against damages produced by the free radicals.

The results of clinical applications showed that the synthesize AgNPs and the aqueous *D. viscosa* leaves extract prolonged the coagulation time by increasing prothrombin time and activated partial thromboplastin time as well as, AgNPs have a low effect on the human red blood cells hemolysis.

List of Content

List of Tables

List of Figures

List of Symbols and Abbreviations

A431	Epidermoid carcinoma
A549	Human Lung Carcinoma
ACT	Activated Clotting Time
AFM	Atomic Force Microscopy
$AgNO_3$	Silver Nitrate
AgNPs	Silver Nanoparticles
AGS	Human Gastric Carcinoma
APTT	Activated Partial Thromboplastin Time
ATP	Adenosine Triphosphate
CAT	Catalase
cm^{-1}	Wavenumber
COLO 205	Colon Carcinoma
CVD	Chemical Vapor Deposition
DPPH	1,1-diphenyl-2-picrylhydrazyl
FT-IR	Fourier- Transform Infrared
GC-mass	Gas Chromatography and Mass spectroscopy
GPx	Glutathione Peroxidase
GR	Glutathione Reductase
HEPG2	Human Liver Cancer
IC_{50}	Inhibitory Concentration that Kill 50% of the cell population
ISO	International Organization for Standardization
LSD	Least Significant Difference

MTT	(3-(4,5-Dimethyl-2-thia-zolyl)-2,5-diphenyl-2H-tetrazolium bromide
Nm	Nanometer
NPs	Nanoparticles
PT	Prothrombin Time
RNS	Reactive Nitrogen Species
ROS	Reactive Oxygen Species
RPMI	Roswell Park Memorial Institute – 1640 Medium
SEM	Scanning Electron Microscopy
SK-OV-3	Ovarian Cancer
SOD	Superoxide Dismutase
SPR	Surface Plasmon Resonance
WRL 68	Human Hepatic Normal Cell Line
XRD	X-Ray Diffraction

Chapter One
Introduction
and
Literature Review

1-1 Introduction

Nanotechnology is concerned with small structures or materials and can be described as the synthesis, characterization, exploration, and application of nanosized materials (1-100 nm). Nanoparticles have entirely different or improved properties as compared to larger particles in bulk materials. Furthermore, due to its cutting-edge nature and broad application spectrum in various branches of science such as chemistry, biology, physics, medicine, material science, and engineering, nanotechnology involving metal nanoparticles has gotten a lot of attention (1). The term "nano" comes from the Greek word "dwarf," and it refers to a reduction in size 10^{-9} time of, which is 1,000 times smaller than a micron (2). The biological activity of nanoparticles increased as the total surface area of the particles increased (3). Owing to their broad range of applications, interest in the synthesis of metallic nanoparticles has risen recently. Metallic nanoparticles are made from metal salts such as silver, lead, titanium, iron, platinum, gold, copper, etc. Silver nanoparticles (AgNPs) are the most widely used metal nanoparticles (MNPs) due to their high antibacterial activity, antioxidant properties, anti-tumor, anti-fungal, and anti-inflammatory properties, as well as a wide range of commercial and industrial applications, especially in the pharmaceutical industry due to the valuable potentials of nanoscale size (4). Nanoparticles are currently used in a variety of fields due to their unique properties. Metallic nanoparticles can be made in various ways, including physical, chemical, and biological methods. Chemical and physical approaches are commonly used to process dangerous toxic byproducts, and the routes are often very costly. There has been a quest for low-cost, healthy, and environmentally friendly, and "green" methods to synthesize stable metal nanoparticles with regulated size and shape (5). Biological methods for nanoparticle synthesis have

proven to be straightforward, cost-effective, dependable, and environmentally sustainable, with a high production yield of AgNPs. As an alternative to chemicals, biological systems used microorganisms (bacteria, fungi, and yeasts), plant extracts, and small biomolecules including vitamins and amino acids to synthesize nanoparticles (6). Nanoparticles made from medicinal plant extracts are also very interesting. Polyphenols, alkaloids, terpenoids, phenolic acids, carbohydrates, and proteins are all critical reducing agents in the bio-reduction of silver ions (Ag^{+}) into (Ag^{0}) (7).

1-2 Literatures Review

1-2-1 *Dodonaea viscosa Lin.*

The Sapindaceae family includes *Dodonaea viscosa Lin*., a shrub. This plant can be found in Africa, the Americas, South Asia, and Australia in tropical, subtropical, and warm temperate climates (2). *Dodonaea* is a genus of about 60 species. The most important feature of this plant is whether it is dioecious or monoecious and whether it is a single or multi-stemmed tree or shrub. The tree can grow up to 7 meters in length and has a blackish-brown bark with varying roughness. The leaves are distinguished by their simplicity, as they have short stems, up to 2.5 mm in size, or none at all, and large, alternate leaves at the end. The leaves are also dark green, with a length of 4 to 7.5 cm and a width of 1 to 1.5 cm. Flowers may be bisexual or unisexual and range in color from white to greenish-yellow (Figure 1-1) (8). This plant thrives in open, sunny areas and is often grown in clay or sandy soils. It can also withstand salt spray, drought, and windy conditions (9). Seeds that are dried retain their viability for a long time. Stem cuttings have been successfully replicated, and seedlings have been successfully grown in nurseries. Throughout its geographic range, the *Dodonaea* has the potential to bloom almost all year. The fruits ripen 11-10 months after the flowers and have long wings, causing them to be dispersed by the wind (10).

D. viscosa has a wide range of medicinal properties that indigenous peoples around the world have used. This plant is used as traditional medicine and is taken orally or topically to treat various ailments. The plant's leaves are used for swelling pain and itching relief, as the stems are essential in the treatment of rheumatism (11). The roots and leaves are used to treat oral discomfort and as a pain reliever. Bruises, sprains, cuts, and burns are treated with parts of the plant. It's also used to treat

gastrointestinal issues, including ulcers, constipation, and diarrhea. On the other hand, in the traditional system of medicine, different plant parts such as roots, seeds, stem, leaves bark and aerial parts are used as antioxidants, anti-bacteria, anti-inflammatories, anti-viruses, and anti-ulcers (8).

Figure (1-1): *Dodonaea viscosa Lin.*

1-2-2 Phytochemicals of *Dodonaea viscosa Lin*.

Plant phytochemicals components offer macronutrients and micronutrients to humans, in addition to biological activity. It also plays a role in taste, color, and aroma, protects plants from damage, and prevents diseases. Phytochemicals are plant components that protect plant cells from contamination, Ultra-Violet ray exposure, stress, environmental hazards, and pathogen attack, to name a few. Plants accumulate them in various places, including leaves, roots, stems, seeds, fruits, and even flowers (12). These compounds are secondary plant metabolites with biological

properties such as antimicrobial activity, antioxidant activity, anti-cancer activity, hormone metabolism regulation, platelet aggregation reduction, detoxification enzyme modulation, and immune system enhancement. There are over a thousand phytochemicals identified, and several more are unknown (13). According to a preliminary phytochemical study, *Dodonaea viscosa* contained flavonoids, phenolic compounds, alkaloids, tannins, hormones, saponins, reducing sugar, and terpenes (Figure 1-2) (14).

Flavonoids, a class of secondary plant metabolites with altered phenolic structures in their molecular system, are widely distributed in the plant kingdom. Many of these substances have anti-cancer properties. Flavonoids can protect the body from free radicals and reactive oxygen species by acting as potent antioxidants.

Phenols are essential secondary metabolites for most medicinal plants. These phenols can use as treatment for neurodegenerative an anti-inflammatory, anti-cancer, cardiovascular diseases, osteoporosis, and diabetes mellitus (15).

Alkaloids are nitrogen-containing organic compounds found in nature. Living species, such as plants, animals, fungi, and bacteria, produce alkaloids naturally. They're characterized by their pharmacological activity, which includes anti-arrhythmic (quinidine, spareien), anti-cancer (dimeric indoles, vincristine, vinblastine), antihypertensive (many indole alkaloids), and antimalarial (quinine) impact (12).

Tannins are the most commonly distributed class of plant secondary metabolites. They are water-soluble polyphenolic biomolecules. Tannins play various plant biology and human life roles, including herbivore defense, UV protection, and pathogen defense. For previous resonance, alkaloids and tannins found in medicinal plants can act as a deterrent to grazers (16).

Saponins are plant glycosides with water-soluble sugars bound to a lipophilic steroid or triterpenoid. Saponins can be found in various plant components, including roots, leaves, fruits, flowers, and stems, and can be found in different plant families. When combined with water, it produces a soapy substance that has been used to treat a variety of diseases, including high cholesterol, blood pressure, physical pressure, diabetes, blood vessels, and hepatitis (17).

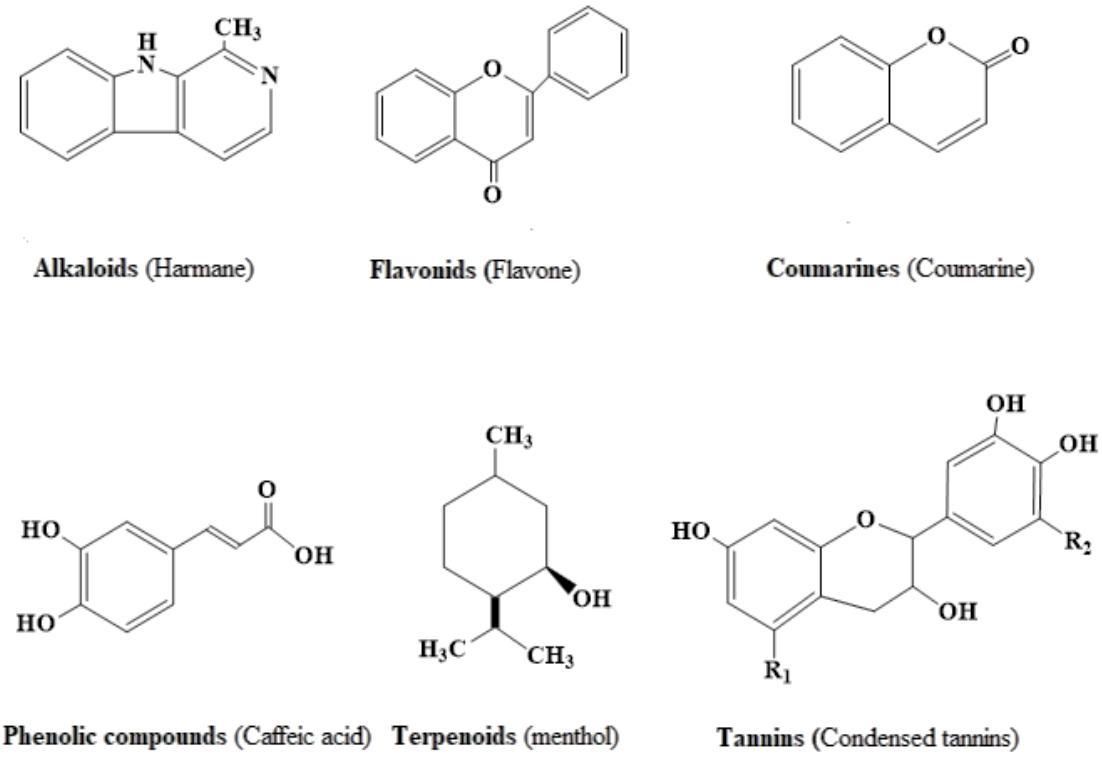

Figure (1-2): Structure of the essential phytochemicals of *Dodonaea viscosa Lin*. (18); (19).

1-2-3 Major Components of Plant

Secondary plant metabolites are chemical compounds generated by plant cells. These components are produced as a result of the primary metabolites' metabolic pathways. All living cells have a standard primary metabolic system, including small molecules like glucose (amino acid, sugars, Krebs cycle intermediates, polysaccharide, nucleic acids, and proteins). Secondary plant metabolites are divided into many groups based

on their chemical structure (phenolic, alkaloid, saponins, terpenes, lipids, and carbohydrates). Due to their ability to protect plants from pathogens. These metabolites have anti-fungal, antiviral, and antibiotic biological activities. The phenolic compound (simple phenols, flavonoids, tannins, coumarins, chromones and xanthones, stilbenes and lignans), alkaloids (nicotine, caffeine, and vinblastine) are examples of secondary plant metabolites (Figure 1-3) (20).

Green synthesis of NPs necessitates the use a combination of metal salts and natural substances such as vitamins, sugars, plant extracts, biodegradable polymers, and microorganisms. When plant extracts are used, they can serve as a reduction agent and contribute to the system's stability (21).

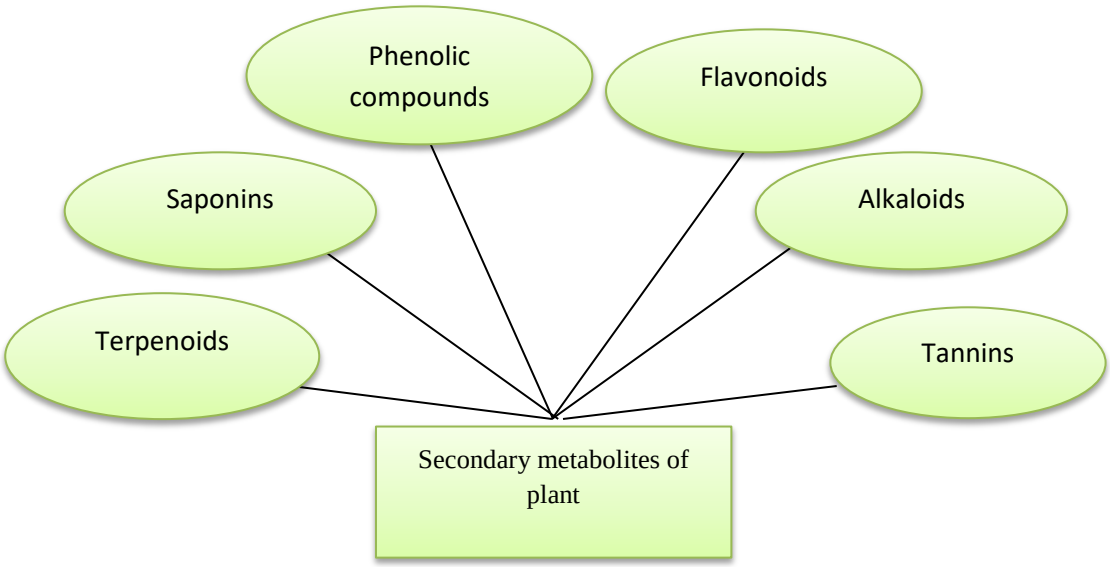

Figure (1-3): Secondary metabolites (22)

1-2-4 Biological Applications of *Dodonaea viscosa*

There are a variety of drugs available to treat various diseases. The advent of intractable diseases and the development of tumors fueled the quest for new drugs with more minor side effects. Natural resources have been used in the treatment of different conditions in the past without any scientific expertise. Many antibiotics were isolated from microorganisms

after the discovery of penicillin (a fugal product). Plants have long been used to treat a variety of diseases, according to previous research, because they contain biologically active substances. The potential activity of the plant extracts could be due to the presence of important phytochemicals constituents in the plant (23).

Flavonoids, saponins, phenols, carbohydrates, tannins, sugar, and gum were all extracted from *D. viscosa* and displayed various biological activities. The leaves of *D. viscosa* are used to treat gastrointestinal and rheumatic diseases in Africa, while the leaves are used to treat wounds in New Zealand. Snake bites and bone fractures are also treated with it, in addition headaches, indigestion, diarrhea, and wound healing. Different polarity crude plant extracts have other behaviors, for example (anti-diabetic activity, antioxidant activity, antimicrobial activity, wound healing activity, and cytotoxic activity). The extract of boiling leaves of the *Dodonaea* plant, which is used as a mouthwash, was used to research another biological application of this plant on stomatitis (24).

Previous pharmacological research on *D. viscosa* revealed that it is used to treat a variety of ailments. It's been used for a long time to treat diarrhea and stomach pain, and it's also good for dermatitis, anti-rash, and scratching on the face. It has also been used as a muscle relaxant (25); (8).

1-3 Synthesis of Nanoparticles (NPs)

The synthesis of NPs can be accomplished using various approaches, which are usually divided into two categories. As seen in (Figure 1-4), there are two approaches: bottom-up and top-down (26). Top-down synthesis is the mechanical grinding of bulk materials to break them down into nanosized particles. This process uses a destructive approach that begins with the larger particle and works its way down to the smaller units, then transformed into suitable NPs (27). For example, mechanical methods

(grinding, ball milling, etching, and cutting), laser beam processing, thermal decomposition, and lithography are examples of this technique (28). The surface chemistry of the structure, this method can cause imperfections in the product's surface structure, posing a significant limitation. Furthermore, the surface structure of NPs has a substantial impact on their physical properties (29).

Chemical reduction, electrochemical methods, and sono-decomposition are all examples of bottom-up synthesis. Since NPs are made from relatively simple substances, this process is often referred to as the building-up procedure. Nanoparticles are prepared using chemical and physical methods in both top-down and bottom-up methods. The chemical process has a high yield instead of the physical route, which has a low yield. Furthermore, these approaches are costly and, more than certainly, environmentally damaging since they necessitate the use of toxic and hazardous substances that pose various biological risks (28).

Green and biogenic bottom-up synthesis has piqued the interest of several researchers due to the processes' feasibility and their low toxicity and environmental friendliness. The synthesis of nanoparticles is carried out using biological reducing agents from plant extracts and microorganisms (30).

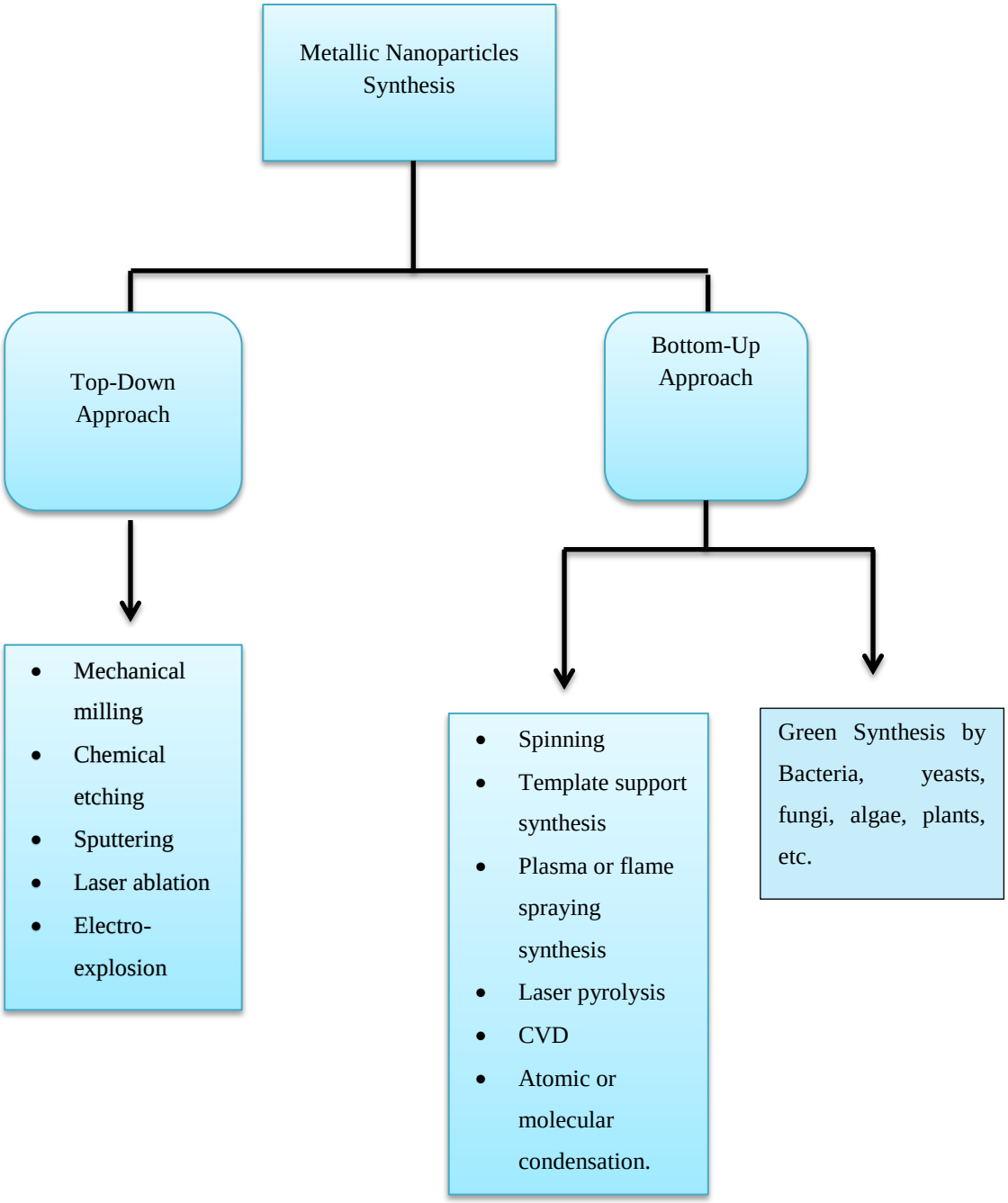

Scheme (1-4): Typical synthetic for nanoparticles for top-down and bottom-up approach (31).

1-4 Types of Nano-synthesis

Metal nanoparticles can be made using a variety of chemical, physical, biological, and hybrid methods. Chemical reduction with stabilizing agents and reducing agents (both organic and inorganic reducing agents) is the most common method for producing NPs (32).

Chemical synthesis, however, involves the use of toxic and volatile chemical compound reactants that are incredibly hazardous and detrimental to the environment, such as vapor aromatic amines and thiols. Reducing substances like sodium borohydride and hydrazine derivatives is especially harmful to the environment (33).

Physical synthesis methods have many benefits over chemical processes, including the absence of solvent contamination in the prepared thin films and the uniformity of NP delivery. Physical methods are costly because they require complex instrument design and use a lot of energy to sustain the high pressure and temperature used in NPs synthesis (34).

The truth is that researchers are interested in developing alternative routes for NP synthesis that are both environmentally sustainable and safe. As a result, the scientific community is beginning to consider green synthetic protocols. The biological synthesis is based on natural principles and includes a natural process that occurs in biological systems. The market for "green" NPs has resulted in new and creative approaches to combating physical and chemical methods.

1-4-1 Biosynthesis of Nanoparticles

Chemical reduction, electrochemical reaction, reverse micelles, microwave process, sonochemical method, and biosynthesis were all used to make metal and metal oxide nanoparticles throughout the past (35). The use of microorganisms, enzymes, and plants or plant extracts in the biosynthesis of nanoparticles has been suggested as a possible environmentally sustainable alternative to chemical and physical methods (6).

Microbial nano-particular synthesis is a highly efficient process because it involves a biological organism, is cost-effective, and has no biotic or abiotic side effects. *Pseudomonas stutzeri* (36), *Escherichia coli*

(37), *Shewanellaalga* (38), and other microorganisms were used to synthesize NPs. Several methods for generating smaller nanoparticles have been proposed. Following the discovery of Ag aggregation inside the bacterial cell, in 1999, Klaus and his colleagues discovered bacterial biosynthesis mediated in NPs (36). The production of non-toxic NPs is well-known among bacteria, yeast, and fungi. However, microbial-mediated NP synthesis is not commercially viable because it necessitates a costly medium and strict aseptic conditions (39).

Microbes are also used as a tool for NP synthesis in various fungi, such as *Fusarium oxysporum* (40), *Cladosporium cladosporioides* (41), and *Fusarium semitectum* (42).

Plant extracts have traditionally been used as reducing agents rather than chemical reducing agents. These extracts have a reducing and capping effect. Researchers were able to successfully stabilize and synthesize NPs using an utterly green approach that did not require the use of any harmful reducing agents. Plant extract nanoparticles can be biosynthesized rather than chemically synthesized, and they can be used for various therapeutic applications. Furthermore, the plant extract was more effective as a reduction and capping agent than microbial synthesis. *Ficus carica* (43), *Crocus sativus L.* (44), *Azadirachta indica* (45), *Annona muricata*, and other plant extracts have been used to make nanoparticles in recent studies (46).

1-4-2 Biosynthesis of NPs from Plants

Plant-assisted nanoparticle synthesis is more efficient than microbial nanoparticle synthesis in terms of yield. Plants have a range of metabolites and biochemicals (such as polyphenols) that can act as both stabilizing and reducing agents in the production of biogenic NPs. Plant-mediated NP synthesis is both environmentally sustainable and cost-effective since it

avoids the use of dangerous chemicals. Plant-derived NPs were much more stable than those generated by microbes and champignons in the studies (47). Compared to medications, food additives, and nutraceuticals, polyphenols are the main natural antioxidant classes with exceptional potential (48).

The synthesis of NPs from plants can be divided into extracellular, intracellular, and phytochemical. Extracellular methods are used when plant extract is used as a raw material for NP synthesis. The intracellular method of nanoparticle synthesis uses cellular enzymes to synthesize nanoparticles within the cells of plant tissue. The NPs are recovered after synthesis by separating the plant cells' cell walls. Although phytochemical-mediated NP synthesis is not a popular method because it necessitates knowledge of the specific phytochemical required to synthesis stabilized NPs, it is a viable option (33).

The most significant advantages of using plants to synthesize nanoparticles are the safety, performance, low energy consumption, and the metabolites that help reduce silver ion. On the other hand, the biological path generates NPs that are less toxic and better suited to a range of biomedical applications. Plant NP formations usually range in size from 1 to 100 nm. (49).

Plant sections such as roots, stems, leaves, bark, and even seeds are used to make nanoparticles. The nature of plant extracts affects NP formation in a salt solution. In addition to the concentration of each extract and salt, pH also played a role in the formation of NPs (50)

1-5 Biosynthesis of Silver Nanoparticles

Chemical and physical methods for synthesizing NPs include various substances that can be harmful to biological and environmental systems. Whereas biologically-mediated NP synthesis is less toxic and produces a

higher yield product. NPs need a good source of metals to be synthesized (51). Silver nanoparticles (AgNPs) are one of the most widely used in various applications as a medicinal and drug delivery, as well as the fact that silver at the nanostructure level has gained considerable attention due to their activity antimicrobial, anticoagulant, biofilm inhibition, anti-cancer, and anti-inflammatory when compared to bulk silver, making them an ideal candidate in the medical a sector (52).

Microorganisms (bacteria, fungi, aquatic algae, yeasts), alcoholic or aqueous plant extracts, and other biosynthesis methods may all be used to make AgNPs (53). The use of plants to synthesize AgNPs has gained popularity in the last decade due to its pace, lack of environmental impact, and lack of pathogens. A two-step method is used. The reduction of Ag^{+} ions to Ag^{0} is the first step. The formation of oligomeric clusters of colloidal silver NPs results from the second stage, which is aggregation and stabilization (54).

Plant extracts provide phytochemicals such as (enzymes, polysaccharides, alkaloids, tannins, phenols, terpenoids, and vitamins). Despite their complex structures and pleasant personalities, these compounds have much medicinal value (55). The synthesis of AgNPs using plants was identified using *Bunium persicum Boiss* fruit extract (56), *Cassia roxburghii* leaf extract (57), and *Piper longum* fruit (58). However, as compared to other biological methods, the synthesis of AgNPs using plant extracts is advantageous because the removal of metal ions is much quicker, resulting in high particle stability (26).

1-5-1 Optimized Conditions for Biosynthesis of AgNPs

Many factors contribute to the increased production, scale, and stability of biogenic AgNPs. In the synthesis of AgNPs, the volume of

plant extract, the concentration of silver salt, the pH, and the temperature at which the reduction occurs all play essential roles (Figure 1-5).

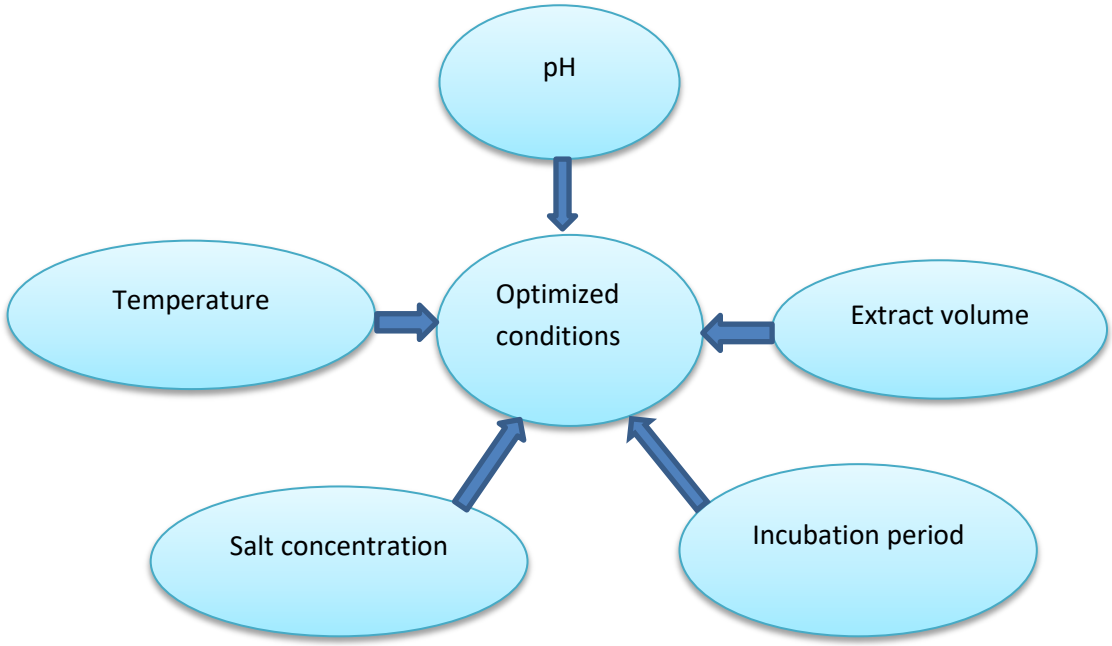

Figure (1-5): Factors affecting to synthesis AgNPs (59).

The scale, shape, and properties of nanoparticles are all affected by these factors. When plant extract and Ag-salt are combined, the color changes from colorless to dark brown, indicating the development of AgNPs for the first time. AgNPs are synthesized at various pH levels (2–14). The different temperatures used to manufacture Ag nanoparticles range from (25^{o}C to 45^{o}C), with low temperatures producing sharp peaks and high temperatures making significant peaks. The optimum temperature for the synthesis of AgNPs at room temperature is 25°C, and the ideal pH is considered pH 7. The most substantial Ag-salt concentrations are between 0.25 and 10 mM, with concentrations above 10 mM causing the silver accumulation. As the salt concentration rises, the surface plasmon bands move to a higher frequency, indicating aggregation. AgNPs efficiency is determined by the reaction's incubation period (60).

1-6 Biological Applications of Silver Nanoparticles

AgNPs have grown in popularity due to their numerous applications in various fields (biomedicine, pharmacy, agriculture, and food industry). Due to their unique properties in industrial applications, silver nanoparticles are one of the most intriguing particles (61).

Since silver products, such as metallic silver and silver salts, have been used as potent antimicrobial agents in medicine for decades, silver nanoparticles are an integral part of nanotechnology (62).

Silver nanoparticles also have effective against a broad spectrum of Gram-positive and Gram-negative bacteria, together with some antibiotic-resistant strains. They have been used to prevent diseases for decades. Furthermore, AgNPs have gained interest in cancer therapeutic applications. The chemical and physical properties of these metallic nanoscale particles are peculiar. Its ease of inactivation limits the antibacterial activity of the Ag^{+} ion by complexation and precipitation. At the same time, silver nanoparticles have a higher bactericidal activity due to its larger surface area. Furthermore, the broad impact of biologically synthesized AgNPs disrupts the bacterial system's protein synthesis mechanism by breaking the cell membrane. These NPs inhibit bacterial cell division at high concentrations, causing an increase in cell membrane permeability. They play a significant role in rupturing the bacteria's cell wall, ultimately leading to cell death (7). It is now possible to synthesize silver nanoscale particles in various shapes that can communicate with microbes, resulting in a difference in antibacterial performance (4).

Plant-derived silver nanoparticles are used not only as antibacterial, anti-fungal, antiviral, anti-inflammatory, wound healing, anti-angiogenic therapy, cancer diagnosis, and drug delivery but also in bio-imaging (Figure 1-6) (63). There may be drawbacks to using silver NPs since they

cause toxicity of varying degrees. Ag nanoparticles in high concentrations can cause a variety of health issues. When appropriately used, these particles are environmentally friendly, but when used randomly, they become a formidable foe (64).

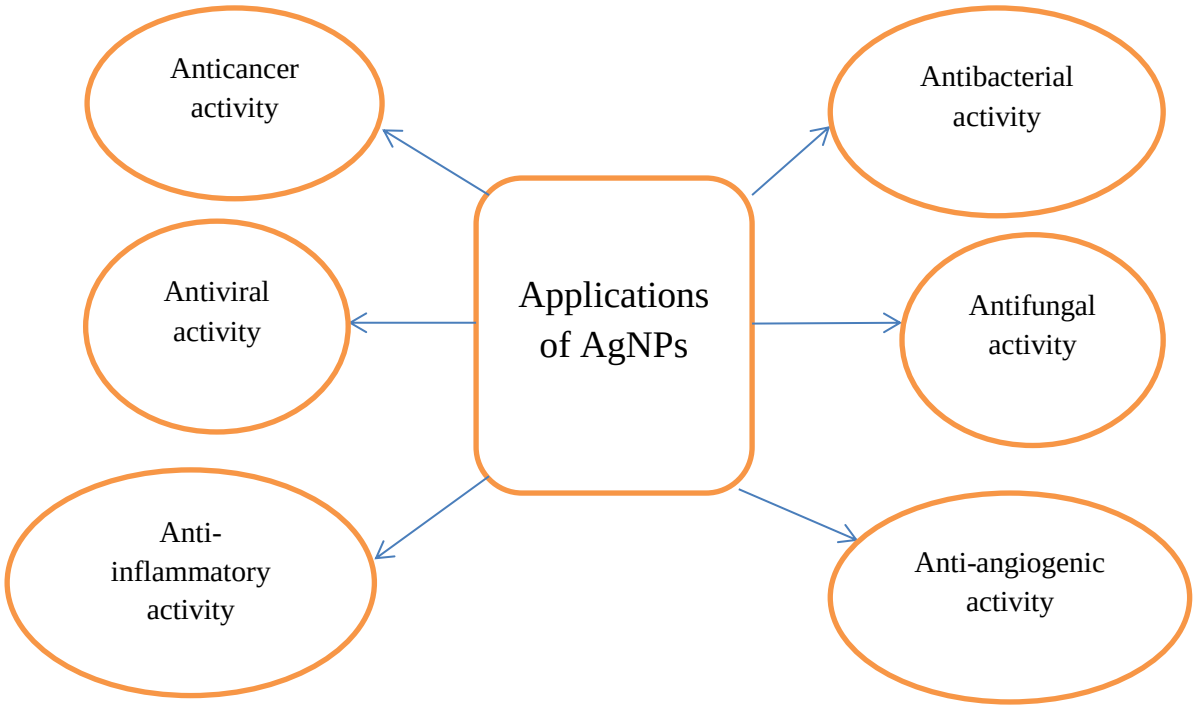

Figure (1-6): Different applications of silver nanoparticles in biomedical fields (61).

1-6-1 Antioxidant Activity

Antioxidants are substances that can defend cells against free radical damage. Free radicals are natural compounds produced in the body due to the breakdown of food within the body or exposure to radiation or pollutants. These radicals are a significant contributor to heart disease, cancer, and other illnesses (65).

Even though free radicals are usually present in the body, tiny amounts are considered toxic molecules. The generation of superoxide radicals is primarily carried out in the mitochondria of a cell. The majority of the adverse effects are caused by radicals, which strike and destroy molecules inside cells due to the continuous production of oxygen. The

reactive oxygen species capable of causing oxidative damage involve superoxide ($O_2^{\bullet-}$), hydroxyl ($OH^{\bullet}$), perhydroxy radical ($HOO^{\bullet}$), alkoxyl radical ($RO^{\bullet}$), and peroxyl ($ROO^{\bullet}$), organic hydroperoxide (ROOH), and monooxygen ($1O_2$), etc. The sources of reactive oxygen species (ROS) include the leak of an electron from electron transport systems, decompartmentalization of iron which facilitates the generation of highly reactive hydroxyl radical, and also various biological redox reactions. Many physiological processes and reactions produce reactive oxygen species (ROS) and reactive nitrogen species (RNS), such as peroxynitrite (ONOO), nitric oxide (NO), and peroxynitrate, among others, in our bodies. Antioxidant protection systems in living organisms include both enzymatic and non-enzymatic antioxidants that sustain the level of ROS/RNS and restore oxidative cells. Antioxidants are classified as either protective or chain-breaking antioxidants based on their mechanism of action. A defensive antioxidant that serves as the first line of protection suppresses ROS and RNS. The active species are easily removed by the scavenging antioxidants until the essential molecules are biologically attacked. For instance, superoxide ($O_2^{\bullet-}$) free radicals are converted to hydrogen peroxide (H_2O_2) and oxygen (O_2) by the enzyme superoxide dismutase (SOD), and hydrogen peroxide is then converted to (H_2O) and (O_2) by catalase (CAT) or glutathione peroxidase (GPx) (Figure 1-7) (66). If CAT does not transform H_2O_2 to H_2O and O_2, it will form an $OH^{\bullet}$ radical, which is the most active radical and causes damage to living cells. The action of the enzyme in scavenging ONOO, ROO, $1O_2$, and $HO^{\bullet}$ is unknown. Enzymes are the first line of defense in the fight against ROS and RNS since they actively engage in their neutralization. The second line of defense is the antioxidants that scavenge the active radicals to suppress chain initiation and or break the chain propagation reactions. They are hydrophilic and other lipophilic.

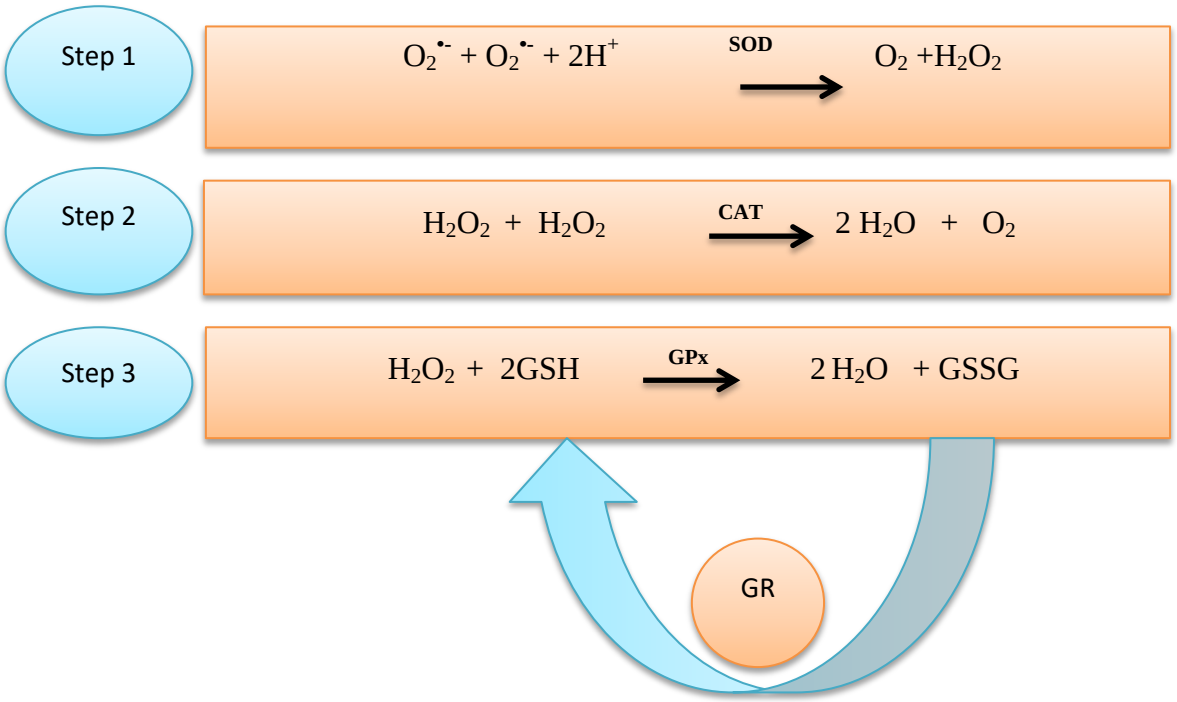

Figure (1-7): The main enzymes responsible for oxidative stress and scavenging free radicals Superoxide Dismutase (SOD), Catalase (CAT), Glutathione Peroxidase (GPx), Glutathione Reductase (GR) (67).

These include vitamin C, vitamin E, uric acid, bilirubin, albumin, and thiols. The antioxidants and repair proteins, proteases, and peptides in mitochondria's cytosol are the third line of protection. Previous research has shown many different types of natural antioxidants, each with its composition, worksite, mechanisms, and properties such as enzymes and high molecular weight compounds. Proteins like (albumin, ceruloplasmin, and transferrin) which limit the production of metal-catalyzed free radicals, minerals like (zinc, manganese, and selenium), and low molecular weight compounds include water-soluble and lipid antioxidants. Uric acid, ascorbic acid, and some other polyphenols come under water-soluble ones, and bilirubin, tocopherol, quinines, and some polyphenols come under lipid-soluble antioxidants (68).

Natural antioxidants can be present in all parts of plants. Vitamins, carotenoids, flavonoids, and phenols are antioxidants that neutralize free radicals by contributing electrons. (Figure 1-8) (69).

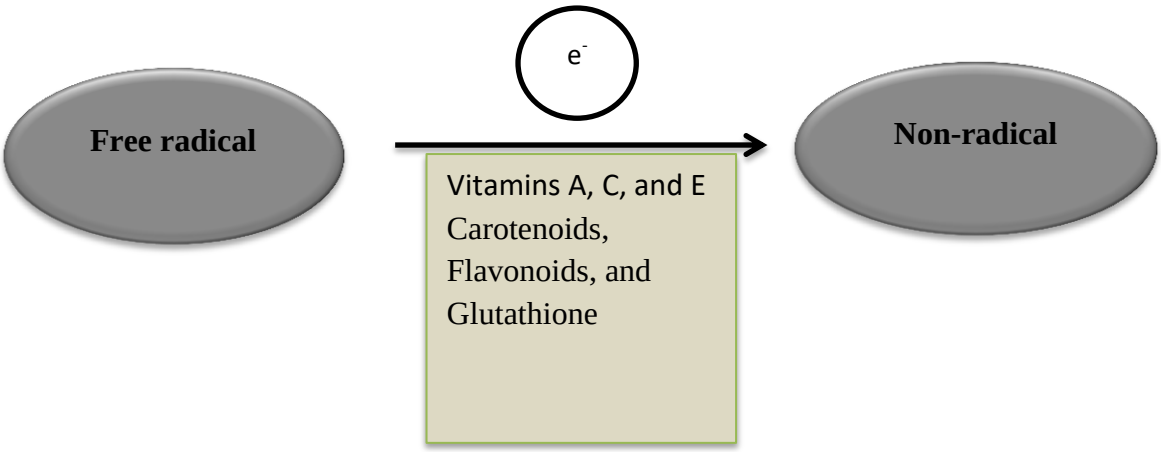

Figure (1-8): The Non- enzymatic Natural Antioxidants (70).

1-6-2 Anti-cancer Activity

Cancer incidence has risen in recent years due to oxidative damage and numerous environmental and genetic factors that have a direct or indirect impact. Cancer is a form of irregular tissue growth in which cells divide uncontrollably. Researchers have been developing therapies that reduce side effects, mainly because administering chemotherapy agents intravenously is a time-consuming process. The majority of the researchers focused on developing nanomaterials as an alternative to chemotherapy that could kill cancer cells directly. Anti-cancer drugs have been used in most *in vitro* and biological model systems by various laboratories. Cell death is programmed based on concentration under certain circumstances, according to the molecular mechanism of AgNPs (4).

Biosynthesis silver nanoparticles have previously been shown to have anti-cancer activity in cancer cell lines such as COLO 205 (colon carcinoma), AGS (human gastric carcinoma), HEPG2 (human liver

cancer), MCF-7 (human breast cancer), and A431 (epidermoid carcinoma) (60); (71).

Silver nanoparticles' anti-cancer activity is mediated by changes in cell morphology, a decrease in cell viability, metabolic activity, and an increase in oxidative stress, which contributes to mitochondrial damage and an increase in reactive oxygen production species (ROS), culminating in DNA damage. The ability of AgNPs to change the morphology of cancer cells is a sign of apoptosis. Apoptosis has been identified as a major mechanism of cells death in exposed to AgNPs synthesized using plant extracts (72).

The human lung (A549) carcinoma cells are more toxic to synthesized AgNPs from plant extract than non-cancer cells, meaning that AgNPs can target cell-specific toxicity, which lowers pH in cancer cells (58).

One study was reported by Muhammad Ovais *et al*. found that silver ions released from colloidal biogenic silver nanoparticles cause cancer cell death. The release of Ag^{+} ions was twice as strong in an acidic medium as it was in a neutral medium. As a result, when the pH is acidic, silver ions are abundant, which increases anti-cancer activity in the acidic environment. The release of silver ions is twice as strong in acidic media, according to the researchers (60).

1-6-3 Anti-bacterial Activity

Silver nanoparticles are distinguished by two main characteristics: their nanoscale size and wide surface area, which enhances their effectiveness. AgNPs are the most widely used nanomaterials due to their strong antimicrobial properties. These interesting particles have been widely studied and are used in a wide range of applications. Despite specific existing antimicrobial and anti-cancer pathways and multiple

studies that have applied the theory, the properties of AgNPs remain unknown. AgNPs can prevent or destroy bacteria growth by inducing membrane destruction, ROS development, DNA damage, enzyme inactivation, and protein denaturation (73).

Antibiotics were used widely for long periods, allowing bacteria to establish resistance. This resistance can happen as a result of gene mutation or as a self-defense mechanism for bacteria. As a result, enzymes that inactivate antibiotics are generated. As a result, the bacteria's resistance to antibiotics grew. Scientists were developing new antimicrobial therapeutics. AgNPs were one of the most effective antimicrobial agents, and they've been used as nano-carriers for drugs and antibiotics to help boost antibiotic activity against resistant bacteria (33).

Silver is now commonly used as an antibacterial and wound dressing ingredient. Silver nanoparticles have good antibacterial activity because of their tiny nanoscale size and broad surface region (74). The antibacterial activity of synthesized AgNPs derived from plant extracts is mediated by (i) the generation of reactive oxygen species (ROS) that cause oxidation of cell components and cell destabilization (Figure 1-9) (ii) As AgNPs enter the cell, they convert to silver ions, which interact with biomolecules (sulfur-containing substances), forming a bond with the sulfhydryl group of enzymatic proteins in bacteria, causing bacterial protein denaturation, and (iii) the release of Ag^{+} ions from AgNPs, which can penetrate the cell membrane, causes further damage to bacteria, eventually killing them (75).

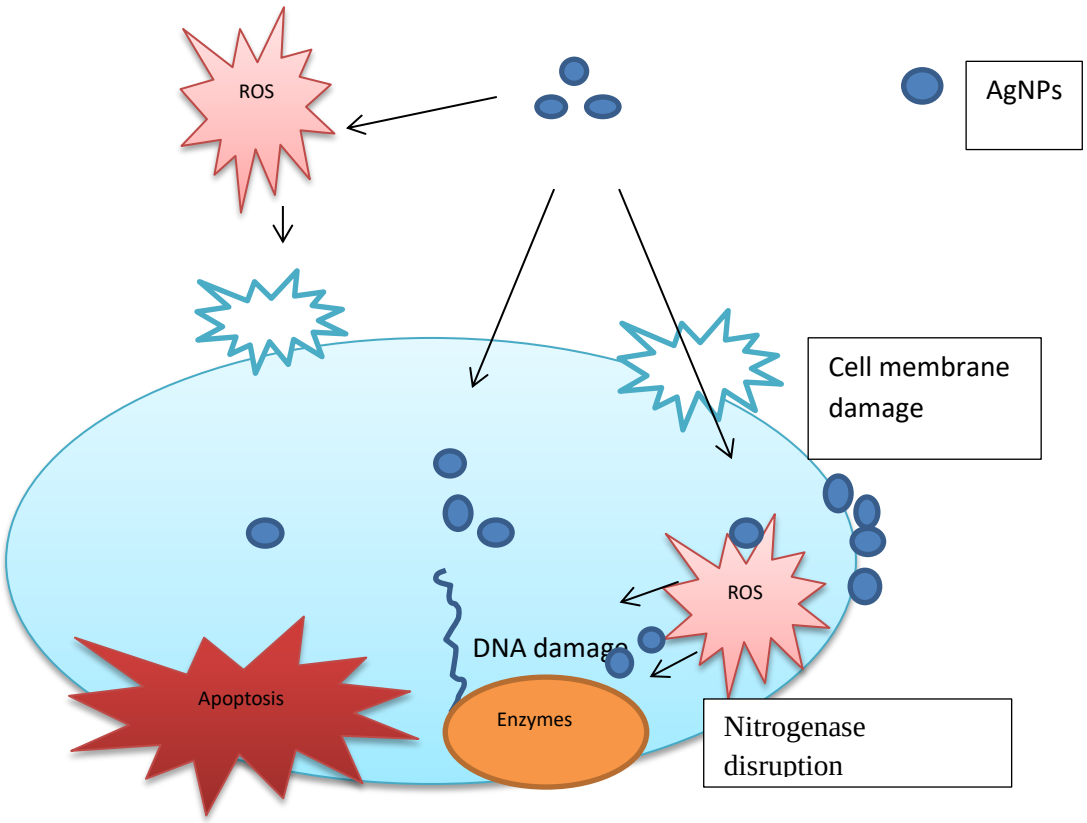

Figure (1-9): Mechanism of action of AgNPs against bacteria (76).

One study was reported by Senthil, B., *et al.* that AgNPs were found to be more effective against Gram-negative bacteria than Gram-positive bacteria. Gram-negative bacteria have lipid polysaccharides on their surfaces that made them negatively charged and are correlated with the positive charge of silver. Gram-negative bacteria have a thin layer of peptidoglycans and linear polysaccharides bonded to each other. In contrast, Gram-positive bacteria have a thick layer of peptidoglycans and linear polysaccharides bonded to each other. In another meaning, the integral proteins provides a cellular rigidity that impedes the attachment of AgNPs to its surface (77).

1-6-4 Coagulation of Blood

One of the most critical characteristics of NPs is their small size, which allows them to enter the circulatory system through the skin, injection, inhalation, or even feeding. When these particles enter the

bloodstream, they contact blood cells and plasma proteins, potentially triggering a pathophysiological response. According to ISO-10993-4, blood compatibility with these NPs must be tested and their relationship with blood, thrombosis, coagulation, platelet aggregation, hematology, and complementary systems. Many experiments were performed to determine the biological effects of AgNPs on blood, but comparisons were difficult due to differences in the materials used (62).

Blood coagulant is vital for maintaining a constant blood flow and preventing bleeding. It also aids the innate immune system in preventing the spread of infection, and this is flow system can malfunction, causing a blood clot to develop, which can lead to organ failure and is most commonly linked to cardiovascular disease. Pro-inflammatory cytokines, the expression of molecules that promote clotting on cancer cells' surfaces, and interactions with platelets can all contribute to blood clotting. Controlling the blood clotting system has become critical for maintaining health and avoiding complications that may occur from coagulation disorders. Since AgNPs are non-toxic to platelets and have strong antimicrobial properties, they could pave the way for new ways to treat blood coagulants. Nanoparticles of various sizes and shapes have been shown to have varying degrees of effect on the blood clotting system in studies. Since the blood clot must be resolved quickly and effectively, it is preferable to improve care with nanotechnology (78).

Coagulation screening tests are traditionally categorized into tests of primary hemostasis (platelet plug formation), secondary hemostasis (fibrin clot formation), or fibrinolysis (clot breakdown). A secondary hemostasis pathway is activated partial thromboplastin time (APTT) studies. It's similar to triggered clotting time in terms of diagnostics, but APTT is less affected by platelet defects or hematocrit. Prothrombin time (PT) is used to estimate the typical and extrinsic pathways and their ability to transform

fibrinogen to fibrin. Both the APPT and the PT are used to detect defects in the extrinsic, intrinsic, or general coagulation pathways as checking tests. Each APTT and PTT test necessitates the addition of specific coagulation activating reagents to citrated plasma, followed by the measurement of the time it takes for the coagulate to shape. The anticoagulant sodium citrate (3.2 or 3.8 percent) in the tubes used to collect blood for PT and APTT (blue top tube) (79).

Previous researchers Katja Heise *et al*. have used silver nanoparticles in a variety of areas, including medicine. It is important to continue to improve this area because it has a direct connection to human life. Enabled partial thromboplastin time (APTT) and prothrombin time (PT) assays with normal citrated human plasma were used to assess the anticoagulant activity of AgNPs and crude extract. The ability to function in the fibrinolytic system is what activated partial thromboplastin time (APTT) and prothrombin time (PT). For PT and APTT research, the clotting time ranges from 10 to 14 seconds and 22 to 40 seconds, respectively. Anticoagulant antibodies or inhibitors of fibrinogen conversion, for example (heparin administration or other anticoagulants), extend the clotting time of both the PT and APTT tests (80).

1-6-5 Hemolysis

Hemolysis is the breakdown or destruction of the membrane of erythrocytes (red blood cells), which is harmed by the release of hemoglobin into the plasma. Red blood cells can break down prematurely due to diseases like hemolytic anemia or processes like blood centrifugation (81). Hemolysis can cause these hemoglobin removal systems to become saturated and depleted, resulting in an accumulation of hemoglobin and heme within the vascular compartment (82).

Extracellular hemoglobin is harmful because it can damage the heart muscle, blood vessels, central nervous system tissues, and kidneys (83). As the clinical use of AgNPs grew, researchers gained a deeper understanding of their safety in the bloodstream. The study of nano-toxicity on blood, especially red blood cells, is critical because the blood that comes into contact with NPs, whether directly or indirectly, can pass the foreign substances to cells, tissues, and organs. The tendency of a blood-contacting medical substance to hemolyze when combined with blood *in vitro* is one of the most basic tests used to determine its protection. Nano-size particles compared with micro-size particles have more potential for hemolysis because their greater surface area would facilitate the release of more silver ions. Accidental exposure to silver nanoparticles through ingestion and inhalation, or even through the skin, may cause them to enter the bloodstream and interact with blood components. Given their associations with blood components and the cardiovascular system, determining AgNPs compatibility with blood is critical (84).

The percent of hemolysis was calculated in most *in vitro* studies using a spectrophotometric assay after incubating the particles with blood and then centrifuging the intact cells (85).

1-7 The Aims of the Study

1. Green synthesis of silver nanoparticles from the environmentally friendly substance (*Dodonaea viscosa* leaves extract).
2. Characterization of synthesized silver nanoparticles.
3. Study the antioxidant activity of synthesized silver nanoparticles.
4. Clinical applications of synthesized silver nanoparticles.

Chapter Two
Materials
and
Methods

2. Materials and Methods

2-1 Materials

2-1-1 Apparatuses

The apparatuses and equipment are summarized in (Table 2-1)

Table (2-1): The apparatuses and equipment used in this study

Instruments	Company
Atomic Force Microscopy AFM	CSEM
Centrifuge	D-78532/Germany
CO_2 incubator	England /Gallenkamp
Cooling centrifuge	D-78532/Germany
Fourier Transform Infrared FT-IR	Shimadzu (8400S)/Japan
GC-mass chromatography– mass spectrophotometer	Aligant / U.S.A
Gemyy orbit shaker	VRN-480/ Germany
Hot plate with magnetic stirrer	LabTech/Korea
Micro pipette	DragoLAB/China
Micro-titer plate reader	Bio-Rad (Germany)
Oven	D-91126 Schwabach FRG/ Germany
Sensitive balance	ABS 220-4/KERN
Tescan Mira3 SEM	French
Ultrasonic cleaner set	WUC-D06H/Korea
UV-Vis spectrophotometer	UV-1800/ Kyoto, Japan
Water distillatory	LabTech/ Korea
Water bath	England /Gallenkamp
X-ray diffraction XRD	Philips Xpert /Holland

2.1.2 Chemicals and Kits

The chemicals and kits are summarized in (Table 2-2)

Table (2-2) Chemicals and kits used in this study

Material	Company
1,1-Diphenyl-2-picrylhydrazyl free radical (DPPH)	Tokyo Chemical Industry TCI
Acetic acid	HiMedia
Ammonium molybedate	BDH Chemical Ltd Pool/England
Anhydrous acetic acid	Chem- Supply
Ascorbic acid	HiMedia
Basic nitrate bismuth	BDH Chemical Ltd Pool
BIO-CK APTT Kaolin Kit	BIOLABO, 02160, Maizy, France
BIO-TP Prothrombin Time (PT) Kit	BIOLABO, 02160, Maizy, France
Calcium chloride	Stago
Chloroform	Gainland Chemical Company
Copper sulphate solution	Analar Trad Mark
Dimethyl sulfoxide (DMSO)	Sigma (USA)
Ethanol	Gainland Chemical Company
Ferric chloride $FeCl_3$	BDH Chemical Ltd Pool
Fetal bovine serum	Sigma (USA)
Hydrochloric acid	BDH Chemical Ltd Pool
L-Ascorbic Acid	HiMedia, India
Lead acetate	BDH Chemical Ltd Pool
Mercuric chloride	BDH Chemical Ltd Pool
MTT kit	Intron Biotech (Korea)
Potassium citrate	Merck
Potassium dihydrogen phosphate	Merck
Potassium ferricyanide	Analar Trad Mark

Potassium iodide	Analar Trad Mark
RPMI-1640 Media	Sigma (USA)
Silver nitrate	Reagent World, Ice / U.S.A
Sodium hydroxide	Analar Trad Mark
Sodium phosphate	BDH Chemical Ltd/England
Sulfuric acid	Belgium
Trichloroacetic acid	Gainland Chemical Company
Triton-X 100	HiMedia

2-2 Methods

2-2-1 The General Procedure for Synthesis Silver Nanoparticles and their Applications.

The general steps for synthesis silver nanoparticles and their applications summarized in scheme (2-1).

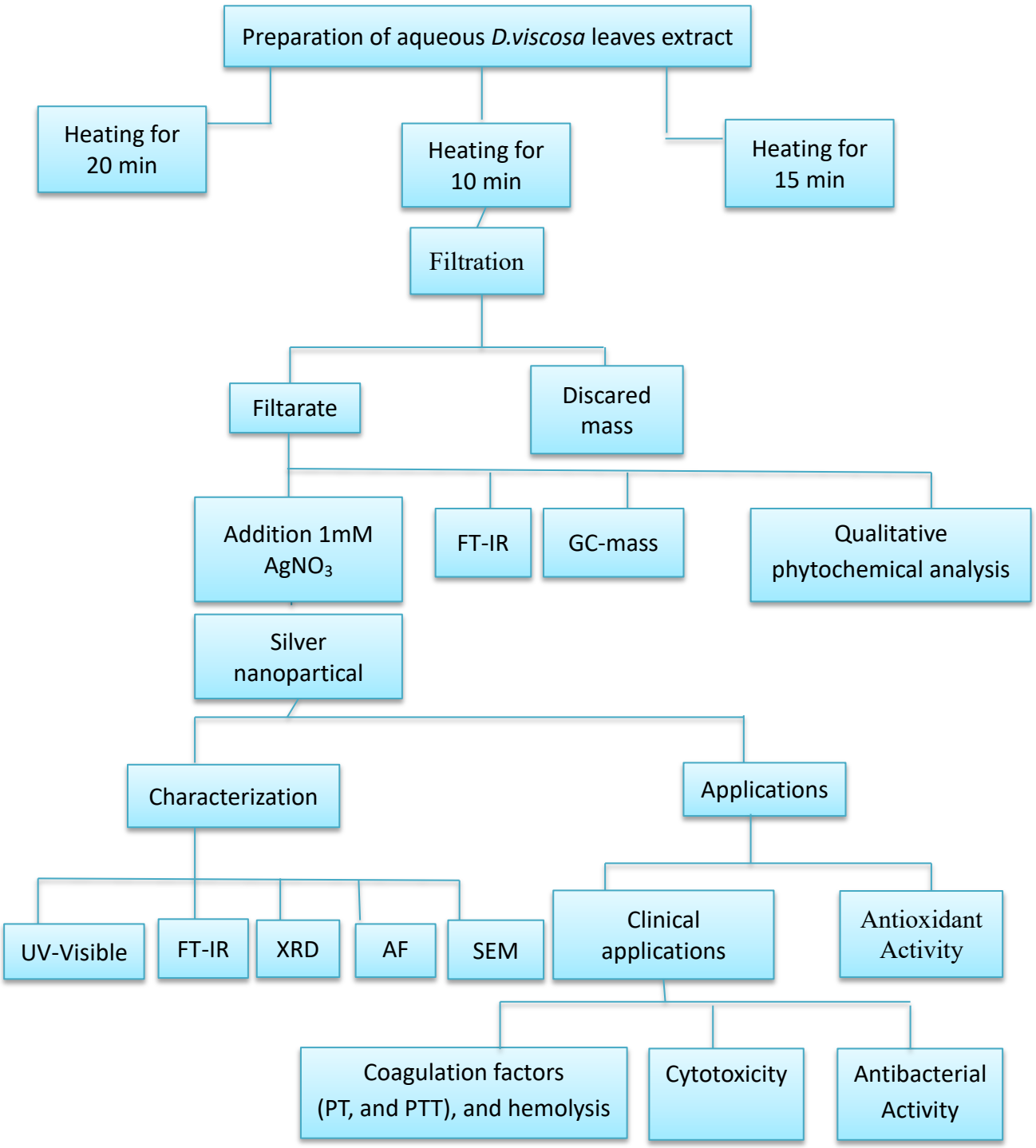

Scheme (2-1): The general steps of synthesis AgNPs and their applications

2-2-2 Collection of Plant

Fresh *D.viscosa* leaves were collected from the garden of the University of Kerbala, College of Science from 1 September to 30 October 2019. First, the leaves were washed using tap water and then deionized water, then they are left to dry at room temperature. Finally, the dry leaves were cut into small slices and stored in a dark and dry place for further use to prepared extract. The identification of the plant species was done by the Botanist Dr. Nibal Muteer at the University of Kerbala, College of Education of Pure Science.

2-2-3 Qualitative Phytochemical Analysis

The crude solution of *D. viscosa* leaves extract was submitted to phytochemical analysis. These phytochemical were alkaloids, flavonoide, coumarins, saponins, sugars, resins, phenolic compound, terpenes, tannins, and steroids.

- **Alkaloid test** [86]

Dragendorff´s reagent is a color reagent to detect alkaloids in a test sample and prepared as following:

Solution A: it was prepared by dissolving 0.85gm of basic bismuth nitrate in a mixture of 10 mL of acetic acid and 40 mL of deionized water in a 50 mL volumetric flask.

Solution B: it was prepared by dissolving10 gm of potassium iodide (KI) in 25 mL of deionized water.

Stock solution: it was prepared by mixing 5 mL of solution A and 5 mL of solution B (equal volumes).

Spray reagent: it was prepared by mixing 10 mL of stock solution with 20 mL of acetic acid and then added into a 100 mL volumetric flask and diluted to volume with deionized water to obtain the Dragendorff's reagent.

Dragedorff's reagent gives orang color when spraying it over a spot of alcoholic extract. That means presence alkaloid in the plant.

- **Coumarin test** [87]

A five mL of alcoholic extract was added to the 5% sodium hydroxide in a test tube and then boiling in water bath for 5 minutes observation of yellow fluorescence, develops when dried paper is place under UV- light for 5-10 minutes.

- **Flavonoid test** [88]

Alcoholic extract was treated with equal volumes of 50 % ethyl alcohol, and 50 % sodium hydroxide with the same volume of extract. Formation of intense yellow indicates the presence of flavonoids.

- **Resins test** [89]

A twenty-five mL of 95 % ethanol was mixed with 5 gm of plant, and then boiled in water bath for 2 minutes. The extract was filtered and treated with a few drops of 4 % HCL. Appearance of the strong turbidity indicate to a positive test.

- **Saponins test** [90]

A one mL of the aqueous extract was added to 2 mL of deionized in a test tube and was shaken vigorously for a few minutes. A thick foaming remained for long time; this is evidence for a positive test.

- **Sugar test** [91]

Bendect´s reagent was used for testing monosaccharide and prepared by dissolving 173 gm of potassium citrate with 100 gm of anhydrous sodium carbonate in 800 mL distilled water. The mixture was boiled and filtrated. The copper sulphate solution 17.3% was added to the filtrate, and then the volume was completed to 1liter of distilled water.

To one mL of plant extract, 2 mL of Benedict´s reagent was added in a test tube. The mixture was heated in a water bath for 5 minutes. A red color precipitate indicates the presence of sugar.

- **Terpene and Steroid test** [90]

A 1 mL of alcoholic extract was treated with 2 mL of chloroform; one drop of anhydrous acetic acid and one drop of concentrated H_2SO_4 were added slowly. Steroid solution is indicated through green blue color while formation terpenoid solution is indicated through red violet color.

- **Phenolic compound test** [91]

The 3-4 drops of 1% (v/v) ferric chloride ($FeCl_3$) solution were added to 1 mL of alcoholic extract of plant. Green, purple, blue or black color, indicates the presences of phenolic compounds.

- **Tannins test** [92]

A one mL of alcoholic extract was added to 1 mL (1%) lead acetate. Appearance of white mucilage precipitate indicates the presence of tannins.

2-2-4 Gas Chromatography and Mass spectroscopy

Gas chromatography and mass spectroscopy, GC-MS, is a type of analysis that incorporates the characteristics of gas-chromatography and mass spectrometry to find various materials in the sample. GC-MS was used to analyze the chemical constituents of *D. viscosa* leaf extract. This analysis was done at the University of Kashan/Iran. In brief, the instruments use electron ionization with two columns, while Helium, Nitrogen, and Zero air was used as carrier gas. The oven temperature was 400°C, and the chromatogram of GC-MS for organic compound was detected by contrasting their spectra with comparing spectra to those stored on the computer library.

2-2-5 Preparation of Aqueous *Dodonaea viscosa* Extract

Ten grams of small pieces of dry leaves were added into deionized water (200 mL) and heated for 10 minutes (2). Followed, the crude extract was filtered by using filter paper Whatman No.1. The same filtrate extract was used to synthesize the silver nanoparticles (AgNPs).

2-2-6 Preparation of 1mM $AgNO_3$ Solutions

A one millimolar (1mM) solution of silver nitrate was prepared by dissolving 0.0425 gm in 250 mL deionized water and stored in a dark and dry place.

2-2-7 Synthesis of Silver Nanoparticles (AgNPs)

An aqueous solution (1 mM) of silver nitrate ($AgNO_3$) was prepared to use in (AgNPs) synthesis and various crude aqueous extract volumes of *D. viscosa* (3, 5, and 7 mL) were added to 45 mL of $AgNO_3$. The mixture was shaken for 4 hours and then incubated for 24 hours at 45 °C. The color was gradually changed from light yellow to dark brown after 24 hours of incubation, indicating silver nanoparticles' formation.

The pellets of formed nanoparticles were collected by Ultra-centrifugation at 5300 xg for 15 minutes. Then the obtained pellets were washed three times with distilled water before they were dried and stored in a dark dry place at room temperature for further use.

2-2-8 Effect of Boiling Time of Extract

The influence of boiling time of the plant leaves to prepare the aqueous extract of *D.viscosa* was considered in this study. Ten grams of dry leaves were heated for (10, 15, and 20 min) respectively with 200 mL of deionized water. Using the UV-vis spectrophotometer (UV-1800/Kyoto), the color change in the solution from yellow to brown was detected at different time periods.

2-2-9 Influence of the Extract Volume

To study the effect of extract volumes on particles synthesis, different volumes of plant extract (3, 5, and 7 mL) respectively were added to 45 mL of $AgNO_3$ (1mM) solution. Synthesized silver nanoparticles were observed using a spectrophotometer (UV-1800/Kyoto) and the change of color was followed with time.

2-2-10 Characterization of Synthesized Silver nanoparticles

2-2-10-1 UV-Visible Spectroscopy

The synthesized AgNPs were characterized using UV-visible spectroscopy (UV-1800/ Kyoto, Japan). The absorbance of the solution mixture was measured at different periods in the range from 300 to700 nm. Free electrons give height to the surface plasmon resonance (SPR) absorption band, and this is due to the oscillation of the electrons of AgNPs when affected by light.

2-2-10-2 Fourier-Transform Infrared Spectroscopy

FT-IR spectra were used to compare the IR spectra before and after formation of AgNPs via *D. viscosa* leaves extract and to identify functional groups for both extract and synthesized AgNPs. The pellets of AgNPs were measured with the KBr disk in the wavenumber ranging from 400 to 4000 cm^{-1} using Shimadzu (8400S)/Japan FT-IR spectrophotometer.

- **Preparation of Sample for FT-IR Spectroscopy**

Silver nanoparticles were washed through centrifugation then the pellets were washed in deionized water. Process was repeated three times, removes the filtrate and the pellet were dried at 50°C. After drying pellet powder well, the pellet were measured with the KBr disk in the wavenumber ranging from 400 to 4000cm^{-1} using Shimaduz (8400S)/Japan FT-IR spectrophotometer

2-2-10-3 X-ray Diffraction (XRD)

The average grain size, crystallinity, strain, and crystal defect were characterized using XRD (Philips Xpert /Holland XRD). Cu-kα radiation (k=1.50456) was used in the range of (10^o to 80^o). Using Scherer's equation, the crystal size of all prepared samples was calculated as follows:

$$D=\frac{0.9\lambda}{\beta\cos}$$

Where D is the average size of crystallite, lambda (λ) is the X-ray wavelength, θ is the angle of Bragg in radians, and β is the full width in radians at half the maximum of the peak.

2-2-10-4 Atomic Force Microscopy (AFM).

The Atomic Force Microscopy (AFM) analysis provides images with near-atomic resolution for measuring surface topography of biological specimens in atmospheric liquid or gas environments. It is capable of quantifying surface roughness of samples down to the nano-scale. In addition to presenting a surface image, AFM is also capable of complementary techniques, which provide information on other surface properties, e.g. hardness, friction or elasticity.

The size and the surface properties of biosynthesized nanoparticles were visualized by atomic force microscopy (CSPM Scanning Probe Microscope). The highest measurement was obtained using AFM image analysis software.

- **Preparation of sample for AFM**

A thin film of the silver nanoparticles was prepared by mixing the powder of AgNPs with ethanol, dropped on glasses slide, and then left on air to dry at room temperature.

2-2-10-5 Scanning Electron Microscopy (SEM)

A scanning electron microscope (SEM) is a kind of electron microscope that scans the surface to create images of a sample with a directed electron beam. The electrons overlap with atoms to reveal information about the surface topography and the sample composition. The sample was examined using Tescan Mira3 SEM /French.

- **Sample Preparation for SEM**

The pellet of AgNPs was treated with ethanol properly and carefully placed on a glass slide, and then left on air to dry at room temperature. The cover slip itself was used during scanning electron microscopy (SEM) analysis.

2.2.11 Biological Activities

2-2-11-1 Antioxidant Assay

The antioxidant activities for both synthesize AgNPs and *D. viscosa* extract were evaluated using three methods. Ascorbic acid has been used as a reference.

2-2-11-1-1 1, 1-diphenyl-2-picrylhydrazyl (DPPH) radical scavenging assay

- **Principle**

The DPPH (1,1-diphenyl-2-picryl-hydrazyl-hydrate) free radical scavenging test is an antioxidant method based on electron-transfer that produces a violet solution in ethanol (93). This free radical, stable at room temperature due to the delocalization of the spare electron on the whole molecule. So, DPPH$^{\bullet}$ does not dimerize, as happens with most free radicals (94).

DPPH• reacts with an antioxidant that can donate hydrogen, the reduced molecular of (DPPH) is form, and the color is change from the violet to yellow. The intensity of the yellow color produced depends on the

amount and existence nature of radical scavenger available in the sample (95).

- **DPPH Solution:**

DPPH solution was prepared freshly by dissolving 0.0053gm of DPPH radical in 100 mL ethanol.

- **Procedure:**

Free radical scavenging of AgNPs and the extract was estimated using DPPH assay (96).

1. A serial of dilutions of each AgNPs, *D. viscosa* extract, and ascorbic acid (ascorbic acid was used as a positive control) were prepared (100, 50, 25, 20, and 15 µg/mL) respectively.
2. An equal volume (1mL) of DPPH (0.135 mM in ethanol) and AgNPs or *D. viscosa* extract was mixed.
3. The mixture was vortexed vigorously and then left in the dark place at room temperature for 30 minutes.
4. The control was prepared as above without adding an extract or AgNPs.
5. The absorbance of the samples and that of control were estimated at 517 nm.

- **Calculation**

The ability of *Dodonaea* extract and Ag NPs to scavenge the DPPH radical was calculated as a percentage of inhibition.

% Inhibition= [(Abs. control –Abs. sample) / Abs. control)] x 100

Where Abs. is the absorbance

2-2-11-1-2 Total Antioxidant Assay

- **Principle**

The total antioxidant capacity test of the AgNPs and *D. viscosa* leaves extract was evaluated by the phosphomolybdenum assay as

described by the method of Prieto *et al* (97). The analysis is based on the ability of a sample to donate electrons and, reduction of Mo (VI) to Mo (V) as a consequence, the formation of a green phosphate/Mo (V) complex with a peak absorption at 695 nm.

- **Solutions**

- **Reagent solution**

The reagent solution (0.6 M sulfuric acid, 28 mM sodium phosphate, 4 mM ammonium molybdate) was prepared by mixing 3.2 mL of concentrated sulfuric acid (18.4 M), 0.0397 gm of anhydrous sodium phosphate, and 0.465 gm of ammonium heptamolybdat, all these materials were dissolved in 100 mL of deionized water.

- **Procedure [98]:**

1. A 0.3 mL of each diluted extract and synthesized AgNPs at concentration (100, 50, 25, 20, and 15 µg/mL) respectively was mixed with 3 mL of the reagent solution.
2. The tubes were covered and incubated at 95°C for 90 minutes.
3. The mixture was cooled.
4. The absorbance of solution was measured at 695 nm.
5. Control was prepared as above except adding AgNPs or extract.

- **Calculation**

The antioxidant activity was calculated a percentage (%) as the following equation:

%Total antioxidant = [(Abs. control –Abs. sample) / Abs. control)] x 100

Where Abs. is the absorbance.

2-2-11-1-3 Reducing power assay

- **Principle**

The potassium ferricyanide reducing power was determined as the method described by Félix-Silva et al. (99). In this method an absorbance increase can be correlated to the reducing ability of antioxidants. The compounds with antioxidant capacity react with potassium ferricyanide, to form potassium ferrocyanide. The latter reacts with ferric trichloride, producing a color complex of ferric ferrocyanide, which is measured with a maximum absorbance at 700 nm.

- **Solutions**

- Phosphate buffer (pH 6.6) was prepared by dissolving 34.83 gm of K_2HPO_4 and 2.7 gm of KH_2PO_4 in 1L of deionize water.
- Potassium ferricyanide K_3 $Fe(CN)_6$(1%w/v) was prepared by dissolving 1 gm of it in 100 mL deionize water.
- Trichloroacetic acid (TCA) solution (10%) it was prepared by dissolving 10 gm in100 mL deionize water.
- Ferric chloride ($FeCl_3$) (0.1%, w/v)) was prepared by dissolving 0.1 gm in 100 mL deionize water.

- **Procedure:**

1. A one mL of AgNPs or *Dodonaea* extract at various concentrations (100, 50, 25, 20, and 15 μg/mL) respectively, was mixed with an equal volume of (0.2 M of phosphate buffer, pH 6.6), and $K_3Fe(CN)_6$ (1% w/v).
2. The mixture was incubated for 20 minutes at 50^{o}C.
3. Tri-chloroacetic acid (TCA) solution (1mL) was added to stop the reaction.
4. The mixture was centrifuged at 7500 xg for 20 minutes.

5. The supernatant solution (1.5 mL) was mixed with the 1.5 mL distilled water and 0.1 mL of ferric chloride solution (0.1%, w/v), and then left for 10 minutes.
6. The absorbance was measured at 700 nm. When the absorbance of the reaction mixture increased, this indicated that the reducing power of the extract or AgNPs increased.

2-2-11-2 Antitumor Assay

To measure the activity of the AgNPs as anti-tumor agent, *in vitro* study was evaluated against both lung cancer cell line adenocarcinoma human cells (A549), which were obtained from human alveolar cell carcinoma and ovarian cancer cell line (SK-OV-3), which were obtained from Homo sapiens, human, ovary: ascites and compared with normal liver cells WRL68. The cell viability was determined using tetrazolium dye(3-(4,5-Dimethyl-2-thia-zolyl)-2,5-diphenyl-2H-tetrazolium bromide) (MTT assay), which is a colorimetric assay for measuring cell metabolic activity and depend on the reduction of the tetrazolium salt by actively growing cells actively to form formazan, which is a purple water-insoluble product (100).

- **Media**
- **Roswell Park Memorial Institute – 1640 Medium (RPMI):**

A ready to use package (100 mL) RPMI was used throughout this study. The medium was already supplied with 4-(2-hydroxyethyl)-1-piperazineethane sulfonic acid (HEPES) and L-glutamine as illustrated by manufacturer.

The medium was completed by adding the following ingredients:

Penicillin G 10^3 IU

Streptomycin 0.001 g

Sodium Bicarbonate 1%

Fetal Bovine Serum 10 %

- **Serum Free Medium**

Serum free medium is RPMI-1460 excluded from fetal calf serum.

- **MTT Cytotoxicity Assay**

- **Principle**

MTT 3-(4,5-dimethylthiazol-2yl) 2,5diphenyl tetrazolium bromide method is colorimetric assay for assessing cell metabolic activity. This method based on the conversion of the soluble tetrazolium, a yellow salt, into purple insoluble formazan, the reaction and produce purple color which indicate to the cell viability and depth of color reflect the number of cell viability in the culture (100).

- **Kit Contents**

1. MTT solution 3-(4,5-dimethylthiazol-2yl) 2,5diphenyl tetrazolium bromide (MW=414) 1mL x 10 vials.
2. Solubilization solution 50 mL x 2 bottle.

- **Procedure [101]:**

1. Tumor cells ($1x10^4$ cells per well) have been grown in 96 micro-liter plates flat well, with a final volume of 200 µL. The type of medium fresh complete Roswell Park Memorial Institute – 1640 Medium (RPMI) from 15 to 20 mL was added and then pipetting was used to disperse cells from the wedding surface into growth medium.
2. Using sterilized parafilm to seal the microplate and it was gently held. Plates flat wells were incubated for 24 hours at 37°C in 5% CO_2.
3. The medium was extracted, and serial dilutions of the appropriate for both AgNPs and extract of *D. viscosa* (100, 50, 25, 20, 15 µg /mL)

respectively were prepared in the mixture (ethanol-deionized water) (1:1 v/v), and then were applied into the wells.

4. For each concentration, triplicates and positive controls (cells treated with the serum-free medium and water) and negative control (cells treated with the serum free medium) were used.
5. The plates were incubated at 37 °C in 5% CO_2 for a selected exposure time of 24 hours.
6. A 10 µL of MTT solution were added to each well. Plates were further incubated in 5% CO_2, for 3-4 hours at 37°C.
7. A 100 µL of Dimethyl sulfoxide (DMSO) was added as solubilization solution to each well for 30 minutes to each well to remove the medium and produce purple color which indicates cell viability.
8. The absorbance of the formazan product which formed by viable cells (purple color) was read using a microplate reader (Bio-Rad (Germany)) at wavelength of 575 nm.

- **Calculation**

The experiment was conducted in triplicate and (IC_{50}) value which expresses half of the inhibitory concentration that kill 50% of the cell population. The percentage of cell viability was calculated using the following formula and expressed as IC_{50} utilizing non-linear regression with graph pad prism statistical program (Version 8).

Viability (%) = OD value of treated cells/ OD value of untreated cells (control) ×100%

Where OD. is the optical density

2-2-11-3 Anti-bacterial Assay

The antibacterial activity of synthesized AgNPs and *D. viscosa* was assessed against Gram-negative bacteria (*E. coli* and *Pseudomonas*

aeruginosa) and Gram-positive bacteria (*Staphylococcus aureus* and *Streptococcus pneumonia*) using the agar well diffusion method (102).

- **Procedure**

1. Mueller-Hinton agar plates were inoculated with tested (10^5-10^6 CFU/mL).
2. Agar wells of 10 mm diameter were made using crok borer.
3. The wells were cultured three times by rotating the plate 60° between streaking, 1-2 cup, 10 mm in diameter were made in each Muller Hinton agar plates.
4. Serial dilution for both extract and AgNPs were prepared at various concentrations (100, 50, 25, 20, and 15 μg/mL), and (5000, 10000, 15000, 20000, and 25000 μg/mL).
5. All wells were filled with (100 μL) of each test sample (AgNPs and *D. viscosa* extract).
6. The plates were incubated at 37 °C for 24 hours.
7. The inhibition zone diameter of each sample was measured in millimeters.

2-2-12 Clinical Application

2-2-12-1 Measurement of Coagulation Factors APTT and PT

2-2-12-1-1 Collection of Blood Specimens

Blood was collected from twenty apparently healthy volunteers (n=20) who were volunteers for this study. Their ages ranged from 18 to 40 years old who were free from any medication for at least two weeks. In addition, we make sure that all of our control group didn't take anticoagulants, antiplatelet, antibiotics drugs, herbal drugs, vitamin or mineral supplements for at least two weeks before blood donation. Two mL of peripheral blood sample was collected by venepuncture in 3.2% sodium citrate tubes.

2-2-12-1-2 Preparation of Samples

The human plasma was obtained from the supernatants of blood after centrifugation at 3000 xg for 10 minutes. The obtained plasma was mixed with different concentration of *D. viscosa* aqueous extract or AgNPs (100, 50, 25, 20 and 15 µg/mL) respectively with the ratio of 1:1 (plasma AgNPs) or (plasma: extract). The mixture was incubated at 37ºC for 2 minutes, this mixture will be used for APTT and PT tests. Plasma alone was as positive control (99).

2-2-12-1-3 Activated Partial Thromboplastin Time (APTT)

APTT Kaolin kit and 0.025 M calcium chloride were used for professional, *in vitro* measurement APTT.

- **Principle**

BIO-CK reagent involves recalcification of plasma in the presence of standardized amount of cephalin (platelet substitute) and a factor XII activator (Kaolin). The use of Kaolin minimizes reading time and optimizes the optical detection.

- **Reagents**

Reagent 1 Vial R1: Cephalin (Rabbit cerebral tissues) Kaolin.

It was prepared by dissolving the contents of one vial of reagent 1 (R1) by added promptly the amount of deionized water (4 mL). The reagent was mixed gently until completely dissolve and left approximately 2 minutes before use. The reagent was stored at (2-8 ºC).

Reagent 2 Vial R2 (Calcium Chloride 0.025 M) It was ready for use.

- **Procedure** [80]

Bio-CK APTT Kaolin 2 kit was used in estimated of APTT

1. A 100 µL of homogenised Bio-CK APTT Kaolin (R1) was added into the 100 µL of human plasma.

2. The mixture in the step above (R1 and human plasma) was incubated at 37 ºC exactly for 3 minutes.
3. Clotting was initiated with the addition of 100 µL 0.025 M aqueous $CaCl_2$ solution (pre-warmed at 37°C).
4. The clotting time was recorded in seconds using the timer.
5. The procedure was repeated with the samples that were prepared as (2.2.14.1.2) at different concentration (100, 50, 25, 20, and 15 µg/mL).

2-2-12-1-4 Prothrombin Time (PT)

BIO-TP Prothrombin Time (PT) BIOLABO kit was used for measurement of prothrombin time.

- **Principle**

The principle of PT test is a universal screening test that measures the efficiency of the extrinsic coagulation system. It contains factors I (fibrinogen), II (prothrombin), V (proaccelerin), VII (proconvertin), and X (Stuart factor). The clotting time is estimated at 37°C in the presence of tissular thromboplastin and calcium (103). The Prothrombin Time is a one-stage test based upon the time required for a fibrin clot to form after the addition of Tissue Factor (TF - historically known as tissue thromboplastin) to platelet poor plasma.

- **Reagents**

Reagent 1: (Vial R1) Thromboplastin. Freeze-dried Thromboplastin (Rabbit cerebral tissue)

Reagent 2: (Vial R2) aqueous solvent (Reconstitution Buffer)

- **Preparation of working reagent**

Working reagent was prepared by adding promptly to the contents of the (vial R1) to the reconstitution buffer (vial R2). It was mixed gently

until complete dissolution. Working reagent (R1+R2) is stable for 8 hours at room temperature.

- **Procedure** [104]

1. A 100 µL of human plasma was incubated at 37 ºC in water bath for 2 minutes.
2. A 200 µL of the working reagent was added to 100 µL of citrated plasma (pre-warmed at 37°C) in the step above.
3. The clotting time in second was recorded starting from the plasma-reagent mixing to clot formation using the timer.
4. The procedure was repeated with the samples that were prepared as (2.2.14.1.2) at different concentration (100, 50, 25, 20, and 15µg/mL).

2-2-12-2 Hemolysis Assay

Five healthy donors were subjected to this study, their ages ranging from 18 to 40 years old. Blood was collected by venipuncture into test tubes containing ethylenediaminetetraacetic acid (EDTA). This method is described by Flaih and Al-Saadi (105).

- **Principle**

In vitro hemolysis assay evaluates hemoglobin release in the plasma (as an indicator of red blood cell lysis) following test agent exposure. Spectrophotometric method reported for hemolytic activity was followed after exposure to various concentrations of AgNPs (106).

- **Procedure** [107]

1. The AgNPs solution (15 µL) at concentration (100, 50, 25, 20, and 15 µg/ml) respectively, was added into 0.1 mL of blood sample and then, mixed well for 5 seconds
2. A 10 mL of normal saline was added to prevent excessive hemolysis.
3. The mixture was centrifuged at 3000 xg for 10 minutes.

4. At 540 nm, the absorbance of mixture was measured
5. Complete hemolysis (100%) was achieved by diluting blood with 100 fold of distilled water.
6. Triton X-100 was used as positive control and normal saline as negative control.

- **Calculation**

After measuring the absorbance, the percentage of hemolysis was calculated by following equation:

% Hemolysis= (AT-AS) /(A 100%-AS) × 100%

AT: Absorbance of test solution.

AS: Absorbance of normal saline.

A 100%: Absorbance of 100% hemolysis (Triton X-100).

2-2-13 Statistical Analysis

All data obtained from the MTT method were expressed as the mean± standard deviation of three independent experiments. Statistical significance was implemented utilizing Graph Pad Prism version 8 (Graph Pad Software Inc., La Jolla, CA). The value was measured from a dose response-inhibition curve (log concentration vs. absorbance) utilizing non-linear regression with graph pad prism statistical program. While the results of (APTT and PT) were statistically analyzed using Statistical Package for the Social Sciences (SPSS) version 24. t-test and One-Way Variance of Analysis (ANOVA) were used. The p-Value at $\leq$ 0.05 considered statistically significant.

Chapter Three
Results
and
Discussion

3. Results

3-1 Qualitative Phytochemical Analysis of *Dodonaea viscosa* Leaves Extract

The aqueous leaves extract of *D. viscosa* was investigated for the presence of phytochemicals important constituents such as alkaloids, coumarins, saponins, flavonoids, resins, sugar, tannins, phenolic compounds, and terpenes (Table 3-1).

Table (3-1): Qualitative phytochemical analysis of *D. viscosa* leaves extract

Phytoconstituents	Reagents	Detection indicator	Results
Alkaloids	Dragendroff's reagent	Orange spots	+
Coumarins	Filter paper saturated with dilute NaOH	Yellow-green	+
Flavonoids	50%ethanol+50% NaOH	Yellow color	+
Phenolic compounds	1% $FeCl_3$	Green color	+
Resins	95% ethanol+ 4% HCl	Turbidity	+
Saponins	Shaking the extract vigorously	Foaming remaining for long time	+
Sugar	Benedect	Red precipitate	+
Tannins	1% lead acetate	White mucilage precipitate	+
Terpenes	Chloroform + glacial acetic acid	Brown color	+
Steroids			–

The plant extracts act as a capping agent and cause metal NPs aggregation in their respective salt solutions. Several researchers have reported the biosynthesis of metal nanoparticles by plant leaves extracts (26); (45). These plant reductants are phytochemicals, including flavonoids, phenol derivatives, terpenoids, and some plant enzymes such as hydrogenases, reductases, and their derivatives (108).

The presence of phytochemicals in different parts of the plants participate in coating produced nanoparticles. So, the plant phytochemicals adhering on the surface of plant-mediated nanoparticles can lead to the synergistic effects and enhance the antimicrobial and anticancer activities of nanoparticles. The significant numbers of plant phytochemicals accumulate in their leaves. So, the majority of research works based on plant-mediated AgNPs synthesizes, have been carried out by using plant leaves extract. Due to complex or even undefined composition of phytochemicals in plant extracts, it is difficult to predict the exact mechanism of plant extract mediated nanoparticles synthesis (12); (109).

Seyed Mohammad Amini in (2019) described the relationship of surface chemistry to biogenic NPs as a major factor that not only determined the several applications of the NPs but also is very important for the stability of synthesized NPs. Where phenolic compound coated metal NPs represent more stability in comparison with NPs that have been synthesized by other chemical reductants such as citrate or sodium borohydride. Various mechanisms were described in the biological synthesis of metal NPs, especially of AgNPs, by a diverse group of plants where the reducing agents were adsorbed on the surface of the particles. The adsorption affinity on the surfaces NPs may be variable for various crystalline orientations (110).

Another mechanism exhibited the synthesis of NPs, the addition of metal salts to the plant extract at optimized conditions, the metal ions

rapidly bind to the functional groups of (-COOH, and -OH) protein molecules available in the solution of the plant extract and are entrapped. This process leads to conformational changes in proteins and exposes its hydrophobic residues to aqueous phases. This causes the introductions of reducing agents from plant extracts and favors the transformations of entrapped metal into metal NPs (111).

A previous study reported that *D. viscosa* is a good source of phenolic compounds, flavonoids, alkaloids, tannins, and sugar. These phytochemicals compounds and vitamins have significant roles in reductant, capping, and stabilizing the nanoparticles. Probably, the flavonoids present in *D. viscosa* leaves can perform the reductant of metals salts, and the tannins and saponins may act as the capping agents. As flavonoids have various functional groups, which are capable of reductant metal ions to NPs (112). Generally, various phytochemicals present in the plant extracts could play a key role in the conversion of the ionic form of silver Ag^{+} into the metallic nano-form Ag^{0}.

3-2 GC-Mass Spectroscopy

In this study GC-MS was utilized to identify the different biological components of *D. viscosa* leaves extract. The chromatogram of the analysis showed six peaks of most constituents (Figure 3-1). Most of these included 1, 3, 6-octatriene, Estragol, pentadecane, hexadecane, 9, 12-octadecadienoic acid, and octadecanoic acid (Table 3-1). The heights of different peaks show the relative concentration of the compounds present in the aqueous extract of *D. viscosa* leaves.

The GC-MS analysis of plant extract results in identification several phytochemicals, which have pharmacologically and industrially potential like antioxidants, phyto-steroids and number of unsaturated fatty acids. The GC-mass analysis displayed the existence of phytochemical components in

D. viscosa leaves extract. As of these compounds have biological activity (113).

Identifying the biological active compounds of *D. viscosa* leaves extract facilitates the therapeutic application of this plant for various diseases. Anethole is such a substance used from ancient times in traditional medicine. Anethole has potent antioxidant activity, anti-inflammatory and anti-nociceptive activity, and antimicrobial properties, against bacteria, yeast and fungi (114). While estragole is a volatile terpenoid, which occurs naturally as a constituent of the essential oils of many plants. Estragole have many biological and pharmacological activities. Pharmacological actions of estragole, like antioxidant, antimicrobial, anti-inflammatory and anti-edematogenic (115).

The primary compound was 9, 12-octadecadienoic-acid, which is the main fatty acid in the extract. This fatty acid is characterized for several applications in the biomedical field (anti-arthritic, anti-inflammatory, and antioxidant properties and used in the commercial preparation of oleates and lotions and as pharmaceutical solvent). Besides, the presence of octadecanoic acid, exhibits biological activity such as antimicrobial activity (116). These molecules clearly indicate the medicinal roles of *D.viscosa*.

A previous study showed that Octadecanoic acid present in most of plant such as *Aesculus hippocastanum, Cassia Obtusifolia, Jasminum Sambac Linn,* and *Cenchrus setigerus, etc.* Several reports claimed that Octadecanoic acid acted as anti-fungal, anti-tumor, and anti-bacterial (117). A 9,12-Octadecadienoic acid (Z,Z) was found in *Morenga oleifera* leaves extract, and *Pleiospermium alatum , etc*. These fatty acid plays an important biological activities (118).

```
File       : C:\MSDCHEM\1\DATA\ZAINAB.D
Operator   : Jafar1
Acquired   :  8 Jan 2020  13:57     using AcqMethod TUNE
Instrument :   Instrumen
Sample Name: 1
Misc Info  :
Vial Number: 1
```

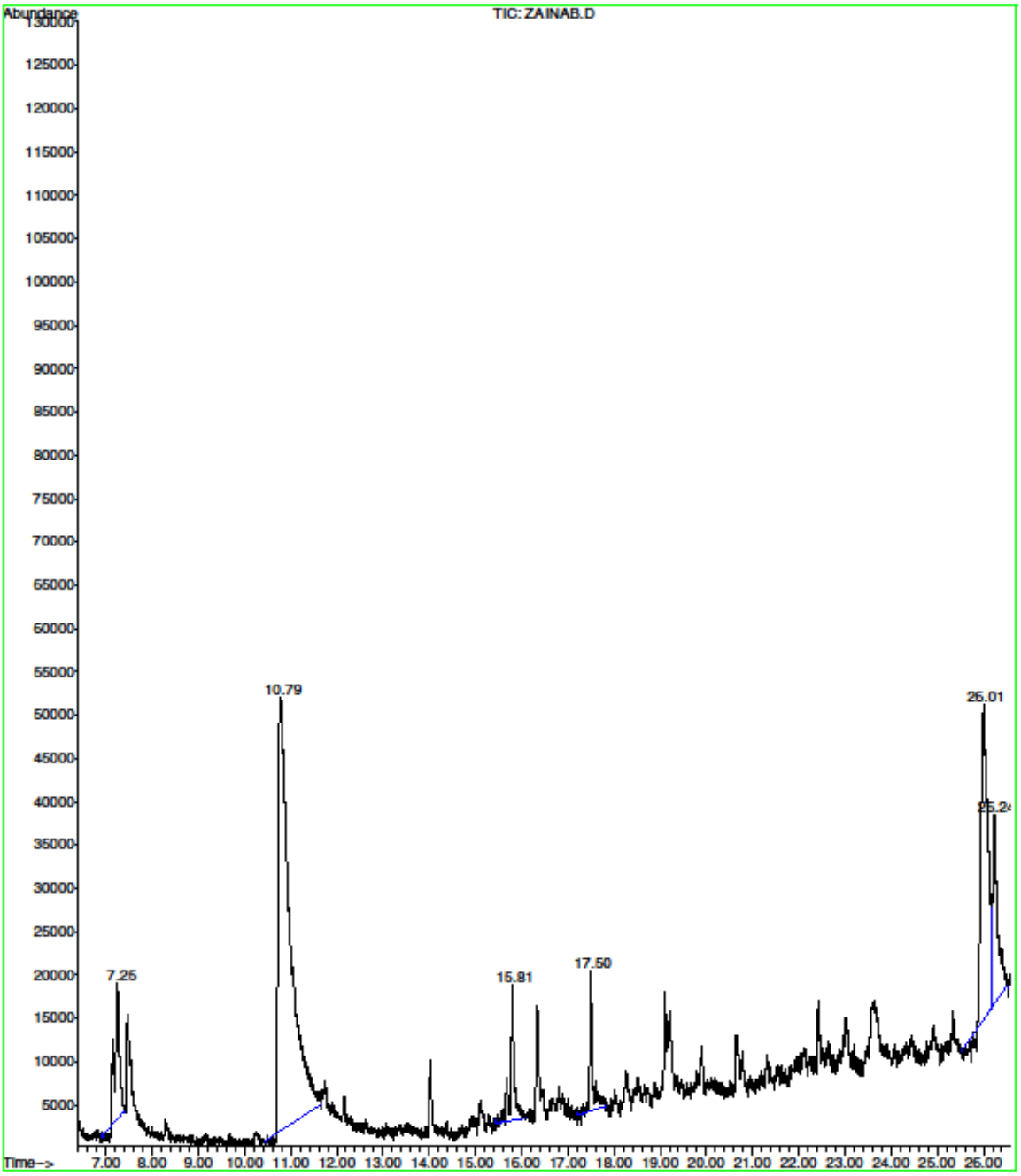

Figure (3-1): GC-mass of *D. viscosa* leaves extract.

Table (3-2): GC-mass analysis of *D. viscosa* leaves extract.

Peak	R. Time	Area %	Name
1	7.25	6.20	Trans -.beta.-Ocimene (+)-4-Carene 1, 3, 6-Octatriene, 3, 7-dimethyl
2	10.79	53.01	Estragole Anethole
3	15.80	5.35	Pentadecane
4	17.50	4.16	Hexadecane
5	26.01	12.34	9, 12-Octadecadienoic
6	26.25	9.95	Octadecanoic acid

3-3 Synthesis of Silver Nanoparticles

Aqueous leaves extract of *D. viscosa* was used to synthesize silver nanoparticles (AgNPs). Ag^{+} ions of $AgNO_3$ were reduced to AgNPs. The crude extract of *D. viscosa* is considered a reducing agent for Ag^{+} and stabilizer for AgNPs. The first indication for AgNPs construction was the color change from light yellow to dark brown within 24 hours, indicating the excitation of surface plasmon resonance of AgNPs. The color intensity increased with time (Figure 3-2). The color change indicates the reduction of Ag^{1+} into Ag^{0} (119). Due to nucleation and growth processes, these free silver atoms (Ag^{0}) accumulated to form AgNPs (120). It is the oscillatory movement of electrons existent in the conduction band that causes the surface plasmon resonance (SPR) phenomenon. The color change gradually was followed via measuring UV-visible absorption with time.

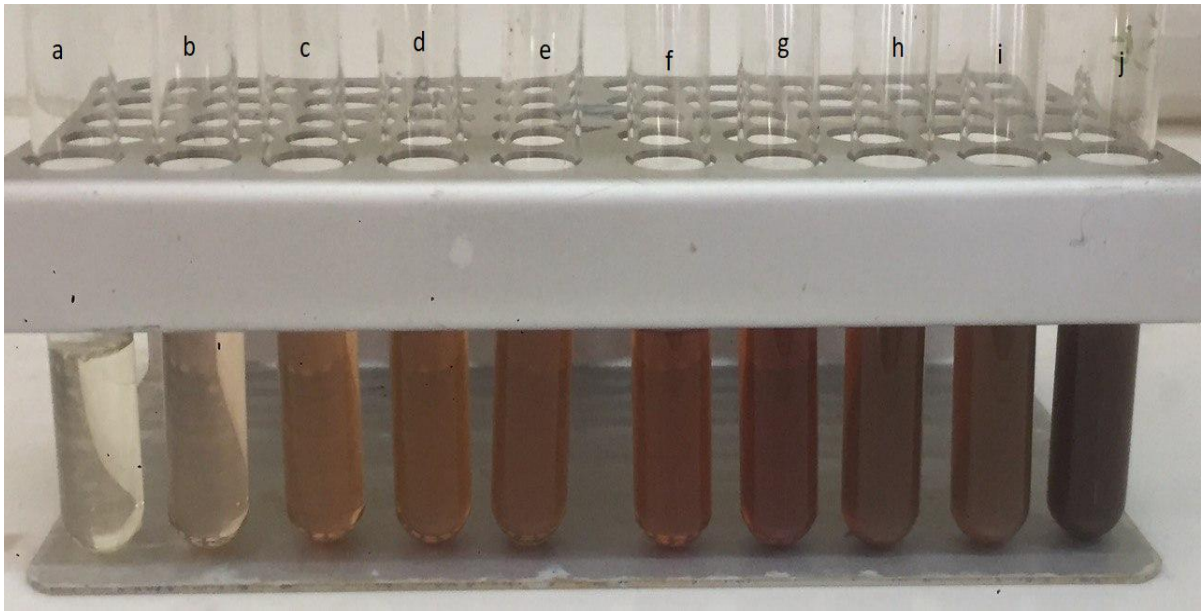

Figure (3-2): Biosynthesis of (AgNPs) showing the color change with time. (a) at zero time (b) after 10 min. (c) after 30 min. (d) after 2 hours (e) after 4 hours (f) after 6 hours (g) after 8 hours (h) after 10 hours (i) after 12 hour (j) after 24 hours.

The formation of AgNPs depends on how long the reducing agents are exposed to metal ions. Therefore, when the incubation period of silver with the reducing agent increase, the synthesis of AgNPs would increase more (121).

The previous study reported that *Lantana camara L.* leaves extract reduced Ag^{1+} ion into AgNPs was followed by color changes in the reaction mixture from yellow to dark brown due to the excitation of surface plasmon resonance (122).

The intensity of absorption peak was increases with increasing time period of mixing plant extract with aqueous solution of $AgNO_3$ (Figure 3-3). This increase in the absorbance intensity was due to growth of silver nanoparticles (5). The mechanism of reduction involved the dissolves silver nitrate (substrate) in water and mixed it with aqueous leaves extract of *D. viscosa*. Probably, the flavonoids in *D. viscosa* leaves act as the reductions of metal ions, whereas saponins and tannins may act as the capping agents.

Moreover, polyhydroxy groups may be responsible for the reduction of Ag^{+} ions into metal NPs (112).

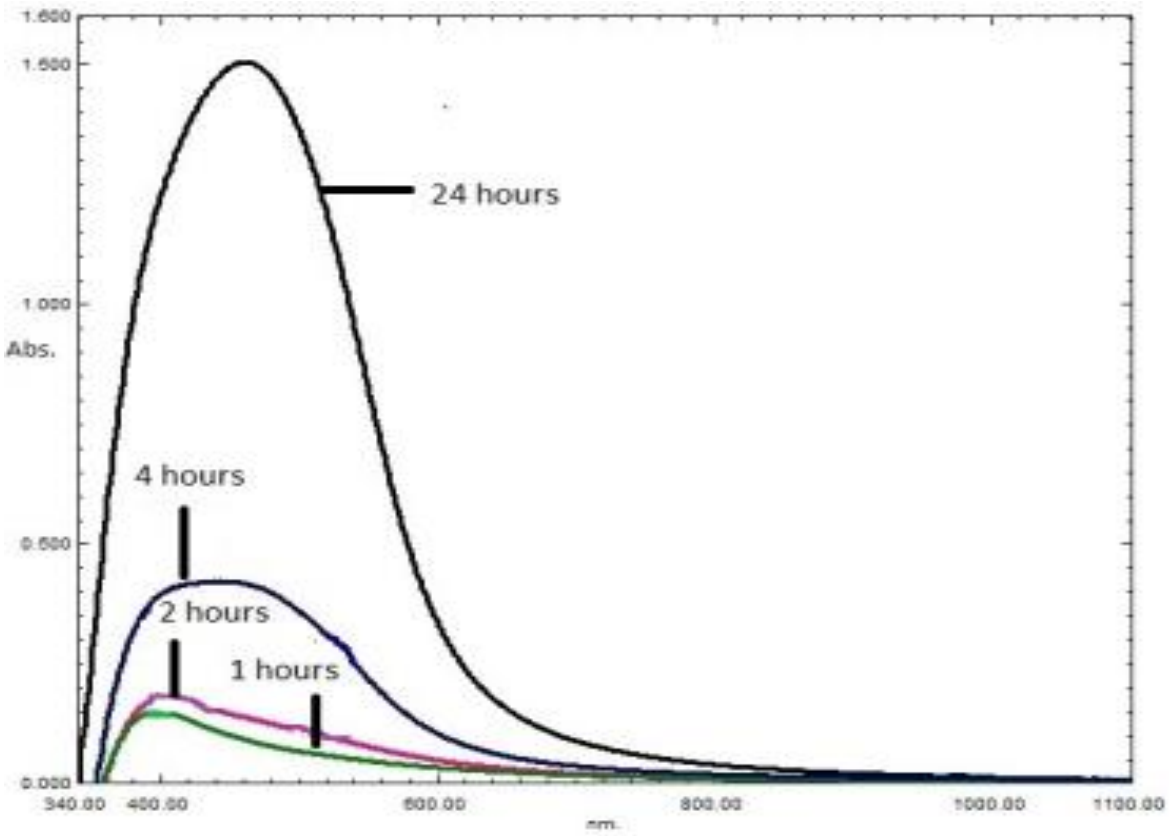

Figure (3-3): UV-visible spectra of AgNPs at different time of incubation

3-4 Characterization of the Synthesized Silver Nanoparticles

3-4-1 UV-Visible Spectroscopy

The synthesized AgNPs from aqueous leaves extract of *D. viscosa* were analyzed using UV-visible spectrophotometer, where Surface Plasmon Resonance (SPR) absorption band at 463 nm after 24 hours of incubation at 45°C (Figure 3-4). The broad, single, and strong absorption peak showed the formation AgNPs in the sample. In order to evaluate the effect of boiling time for the plant aqueous extract of *D. viscosa*, the dry leaves were boiled for 10, 15, and 20 minutes. The UV–vis. absorption spectra of AgNPs were recorded at different time. There was very little

difference in the formation of AgNPs by 15 and 20 min boiling time but 10 min boiling time increased the formation of AgNPs (Figure 3-5).

The effect of amount of plant extract of *D.viscosa* to be added to aqueous solution of silver nitrate for the formation of AgNPs, different volumes of 10 minutes boiled leaves extract (3, 5 and, 7 mL) respectively were added to 45 mL of $AgNO_3$ (1mM) solution. The UV–vis. absorption spectra of AgNPs were recorded at different time. At the wave length 463 nm, the volume 3 mL of *Dodonaea* extract was the best than 5 and 7 mL and the nanoparticles synthesis occurred faster (Figure 3-6). While the effect of temperature on the biosynthesis of AgNPs was studied by performing reactions at different temperatures (25 ^{o}C), and 45^{o}C. The UV–vis absorption spectra of the synthesized AgNPs at different temperatures are illustrated in (Figure 3-7). At relatively low temperature, the intensity of the Surface Plasmon Resonance peak was a little weak and the width of the SPR band was broad, which means few nanoparticles are formed.

Hence, the optimal formation of AgNPs was obtained using 10 minutes boiling time of the leaves extract, 3 mL volume of *D. viscosa* extract. Incubated at 45^{o}C, the absorbance was constant even after 24 hours, indicating the completion of the reaction and the obtained results showed that AgNPs were stable even after 48 hours at room temperature, that is mean that AgNPs prepared are not aggregate (Figure 3-8). All these conditions were selected for synthesizing Ag NPs.

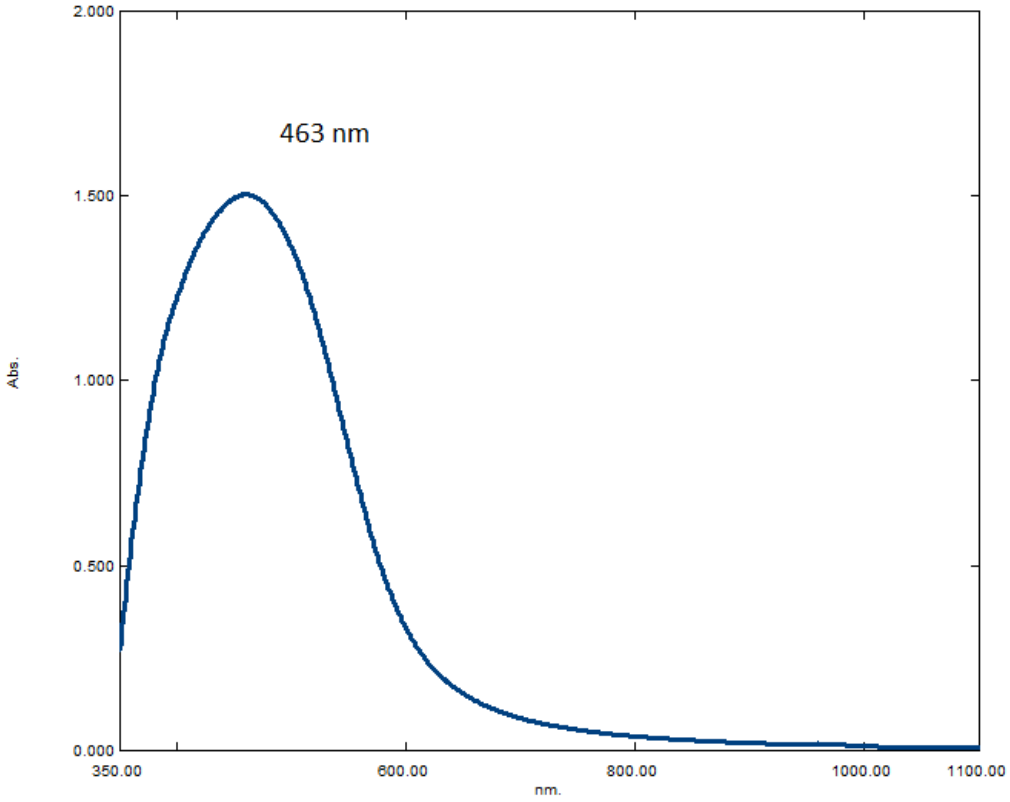

Figure (3-4): UV-Visible spectra of Ag NPs at 463 nm.

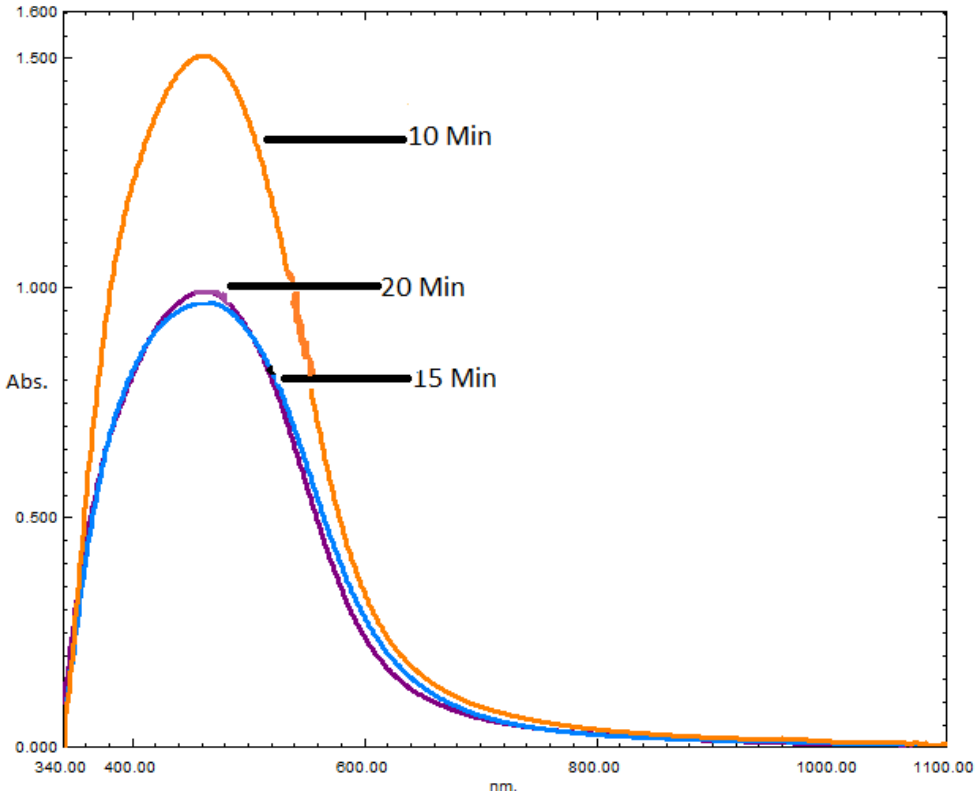

Figure (3-5): UV-Visible spectra for AgNPs at different boiling time of extract.

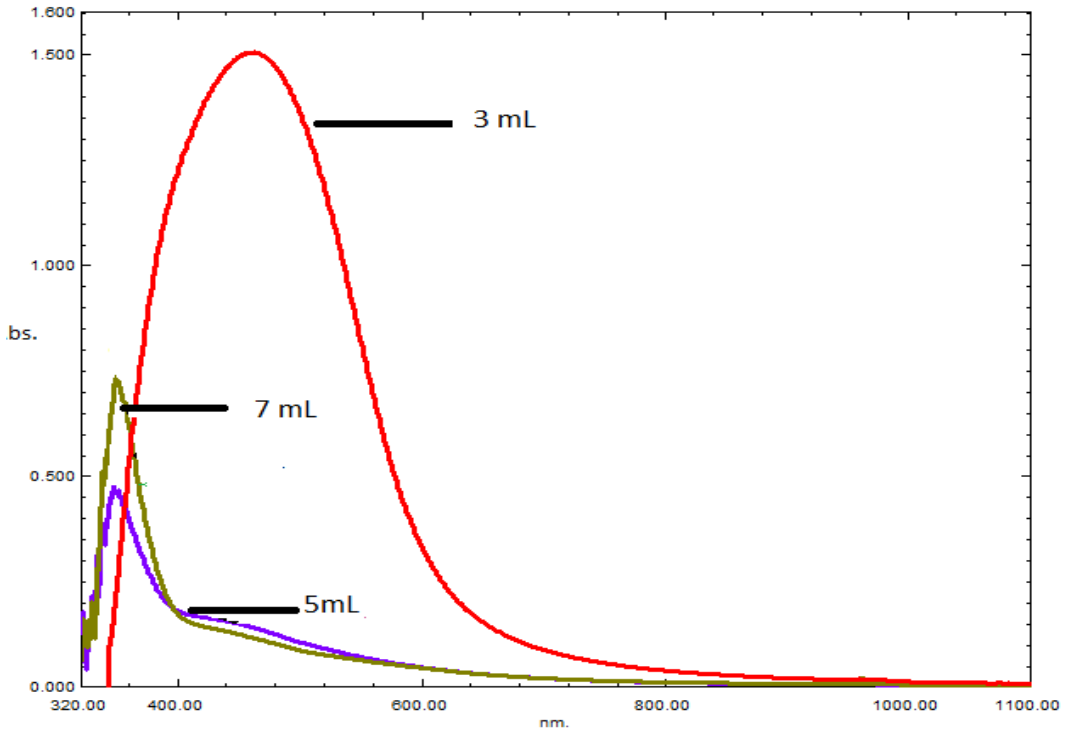

Figure (3-6): UV-Visible spectra for AgNPs at different volumes of extract

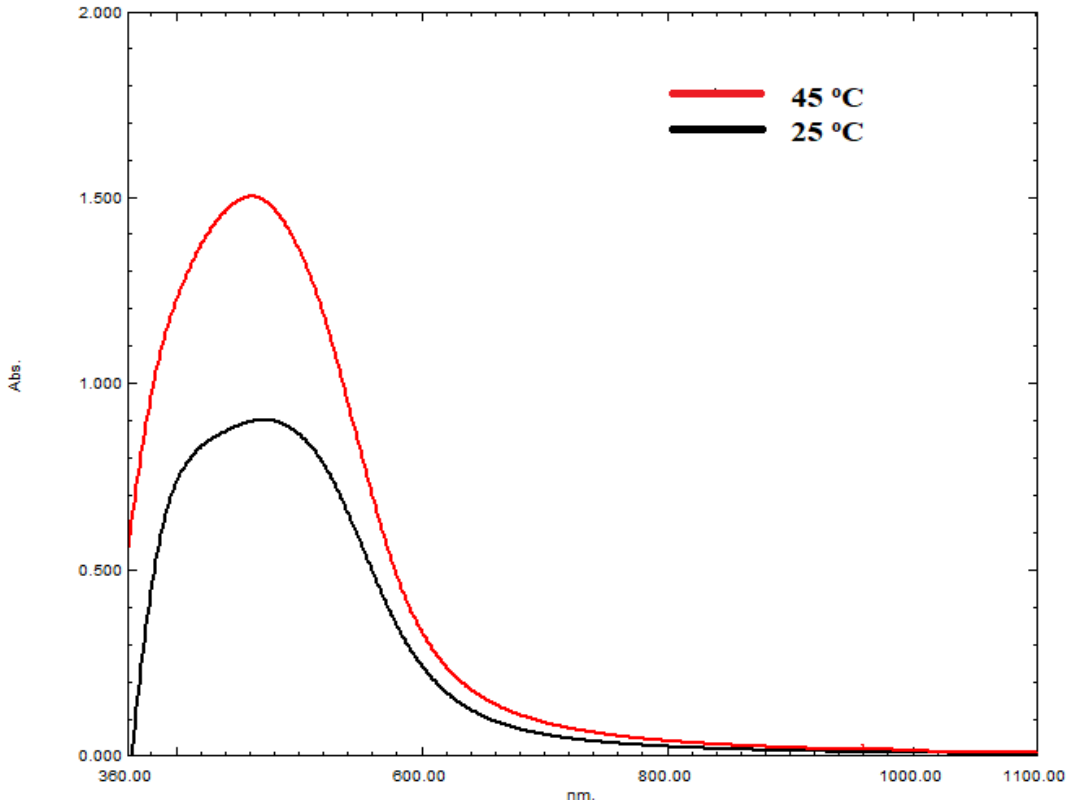

Figure (3-7): UV-Visible spectra of effect temperature on AgNPs synthesis at 25°C, and 45°C.

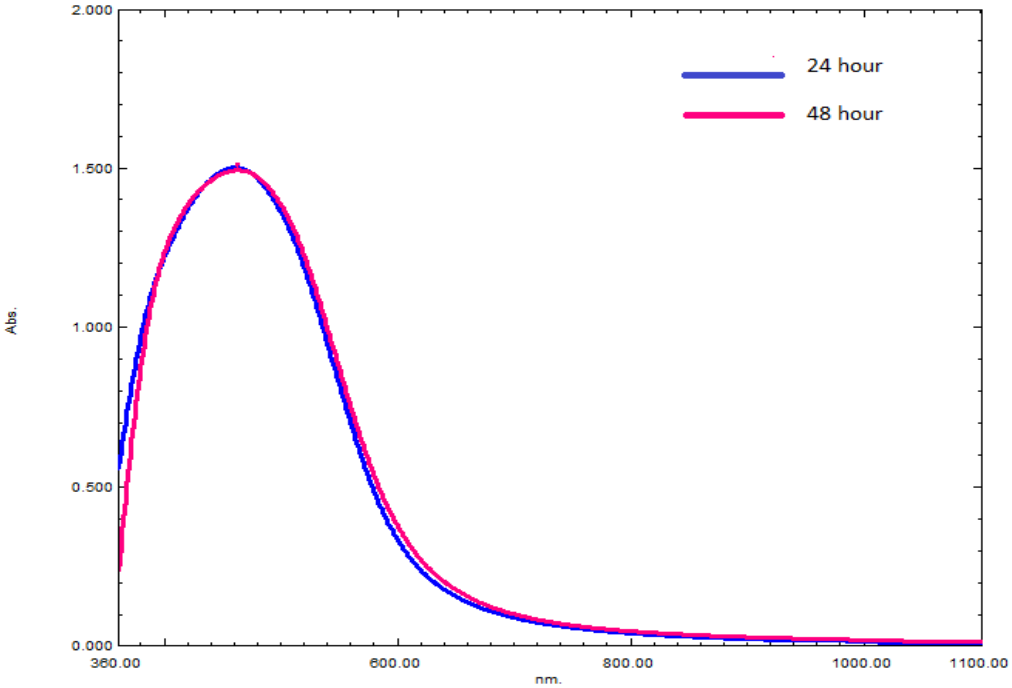

Figure (3-8): UV-Visible spectra of AgNPs with the time

Characterization of Ag nanoparticles is essential to assure the synthesis of AgNPs and know whether the preparation is suitable for a specific application. UV-visible spectroscopy exhibited a clear peak at a wavelength of 463 nm. Similarly, the same the maximum absorbance 463 nm of the synthesized AgNPs from aqueous leaf extract of *Parkia speciose* (123).

Formation and stability of AgNPs by *D. viscosa* extract in an aqueous medium is due to the effect of surface plasmon resonance (SPR) of an electron in the reaction mixture (124). Dependent on the quantum size effects, these (SPR) bands undergo red-shift or blue-shift. The plasmon absorption shifts toward red, when particles size increased. The conduction electrons move collectively in order to examine the turbulent charge distribution known as the plasma localized that is near the surface of metal, when an external electro-magnetic field such as light is applied to a metal occurs what is known as plasma localized near the surface of the metal (125). The broad absorption band is perfect for silver nanoparticles

due to excitation of SPR where the peak shows that the particles are spherical with an extensive range of size distribution (120).

The intensity of Surface Plasmon Resonance increased with the temperature increase. These results reveal that higher temperature is in favor of the formation of AgNPs with higher yields (126). Mostly sharp peak is associated with low temperature-mediated synthesis, which produces uniformly sized AgNPs, while broad peak is associated with higher temperature-mediated synthesis. In sum, the temperature chosen in this study to fabricate AgNPs was 45 °C. A similar result was found in the extract of Oak Fruit Hull *Quercus infectoria* and the optimal temperature for synthesizing AgNPs was at 45°C (127).

3-4-2 Fourier Transform Infrared Spectroscopy (FT-IR)

Identifying the functional groups for both leaves extract (Figure 3-9) and the synthesized AgNPs (Figure 3-10) were carried out using the FT-IR spectrum. The FT-IR spectrum of *D. viscosa* leaves extract showed peaks at 3394.84, 2929.97, 1610.61, 1514.17, 1400.37, 1271.13, 1062.81, 868.00, 650.03 and 542.02 cm^{-1}; while synthesized AgNPs synthesized from *D. viscosa* had spectrum peaks at 3448.84, 2929.97, 1620.26, 1518.03, 1388.79, 1057.03, 873.78 and 692.47 cm^{-1}. The synthesized AgNPs had shifted the absorption peaks from 3394.84 cm^{-1} to 3448.84 cm^{-1} indicating the existence of O-H vibration of alcohol, and phenol with stretching linkage of N-H of primary, secondary, amides, and amine. In addition, a peak of 2929.97 cm^{-1} was observed, which represents the stretching vibrations of methyl groups (C-H) in *D. viscosa* leaves extract and AgNPs.

Other peaks in leaves extract such as 1610.61and 1514.17 cm^{-1} represent the existence of (C=O), and (C=C), respectively. Moreover, the peaks of extract 1400.37and 1271.13 cm^{-1} were shifted to 1388.79 and 1057.03 cm^{-1}, respectively in the synthesized AgNPs.

In addition, the band at 650.03cm^{-1} in the leaves extract shifted to 692.47 cm^{-1} in chart of AgNPs. As observed in both leaves extract, and the synthesized AgNPs a distinct shift of functional groups' peaks. The distinct bands may reveal some organic compounds like protein, phenolic, or glycosides in plant extract that can act as a reducer to Ag^{+} and stabilizer to the AgNPs. Stability of AgNPs can be attributed to existence of these compounds in shell of silver nanoparticles in the aqueous medium (127).

To determine the interaction of NPs and biomolecules, FT-IR analysis was performed to identify the active groups of these molecules. These groups are responsible for the capping, performance, and stabilization of metal nanoparticles (112). FT-IR measurement of *D. viscosa* extract and AgNPs showed several peaks that represent several functional groups such as hydroxyl group (-OH) 3394.83 cm^{-1} and carboxyl group (-C=O) 1610.61 cm^{-1} related to extracting and shifted to 3331.18 cm^{-1} and 1620.26 cm^{-1} respectively. These groups act as reducing and stabilizer agents which and prevent particles agglomeration. The bending and stretching sensations display that biomolecules such as alcoholic groups, polyphenols, carboxylic acid, and proteins are responsible in the reduction Ag^{+} and stabilizing of the AgNPs (128). Supposedly the water soluble compounds of plant extracts such as flavonoids, terpenoids are the adsorbed molecules on the surface of NPs.

Bethu *et al*. study using FT-IR analysis showed that flavonoids and phytochemical compounds of the plant extracts act as reducing and stabilizing agent through the biosynthesis of NPs (101). Previous studies have proven that proteins can bind with minerals and metallic nanoparticles through free amine groups or reduce cysteine in the proteins (129). Many other researchers found similar FT-IR spectra of AgNPs using *Cassia obtusifolia* and *Cassia roxburghii* leaves extract (105); (57). Similarly, the same phytochemical compounds (flavonoids, phenolic, triterpenoids,

proteins or organic acid, and polysaccharides) and the active groups (O-H, C-H, C=O, and C=C) that are present in plant extract of *Fumaria officinalis L.* have been reported to be capable of acting as the important roles of reducing and capping agents in the synthesis of AgNPs (130) .

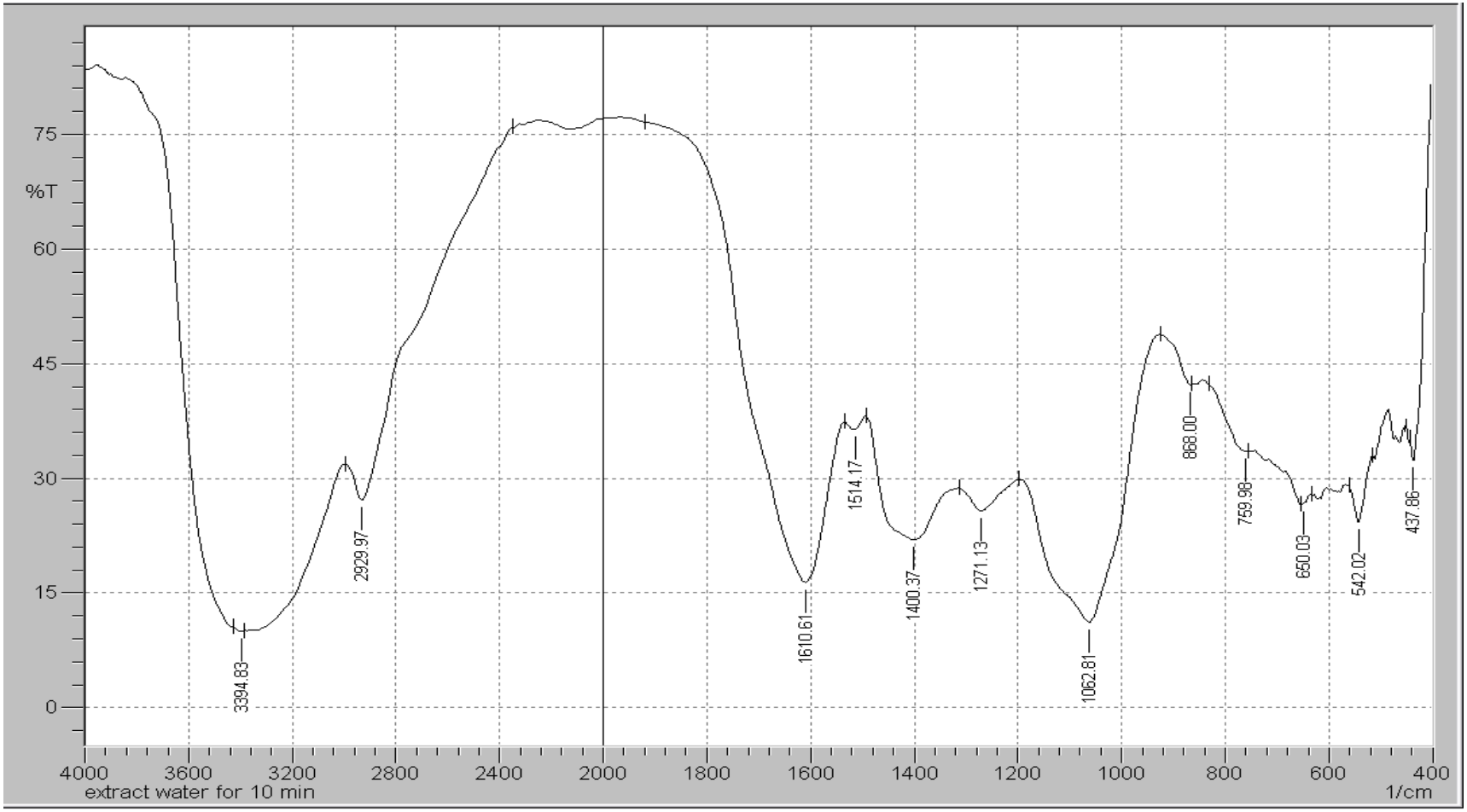

Figure (3-9): FT-IR spectrum of *Dodonaea* leaves extract

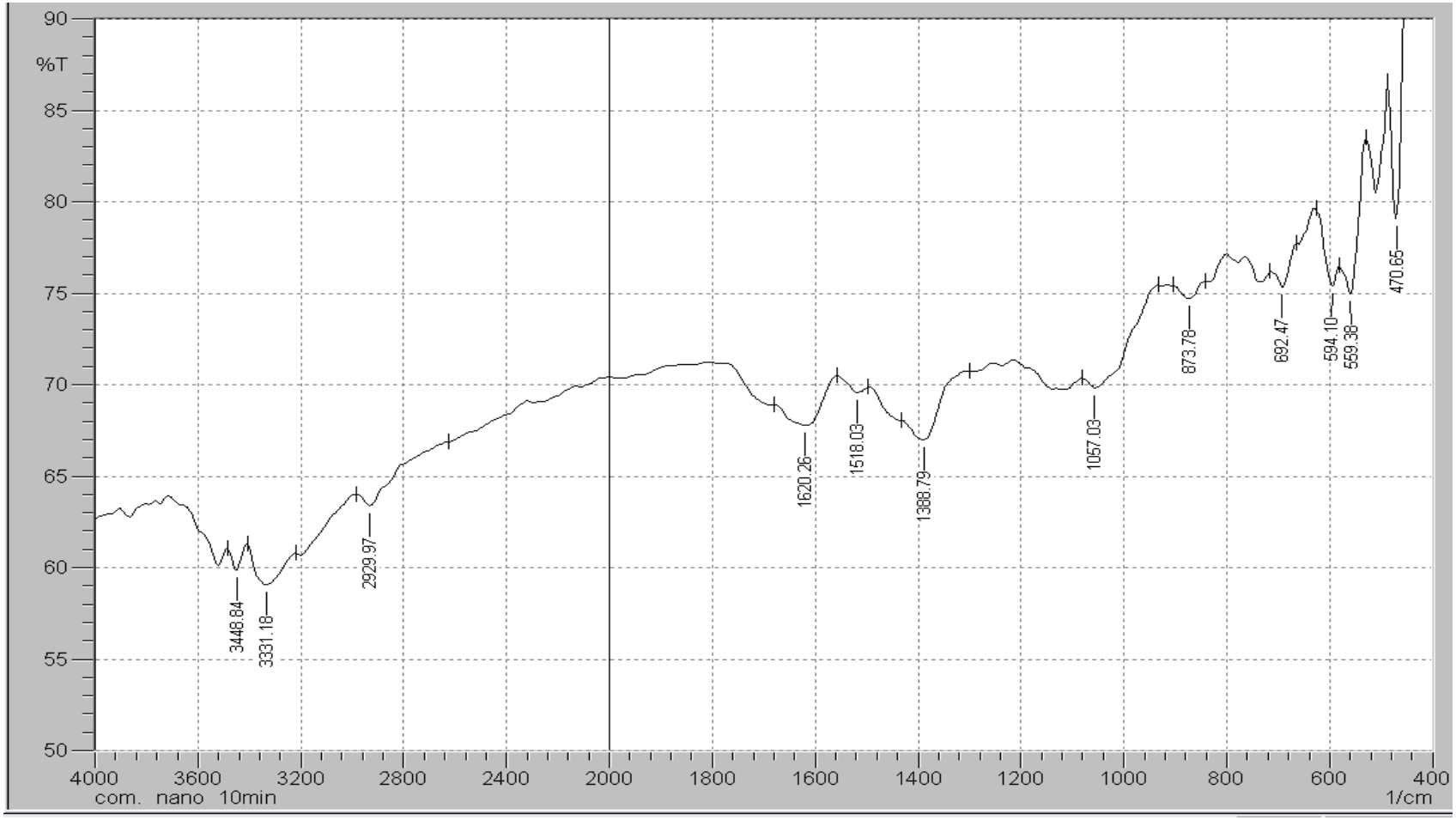

Figure (3-10): FT-IR spectrum of synthesized AgNPs.

3-4-3 X-Ray Diffraction (XRD)

The crystalline nature of the AgNPs and the poly-crystals' lattice parameters were verified using X-ray diffraction analysis. The X-ray diffraction analysis revealed five featured peaks at 2θ values of 38.1874°, 46.2491°, 54.8851°, 57.5409°, and 76.8313° were indexed to Bragg reflections (111), (200), (220) and (311) planes of silver (Figure 3-11). The extra peaks near to 54.8851°, and 57.5409° are due to the presence of biomolecules on the surface of particles (131). The diffraction peaks and Miller indices (*h k l*) to each peak are assigned in (Figure 3-11). Values of these angles were comparing with those 2θ of AgNPs standard sample (JCPDS PDF card 87-0718), which confirmed the Face Centered Cubic (FCC) structure of the formed AgNPs by aqueous extract *D. viscosa* and indicated that the particles were crystalline. The crystallographic planes of each angle value were also demonstrated and compared with the standard data file of AgNPs. The average crystal size of AgNPs was estimated to be 37.665 nm. The intensity of 100% was observed at 2θ with 46.2491°.

XRD results illustrate the crystalline structure and purity of the produced NPs. The Brag reflection at 38.1874°, 46.2491°, 54.8851°, 57.5409°, and 76.8313° at 2θ values confirmed the crystalize structure of silver nanoparticles. Bragg's law is a principle for the action of X-ray diffraction (132). Generally, X-ray diffraction is based on X-ray elastic wide-angle scattering. Using the Debye Scherrer equation, the average crystallite size was determined, where full width at half maximum (FWHM) data was used (122). When X-ray passing through a crystal of particle was produced a diffraction pattern, that diffraction provides the information about the atomic arrangement within the crystals (1). Other peaks in the diffraction can be detected because of $AgNO_3$ as, not all $AgNO_3$ reduced and remained in the sample in a precise quantity.

Table (3-3) shows a comparison of our XRD spectrum with standard value of the theoretical values of standard X-ray diffraction powder patterns (JCPDS PDF card 87-0718).

The obtained XRD results were similar with previous study which showed synthesis of AgNPs *by Ricinus communis* var. *carmencita* leaves extract (7).

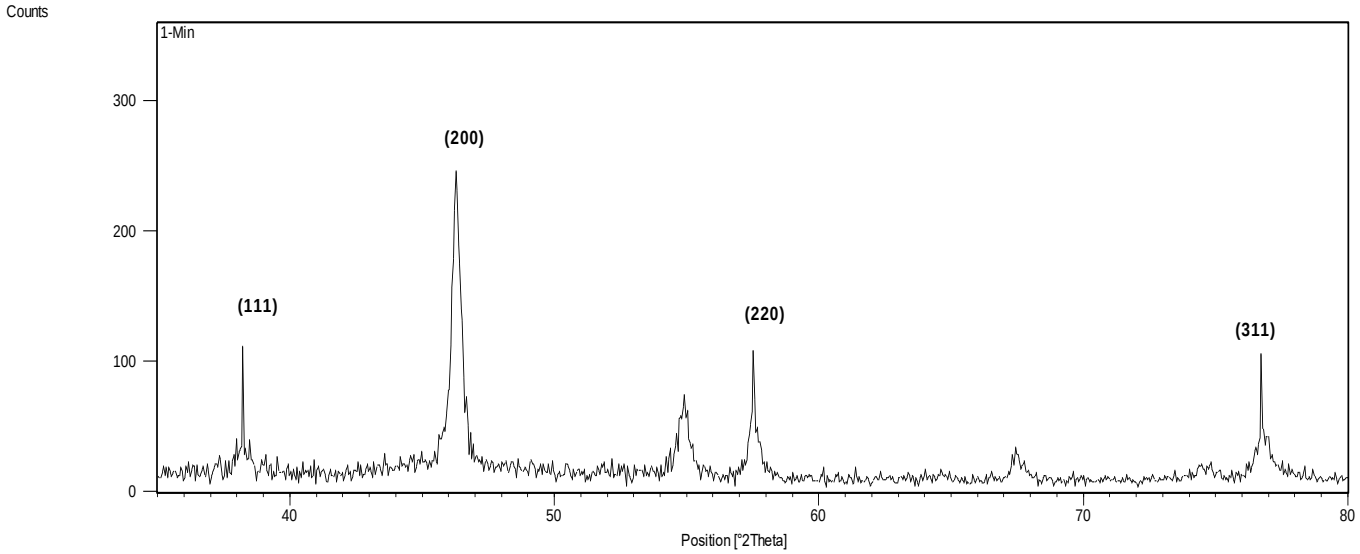

Figure (3-11): X-Ray diffraction (XRD) of synthesized AgNPs from *D. viscosa* leaves extract.

Table (3-3): The result of the XRD for synthesized and standard AgNPs.

Pos. [°2Th.]	FWHM [°2Th.]	d hkl Exp (A°)	d hkl Std. (A°)	Hkl
38.1874	0.5904	2.35678	2.3723	111
46.4491	0.2460	1.96301	2.0545	200
54.8851	0.3936	1.67283	1.6730	202
57.5409	0.3936	1.60187	1.6016	220
76.8314	0.6000	1.23969	1.2389	311

hkl: Miller indices
d hkl Std.: is the distance between parallel planes of atoms for standard
d hkl Exp. is the distance between parallel planes of atoms for experiment

3-4-4 Atomic Force Microscopy (AFM)

The AgNPs surface morphology (the topography of the surface and the particles' size) of nanoparticles was determined using the AFM. AFM holds many advantages in measuring dispersion and particles, as this test would not be affected by the surface oxidation and conductivity. AFM can also measure as small particle size as a sub-nanometer in aqueous fluids (4). The measured AgNPs in this study had an average size of 60.22 nm. The two-dimensional and three-dimensional images of the particles, revealed homogenous uniform size and shape of synthesized AgNPs by 3 mL of *D. viscosa* aqueous leaf extract for boiling 10, 15, and 20 minutes (Figure 3-12), (Figure 3-14), and (Figure 3-16)

The typical AFM analysis confirmed the average particle diameter of the synthesized Ag nanoparticles for the leaves extract of boiling for 10 min with the average size of 60.22 nm (Figure 3-13). In addition, the average particle diameter of the synthesized silver nanoparticles for the extract boiling for 15 and 20 min was 57.26, and 42.57 nm. respectively (Figure 3-15), and (Figure 3-17).

The surface properties and the average size of silver nanoparticles prepared in aqueous solution 3 mL of *D. viscosa* aqueous leaf extract boiling for 10, 15, and 20 min and incubated at $45^{o}C$ for 24 hours respectively was indicates in Table (3-4).

The size of Ag nanoparticles is mainly determined by the rate of reaction and involvement of phytochemicals, when $AgNO_3$ is reduced to Ag^0, Ag^0 undergoes nucleation to form AgNPs in the presence of leaves extract. After fractionation, the majority of the phytochemicals might be lost leading to aggregation of AgNPs. If the reacting solution contains more reducing molecules and less phytochemicals, then the size of synthesized AgNPs would be larger. This might be one of the reasons for the synthesis of larger-sized AgNPs by leaves extract, where reducing molecules were

increased but phytochemicals were reduced. Similarly, less reducing species and more capping agents in the leaves extract could be responsible for smaller AgNPs (133).

Previous studies have presented that the synthesis of AgNPs from commercially available plant extracts such as (*Centella asiatica*, *Solanum tricobatum Citrus sinensis*, and *Syzygium cumini)* have different unorganized forms with the particles size 53, 41, 52, and 42 nm respectively (105). In this study, the synthesized AgNPs in aqueous solution (3 mL) of aqueous leaves extract boiling for 10 minutes and incubated at 45^{o}C for 24 hours have an average size of 60.22 nm, much bigger than the previously reported papers (112); (134). In the another study, the average size of AgNPs synthesized from the *Peltophorum pterocarpum* plant extract was in the same average size of the particles in the current study (135).

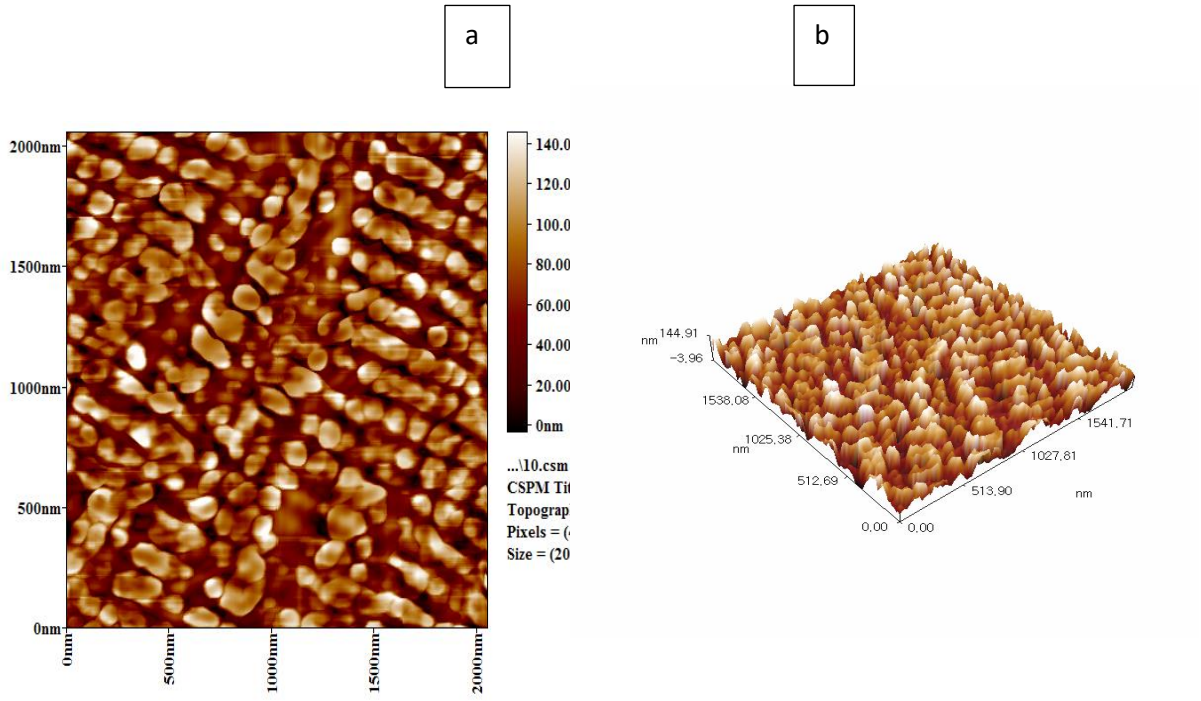

Figure (3-12): AFM assay of AgNPs, synthesized by 3 mL of *D. viscosa* aqueous leaves extract for 10 min. (a) Two dimensional image (b) Three dimensional image.

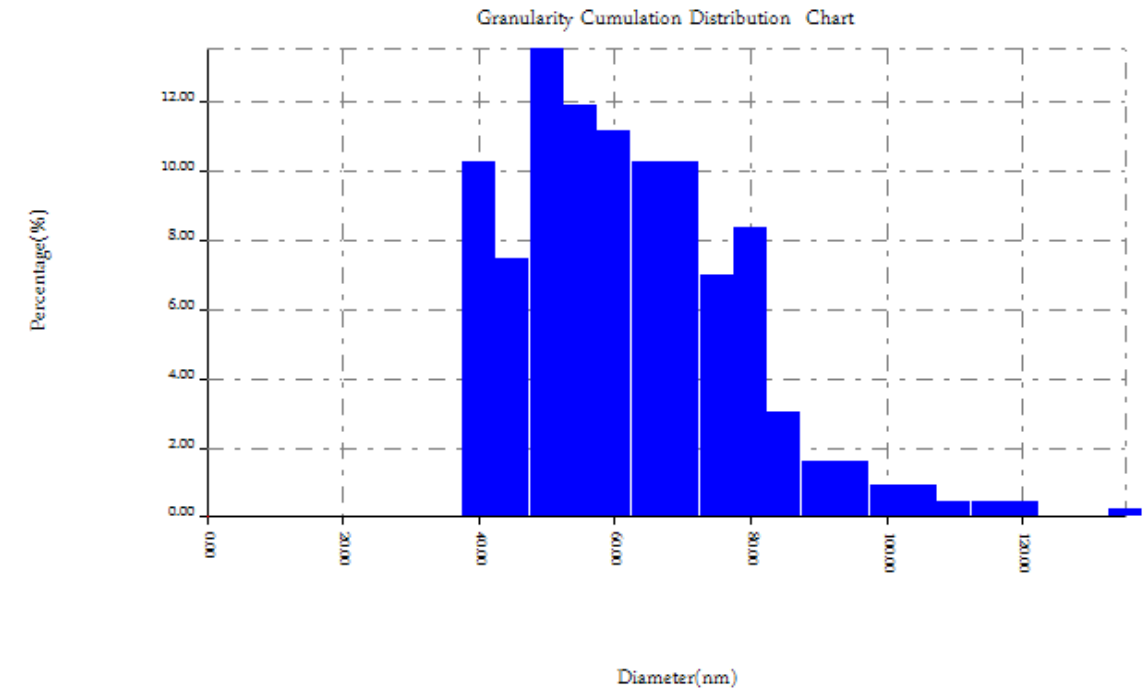

Figure (3-13): Distribution of flow diameter of the silver nanoparticles for 3mL extract and boiling for 10 min.

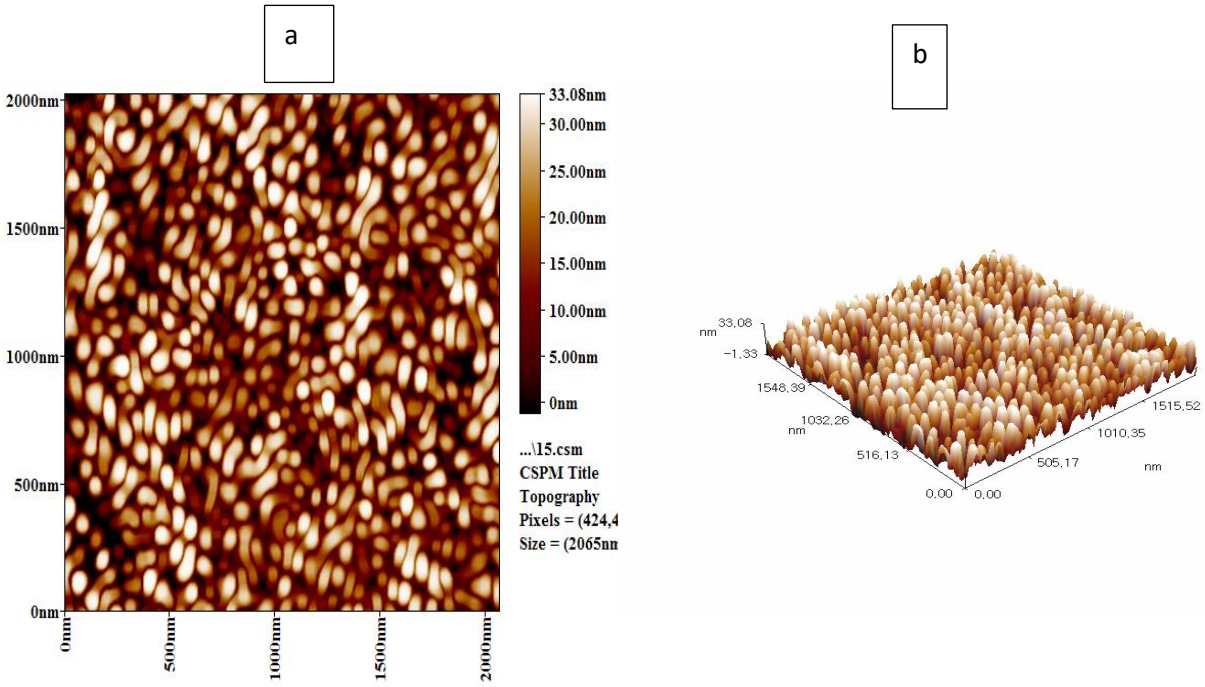

Figure (3-14): AFM assay of AgNPs, synthesized by 3 mL of *D. viscosa* aqueous leaves extract for 15 min. (a) Two dimensional image (b) Three dimensional image.

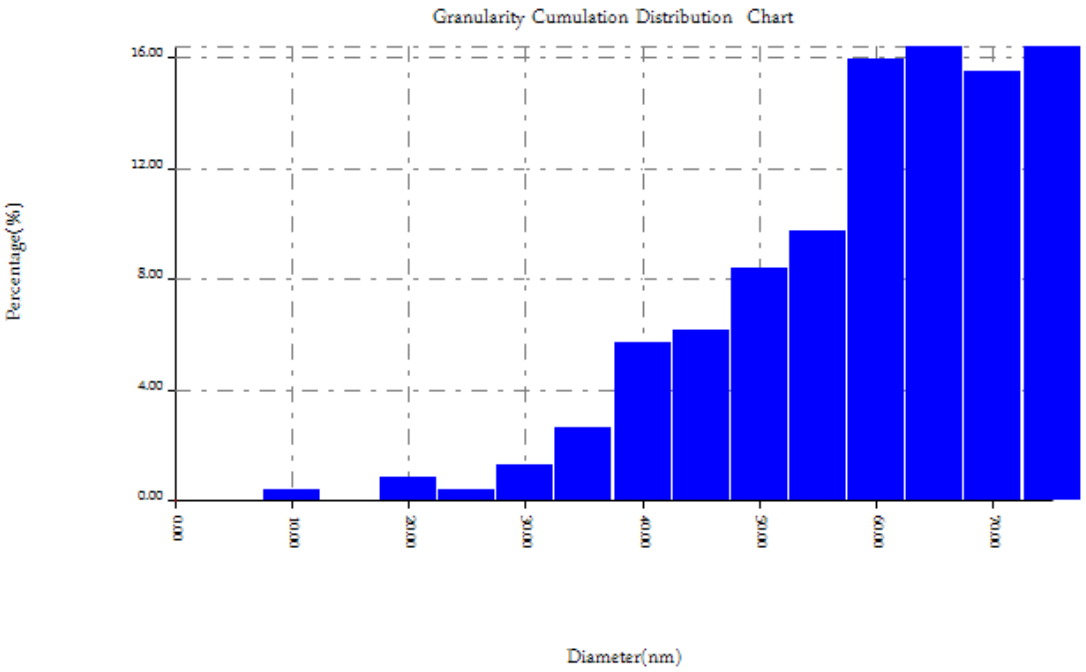

Figure (3-15): AFM assay of AgNPs, synthesized by 3 mL of *D. viscosa* aqueous leaves extract and boiling for 15 min.

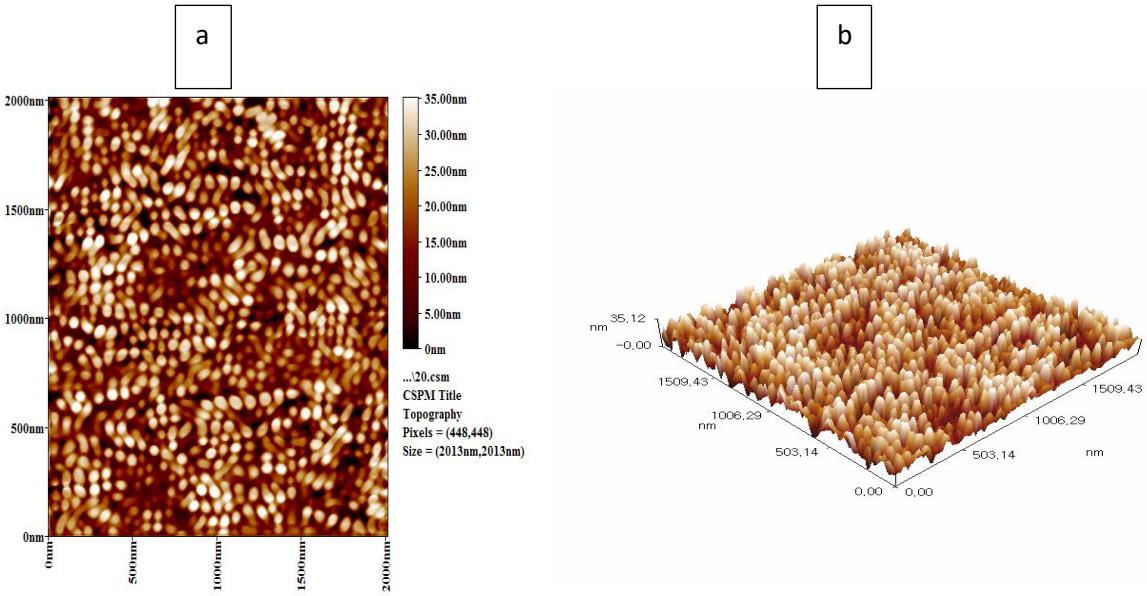

Figure (3-16): AFM assay of AgNPs, synthesized by 3 ml of *D. viscosa* aqueous leaves extract for 20 min. (a) Two dimensional image (b) three dimensional image.

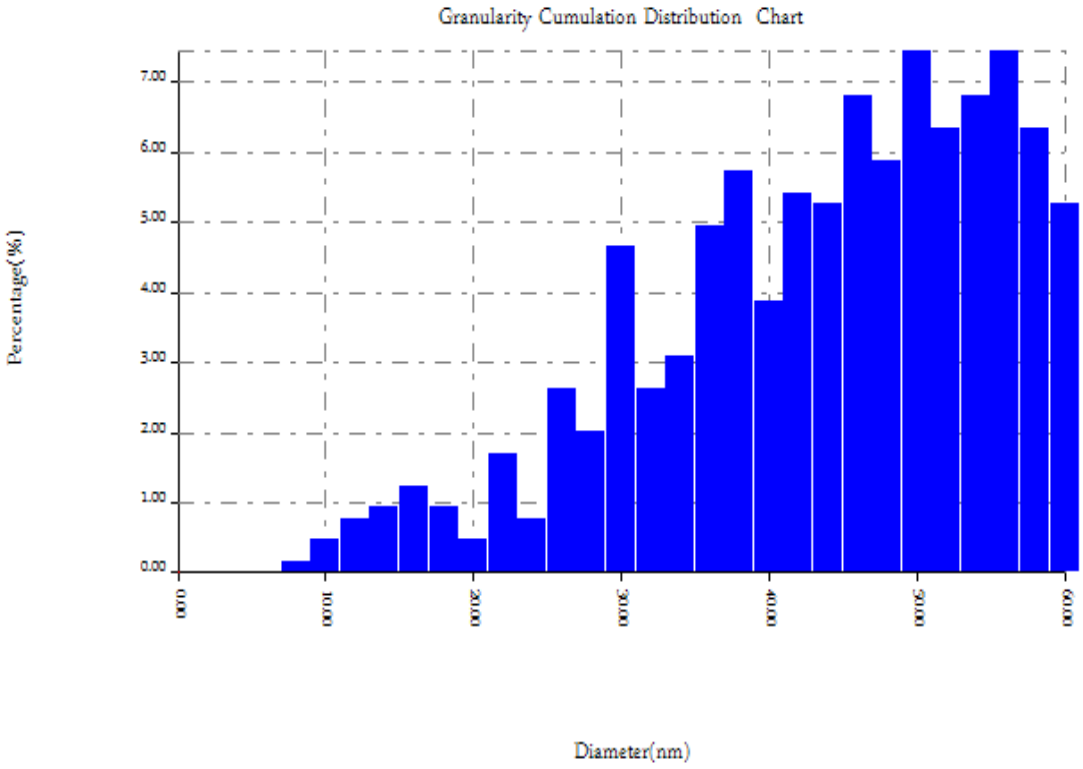

Figure (3-17): AFM assay of AgNPs, synthesized by 3 mL of *D. viscosa* aqueous leaves extract and boiling for 20 min.

Table (3-4): Values of surface roughness analysis

		3ml-10min boiling	3ml-15min boiling	3ml-20min boiling
Amplitude Parameters	**Average diameter**	60.22 nm	57.26 nm	42.57 nm
	Root mean square	33.9 nm	9.92 nm	8.88 nm
	Average Roughness	28.4 nm	8.6 nm	7.54 nm

3-4-5 Scanning Electron Microscopy SEM

AgNPs high magnification images were obtained using SEM technique. This technique can determine morphological features (number, dimension, and shape) of small particles by scanning reflections of a focused beam of electrons over the particles' surfaces. SEM images of the particles showed spherical shape particles and having different average diameter D1 (21.10), D2 (21.39) and D3 (11.86) nm with smooth surfaces morphology, and well scattered with a nearly compact arrangement (Fig. 3-18).

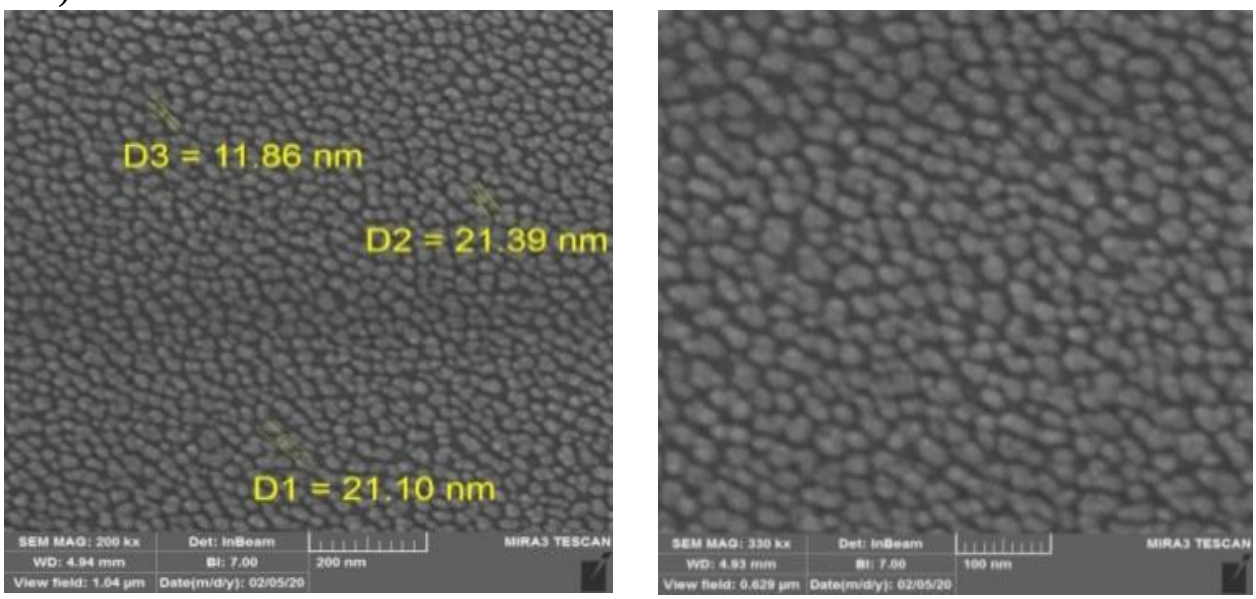

Figure (3-18): SEM image of biosynthesized silver nanoparticles (a) The particle size at different average diameter D1, D2 and D3. (b) SEM shows the spherical shape of particles.

SEM image analysis of surface morphology of AgNPs showed a precise spherical shape without any agglomeration (136).

3-5 Biological Activities

3-5-1 Antioxidant Activity

The antioxidant activity of synthesized AgNPs was measured via three different assays, DPPH free radical scavenging, total antioxidant, and reducing power, and ascorbic acid was used as a reference. Among the three methods used, DPPH scavenging capacity assay is the best choice

because characterized by fast, stability, and simplicity. The results introduced that the AgNPs have a high antioxidant activity, which increased gradually with the concentration compared to the aqueous extract of *D. viscosa* when using the DPPH method (Fig. 3-19).

The total antioxidant assay was performed using the phosphomolybdenum which, based on reducing Mo (VI) to Mo (V) by the antioxidant compound and formation of a green phosphate/ Mo(V) complex. The total antioxidant activity of *D. viscosa* leaves extract was a little more than AgNPs comparing with the ascorbic acid (Fig. 3-20).

Besides, the results revealed that the synthesized AgNPs have a reducing power more than *D. viscosa* leaves extract (Fig. 3-21).

Free radicals and other ROS are continuously formed in many organisms due to the oxidative processes produced to produce energy. Free radicals can be formed from enzymatic and non-enzymatic reactions of oxygen with organic compounds. The antioxidant activity of AgNPs and *D. viscosa* extract was determined using three methods. To assess the antioxidant activity that cannot be accurately determined in one way. DPPH scavenging capacity test is the best method for evaluating antioxidant activity because DPPH• is a stable free radical, not dimerize because of the delocalization of the spare electron on the whole molecule (94).

Silver nanoparticles demonstrated a good ability to scavenge free radicals when comparing it with the *D.viscosa* leaves extract and ascorbic acid, which is used as a well-known standard antioxidant.

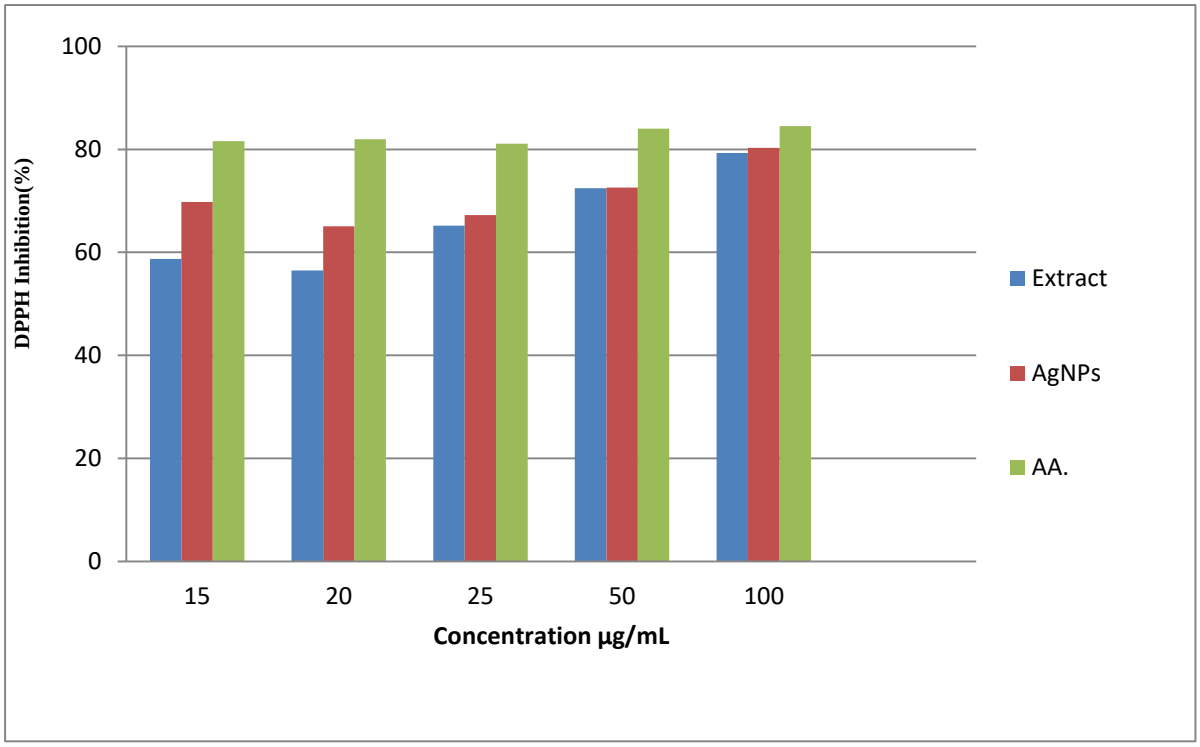

Figure (3-19): Antioxidant activity of the phyto-synthesized AgNPs and plant extract by using DPPH free radical scavenging. Ascorbic acid (AA.) as a reference (positive control).

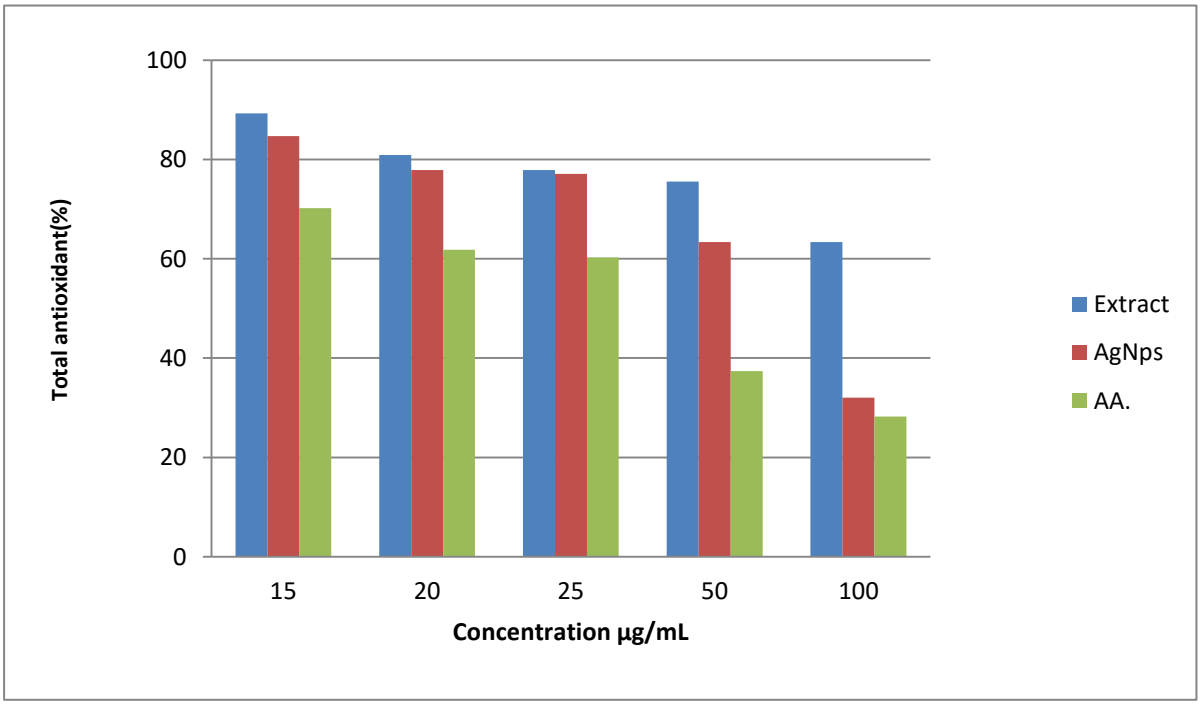

Figure (3-20): Total antioxidant ability of AgNPs, *D. viscosa* extract and Ascorbic Acid (AA).

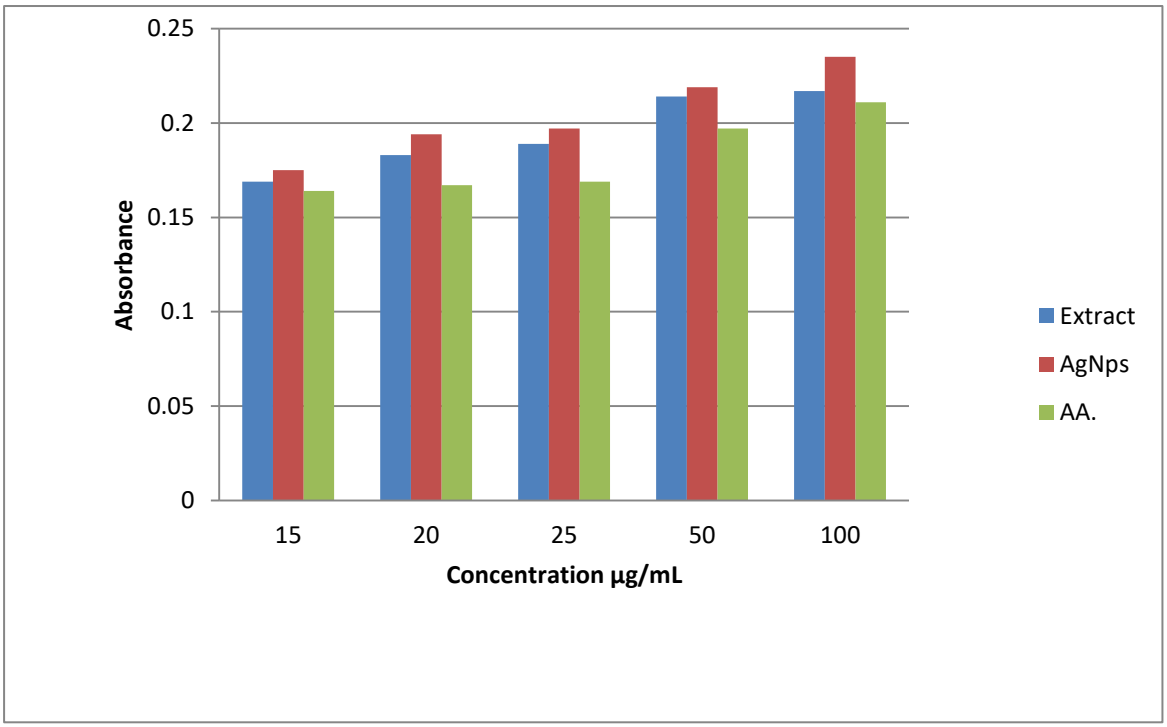

Figure (3-21): Reducing power of AgNPs, *D. viscosa* extract and Ascorbic Acid (AA)

Previous studies have shown that phenolic compounds are commomly present in plants that are both edible and inedible. In addition to the presence of various other phytochemicals including carbohydrates, saponins, tannins and terpenoids. These compounds have biological effects, including their antioxidant activity (99). Antioxidant activity of plant extracts due to the ability of phytochemicals (phenolics, flavonoids, and tannins) to oxidize and could play an important role in satiating singlet and triplet oxygen, rotting the peroxides or nullifying the free radicals. Since phenolics and flavonoids are responsible for the antioxidant activity, and high amount present in the extract indicates good antioxidant activity (137).

Similar reports indicated that the AgNPs have high antioxidant activity against DPPH (138); (139). The antioxidant capacity methods determines the ability of a sample to donate electrons and neutralizing free radicals.

3-5-2 Anti-tumor Activity

The 3-(4,5-dimethylthiazol-2-yl)-2,5-diphenyl-2H-tetrazolium bromide (MTT) assay was used to assess cytotoxic potency for each synthesized AgNPs and *D. viscosa* leaves extract. MTT assay in this study tested the viability of two cell line human cancer cell lines A549 (lung cancer) and SK-OV-3 (ovarian cancer) and compared with normal liver cells line WRL68. After 24 hours of treatment with various concentrations of leaves extract and AgNPs (15, 20, 25, 50 and 100 $\mu g.ml^{-1}$) respectively. The cytotoxicity results showed reduction in cell viability in a dose-dependent manner.

Besides, AgNPs and extract of *D. viscosa* shows weak cytotoxic on normal WRL68 and ovarian SK-OV-3 cell lines as IC_{50} range between 2.45-2.76 $\mu g\ mL^{-1}$ and 2.23-2.42 respectively. These results indicate does not get IC_{50} in SK-OV3 and normal cell lines WRL68 due to the inability of AgNPs and extract of *D. viscosa* to inhibit 50% from cell viability at the chosen concentrations (Fig. 3-23).

The A549 cell proliferation was significantly repressed by AgNPs at concentration (100 $\mu g.ml^{-1}$) with an IC_{50} value of 1.73 $\mu g.ml^{-1}$, as demonstrated in (Table 3-5). The A549 cell lines treatment with the various concentration of *D. viscosa* plant extract (15, 20, 25, 50, and 100 $\mu g.mL^{-1}$) was did not exhibit any significant cytotoxicity with an IC_{50} value of 1.96 $\mu g.mL^{-1}$, the results exhibited AgNPs more sensitive towards A549 cell lines than SK-OV-3.The use of plants as a source for the synthesis of AgNPs showed more of an effect and sensitivity on cancer cell lines A549 than SK-OV-3 and normal cells.

In one study was reported by Asra Parveen and Srinath Rao display that on the effects of AgNPs on cancer cells, AgNPs act on disrupts normal cellular function affects the membrane integrity, and induces different apoptotic of mammalian cells leading to programmed cell death. The

cytotoxic effects of AgNPs were due to active physicochemical interaction between Ag atoms with the functional groups of intracellular proteins, as well as with the nitrogen bases and phosphate groups in DNA (140).

The finding of this study is in a good agreement of previous studies where they showed anti-cancer activity of produced AgNPs from *Cleome viscosa* fruit extract against A549 (lung) and PA1 (ovaries) cell lines. The anticancer effect of AgNPs was more obvious on lung cancer cells than ovarian cancer cells (141). Sriranjani *et al*. showed cytotoxic effect of biosynthesis silver nanoparticles against human colorectal adenocarcinoma (HT29) and Ehrlich ascites cell carcinoma (EAC) (142). As well as, biosynthesized AgNPs from *Chaenomeles sinensis* and *Cibotium barometz* demonstrated anti-cancer efficacy against breast cells cancer (MCF-7) (143); (144). Based on the similar study showed the cell exposure to AgNPs could lead to different changes in cell morphology and reduce cell vitality. Generally, cellular morphological changes in the cell might be due to the disturbance in cell composition due to interaction between the cell surface and AgNPs (145).

The mechanism of the anticancer activity of silver nanoparticles involve, the entry of AgNPs into the cell lead to its damage by forming stable S-Ag bond with a thiol group of enzyme in cell membrane and its deactivation; or breaking hydrogen bonds between nitrogen bases of DNA and thereby denaturing it (122). In general, it was found that the AgNPs synthesized in the green methods have broad activity against cancer cells in dose-dependent manner with no or little toxicity to normal cells.

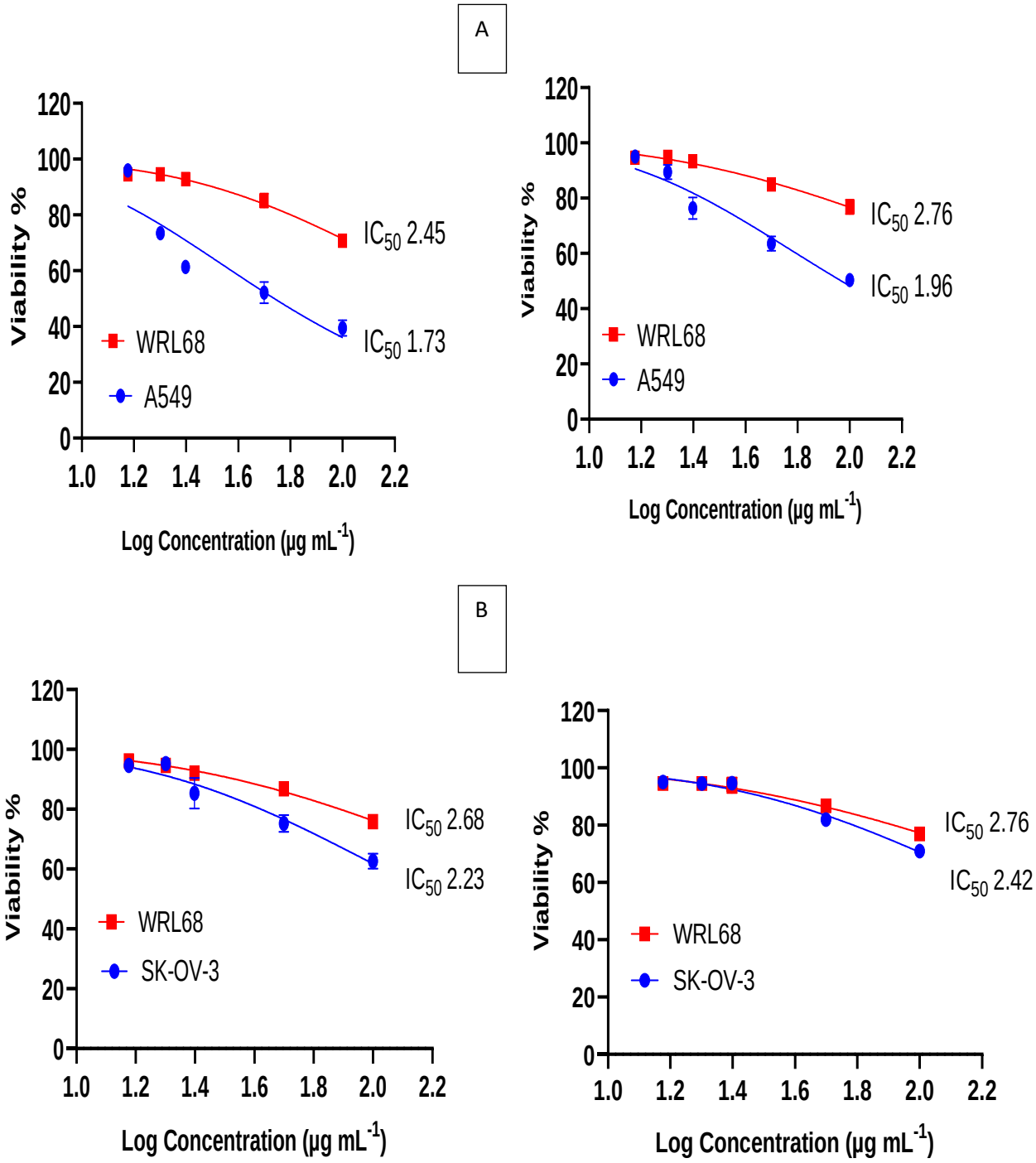

WRL68: liver normal cells
A459: human lung cancer
SK-OV-3: ovarian cancer
IC_{50}: Inhibition concentrations

Figure (3-22): The viability of (A) A549 cells for AgNPs and *D. viscosa* extract (B) SK-OV3 cells for AgNPs and *D. viscosa* extract comparing with normal cell WRL68.

Table (3-5): Inhibition concentrations (IC_{50}) for cytotoxic activity of *D. viscosa* extract and synthesized silver nanoparticles on human lung cancer (A549) and ovarian cancer (SKOV3) compared with the liver normal cells (WRL68).

Log Concentration (µg/mL)	Cell line	%Cell viability	%Cell inhibition	IC_{50} (µg /mL)	Normal cell	%Cell viability	%Cell inhibition	IC_{50} (µg /mL)
2.000	A549	39.429	60.571	1.73*	WRL68	70.795	29.205	2.45
1.699	(Nano)	52.122	47.878			85.185	14.815	
1.398		61.381	38.619			92.824	7.176	
1.301		73.457	26.543			94.560	5.440	
1.176		95.949	4.051			94.560	5.440	
2.000	A549	50.309	49.691	1.96	WRL68	76.890	23.11	2.76
1.699	(Ex.)	63.503	36.497			84.915	15.085	
1.398		76.350	23.650			93.326	6.674	
1.301		89.429	10.571			94.946	5.054	
1.176		95.023	4.977			94.637	5.363	
2.000		62.654	37.346			75.810	24.19	2.68
1.699	SKOV3	75.270	24.730	2.23	WRL68	86.806	13.194	
1.398	(Nano)	85.340	14.660			92.052	7.948	
1.301		95.216	4.784			94.637	5.363	
1.176		94.637	5.363			96.181	3.819	
2.000	SKOV3	70.988	29.012	2.42	WRL68	76.968	23.032	2.76
1.699	(Ex.)	81.983	18.017			86.728	13.272	
1.398		94.637	5.363			93.981	6.019	
1.301		94.560	5.440			94.599	5.401	
1.176		95.062	4.938			94.599	5.401	

Ex.: *D. viscosa* extract
Nano: Synthesized silver nanoparticles
*Significant difference (P-value <0.001)
A459: human lung cancer
SKOV3: ovarian cancer
WRL68: liver normal cells
IC_{50}: Inhibition concentrations

3-5-3 Antibacterial Activity

The antibacterial activity for each AgNPs and *D.viscosa* leaves extract were tested against Gram-positive bacteria (*Staphylococcus aureus* and

Streptococcus pneumonia) and Gram-negative bacteria (*E.coli* and *Pseudomonas aeruginosa*). The results did not show any antibacterial activity at various concentrations of leaves extracts and AgNPs at the concentrations (15, 20, 25, 50 and 100 $\mu g.ml^{-1}$) respectively (Figure 3-23), whereas the synthesized AgNPs at the concentrations (5000, 10000, 15000, 20000, and 25000 μg/mL) respectively revealed antibacterial activity against all tested bacteria compared with the *D. viscosa* leaves extract, which did not show any antibacterial activity (Fig. 3-24). The highest activity of AgNPs was noticed against *Staphylococcus aureus* with an inhibition zone of 20 mm at the concentration of 5000 (μg/mL) (Table 3-6).

These results of antibacterial activity of AgNPs were compared with the positive control (Amoxicillin antibiotic), and *D. viscosa* leaves extract. The antibacterial activity of AgNPs due to the size, shape, and large surface area of AgNPs relative to the small size as the smaller NPs have more antibacterial activity due to them providing more surface exposure to the bacterial membrane. The decreased size and increased surface area of AgNPs lead to the interaction with the cell wall of bacteria and binding to the cell membrane, and change the permeability by changing the membrane potential (146). When AgNPs enter the cell, it turns into silver ions that interact with the biomolecules, causing cell damage due to binds to DNA, which hinders its replication. Besides, these ions interfere with cell division via binding to membrane proteins and cell proteins, which help division cells (33). Also, AgNPs can cross the wall and bacterial membrane and increase the production of ROS by inhibiting respiratory chain enzymes and promoting their accumulation inside bacteria (147).

In a previous study of the effect AgNPs against bacteria, it was shown that the AgNPs interact with the membrane components causing the alteration and damage to the membrane structure and the excretion of cellular components which leads to the cell's death (79); (148).

Table (3-6): Anti-bacterial assay of AgNPs and *D. viscosa* extract against some pathogenic microorganisms.

Test sample	Concentration (µg/mL)	Inhibition zone diameter (mm)			
		Gram-negative		Gram-positive	
		E. coli	*Pseudomonas aeruginosa*	*Staphylococcus aureus*	*Streptococcus pneumonia*
AgNPs	5000	10±0.40	13±1.64	20±0.60	15±0.94
	10000	10±0.13	15±0.81	12±1.30	15±0.65
	15000	10±0.52	15±0.87	12±0.86	12±1.27
	20000	10±0.82	10±1.63	15±0.43	-
	25000	12±1.23	10±1.09	15±1.15	-
Extract	5000	-	-	-	-
	10000	-	-	-	-
	15000	-	-	-	-
	20000	-	-	-	-
	25000	-	-	-	-
Positive control Antibiotic (Amoxicillin)		32±0.41	21±0.17	20±0.23	26±0.15
Negative control (solvent)		-	-	-	-

Values are expressed as mean SD of triplicates

± indicates Standard Error

- indicates no inhibition zone

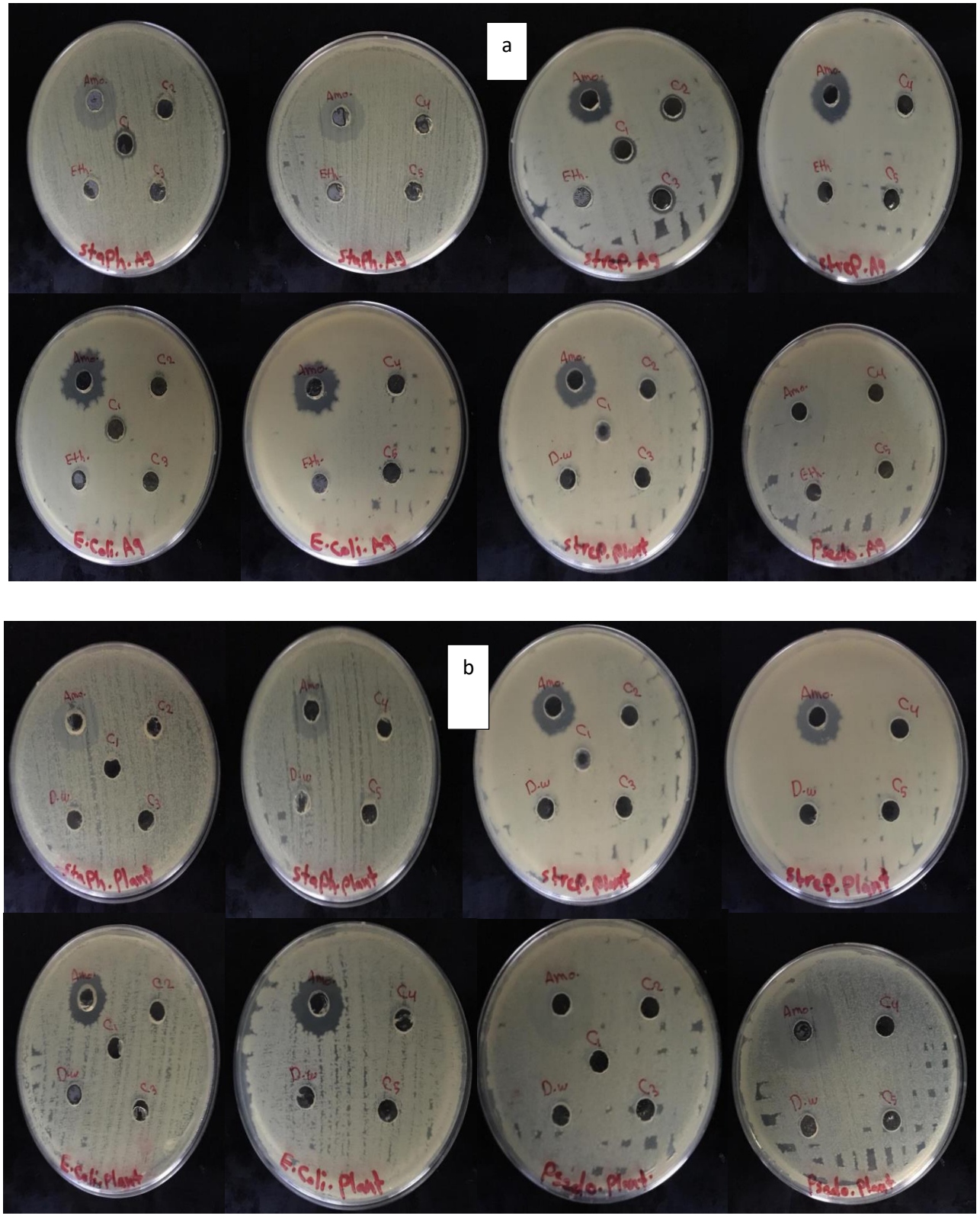

Figure (3-23): The antibacterial activity of (a) AgNPs (b) *D.viscosa* leaves extract against Gram-positive bacteria (*Staphylococcus aureus.)* and *Streptococcus pneumonia* and Gram-negative bacteria (*E.coli* and *Pseudomonas aeruginosa)*(C_1, C_2, C_3, C_4, and C_5) represents the concentrations of AgNPs and extract (15, 20, 25, 50, and 100 µg/mL). Negative control represents solvent Amo. (Amoxicillin) positive control.

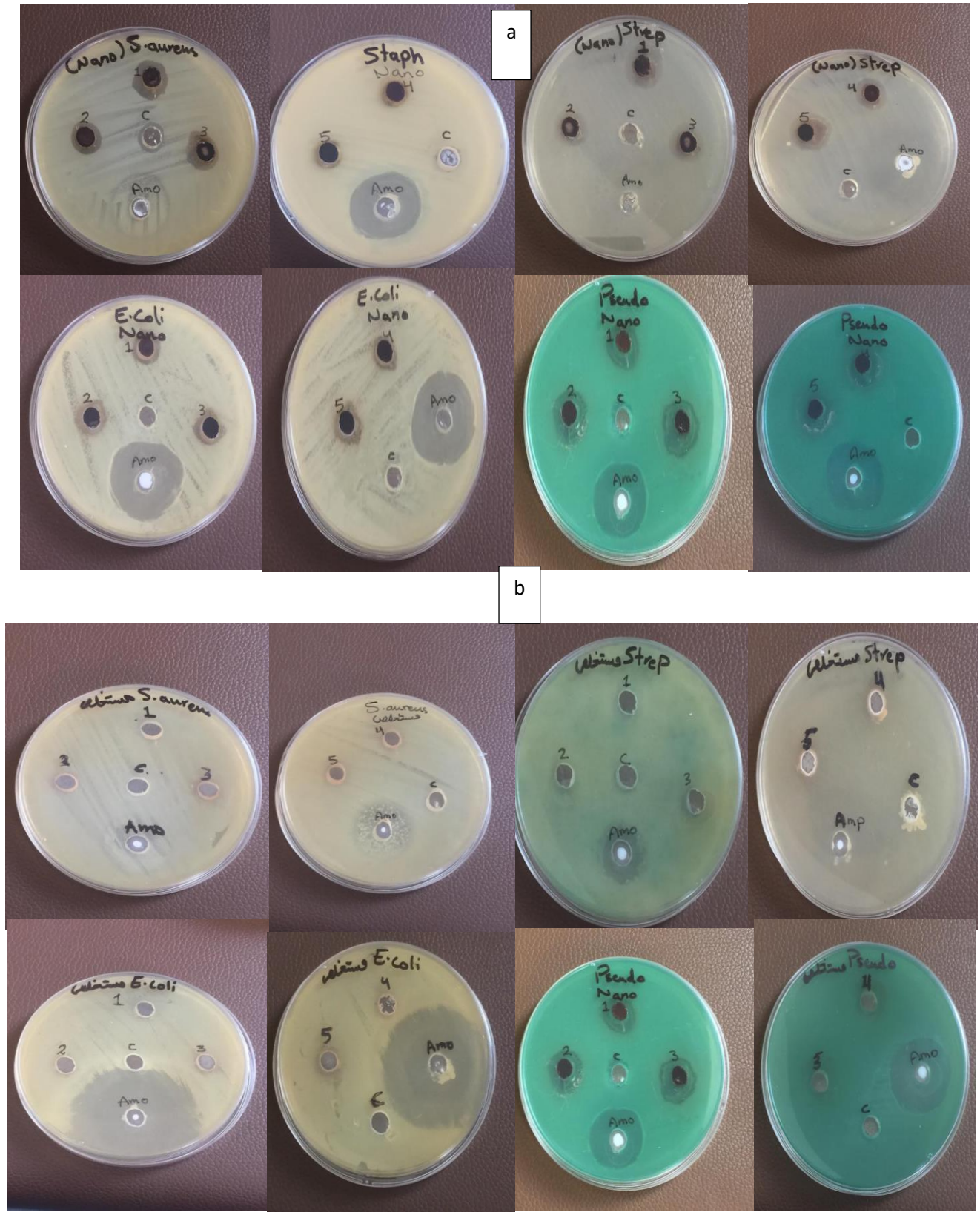

Figure (3-24): The antibacterial activity (1) silver nanoparticles (AgNPs) and (2) *Dodonaea viscosa* leaves extract against Gram-positive bacteria (*Staphylococcus aureus* and *Streptococcus pneumonia* and Gram-negative (*E.coli* and *Pseudomonas aeruginosa*). (C_1, C_2, C_3, C_4, and C_5) represents the concentrations of AgNPs and extract (5000, 10000, 15000, 20000 and 25000 µg/mL) Negative control represents solvent. Amo. (Amoxicillin) positive control.

3-5-4 Coagulation Factors

The anti-coagulant activity of *D. viscosa* extract and AgNPs were evaluated via prothrombin time (PT) and activated partial thromboplastin time (APTT) tests using normal citrated human plasma. The results were expressed as mean and standard deviation (SD). AgNPs cause a highly significant increase in PT at concentrations (15, 20, 25, 50, and 100 µg/mL) comparing with the control and there is a highly significant difference ($p<0.001$) between all groups (Table 3-7).

In addition, APTT increased significantly with an increased concentration of AgNPs in comparison with the control and there is a highly significant difference ($p<0.001$) between all groups. Normal citrated human plasma was used as control (Table 3-8).

Also, the results of clotting times appeared that *D. viscosa* extract causes a highly significant increase in PT at the concentrations (15, 20, 25, 50, and 100 µg/mL) respectively compared with the control and there is a significant difference ($p<0.001$) between all groups (Table 3-9).

Besides, the results of anticoagulant activity of *D. viscosa* showed that there were significant increase in APTT at concentrations (15, 20, 25, 50, and 100 µg/mL) respectivly comparing with control (Table 3-10).

Also, in order to comparison between the effect of AgNPs and *D. viscosa* extract on the coagulation factors, the results showed that there was a highly significant increase ($p= 0.02$, 0.05, and 0.01) in PT at concentrations (15, 50, and 100 µg/mL) respectivly of AgNPs comparing with the extract (Table 3-11), whereas there was a highly significant difference in APTT at all concentrations (15, 20, 25, 50, and 100 µg/mL) in both values to AgNPs and *D. viscosa* extract (Table 3-12).

In this study, PT and APTT are performed in citrated plasma and are the most commonly employed laboratory tests in patients suspected of

having a coagulopathy. This study showed that both PT and APTT were significantly prolonged.

Table (3-7):Prothrombin Time (PT) of blood samples with and without Ag NPs.

Groups	Mean± SD N=20	P-value	P-value	LSD
Control	13.93±0.62		<0.001	2.86
15 µg/mL	15.93±0.24	0.17*		
20 µg/mL	17.85±3.21	0.008*		
25 µg/mL	20.4±5.1	<0.001*		
50 µg/mL	22.58±6.3	<0.001*		
100 µg/mL	25.38±6.8	<0.001*		

P-value≤0.05 is significant
*AgNPs vs. Control
LSD: least significant difference
SD: Standard Deviation
N: Number of volunteers

Table (3-8): Activated Partial Thromboplastin Time (APTT) of blood samples with and without AgNPs

Groups	Mean± SD N=20	P-value	P-value	LSD
Control	30.67±2.02		<0.001	2.72
15 µg/mL	33.29±3.35	0.05*		
20 µg/mL	34.89±3.76	0.003*		
25 µg/mL	37.23±4.29	<0.001*		
50 µg/mL	38.76±4.66	<0.001*		
100 µg/mL	42.64±6.56	<0.001*		

P-value≤0.05 is significant
*AgNPs vs. Control
LSD: least significant difference
SD: Standard Deviation
N: Number of volunteers

Table (3-9): Prothrombin Time (PT) of blood samples with and without *Dodonaea viscosa* extract

Groups	Mean± SD N=20	P-value	P-value	LSD
Control	13.93±0.62		<0.001	1.64
15 µg/Ml	15.12±0.99	0.15*		
20 µg/mL	16.45±2.3	0.003*		
25 µg/mL	18.14±2.84	<0.001*		
50 µg/mL	19.35±3.82	<0.001*		
100 µg/mL	20.92±3.82	<0.001*		

P-value≤0.05 is significant
**Dodonaea viscosa* extract vs. Control
LSD: least significant difference
SD: Standard Deviation
N: Number of volunteers

Table (3-10): Activated Partial Thromboplastin Time (APTT) of blood samples with and without *Dodonaea viscosa* extract

Groups	Mean± SD N=20	P-value	P-value	LSD
Control	30.67±2.02		<0.001	2.72
15 µg/mL	31.12±1.72	0.059*		
20 µg/mL	32.37±2.59	0.05*		
25 µg/mL	33.68±2.32	0.001*		
50 µg/mL	35.91±3.1	<0.001*		
100 µg/mL	37.57±3.9	<0.001*		

P-value≤0.05 is significant
**Dodonaea viscosa* extract vs. Control
LSD: least significant difference
SD: Standard Deviation
N: Number of volunteers

Table (3-11): Comparison between the effect of AgNPs and *D. viscosa* extract on Prothrombin Time (PT)

Groups	Mean±SD N=20	P-value
15 µg/mL AgNPs	15.93±1.11	0.02
15 µg/mL Extract	15.12±0.99	
20 µg/mL AgNPs	17.85±3.21	0.12
20 µg/mL Extract	16.45±2.3	
25 µg/mL AgNPs	20.4±5.19	0.09
25 µg/mL Extract	18.14±2.84	
50 µg/mL AgNPs	22.58±6.3	0.05
50 µg/mL Extract	19.35±3.4	
100 µg/mL AgNPs	25.38±6.8	0.01
100 µg/mL Extract	20.92±3.82	

P-value≤0.05 is significant
SD: Standard Deviation
N: Number of volunteers

Table (3-12): Comparison between the effect of AgNPs and *D. viscosa* extract on Activated Partial Thromboplastin Time (APTT)

Groups	Mean±SD N=20	P-Value
15 µg/mL AgNPs	33.29±3.35	0.01
15 µg/mL Extract	31.12±1.72	
20 µg/mL AgNPs	34.89±3.7	0.01
20 µg/mL Extract	32.3. ±2.5	
25 µg/mL AgNPs	37.23±4.29	0.003
25 µg/mL Extract	33.68±2.32	
50 µg/mL AgNPs	38.76±4.66	0.02
50 µg/mL Extract	35.91±3.1	
100 µg/mL AgNPs	42.64±6.56	0.005
100 µg/mL Extract	37.57±3.9	

P-value≤0.05 is significant
SD: Standard Deviation
N: Number of volunteers

Prolongation of APTT is related to inhibition of the common pathway or intrinsic of coagulation, whereas not showing prolongation of PT does not indicate inhibition of the external pathway (99).

Nanoparticles can have harmful or beneficial effects on the coagulation system depending on whether they are desired or not. Also, the nanoparticles can be contrived to exclusively work together with the blood coagulation system to circumvent various blood disorders (149).

Similar studies indicated the anticoagulation properties of biosynthesized AgNPs had also been previously reported by Flaih and Al-Saadi; and Muhammad *et al*. the presence of flavonoids and phenolic acids in plant caused highly significant prolonged PT and APTT (105); (150). Some studies have indicate that AgNPs possessed antiplatelet activity as well as fibrinolytic activity which prevented blood coagulation. The blood clotting system is a complex system that includes series of coagulation factors. Until now it is not understood whether AgNPs are related to inhibiting the real prothrombin (factor II), proconvertin (factor VII), and Stuart's factor (factor X) to prevent the formation of thrombin (factor IIa). However, the anti-fibrinogen, anti-platelte, and anti-fibrin combined are undoubtedly contribute to the anticoagulant activity of AgNPs as obtained in this study (151). Recently, nanomaterials are being positioned for use as anticoagulants with incredible performance in forestalling coagulation of blood (152).

3-5-5 Hemolytic activity

Hemolysis is a phenomenon in that the breakdown or destruction of red blood cells (RBC) takes place, so that, the contained hemoglobin is released into the supernatant plasma. The results of the hemolytic activity of AgNPs synthesized from *D.viscosa* were tested on human whole blood as a percentage hemolysis and reported for ten healthy nonsmoker donors. The results showed the percentage of hemolysis, which was 3.16%, 3.53%,

4.3%, 5.1%, and 5.8% respectively at a concentrations (15, 20, 25, 50, and 100 µg/mL) (Fig 3-24). The synthesized AgNPs at all concentrations showed a reduction of absorbance values. The percent hemolysis was determined using colorimetric detection of hemoglobin in the supernatant in normal saline-treated with AgNPs. Triton X-100 was used as a positive control and normal saline as negative control. The concentration and surface area to the ratio of the volume of AgNPs greatly influence on the hemolysis. In this study, the synthesized AgNPs showed a little effect on heamolytic.

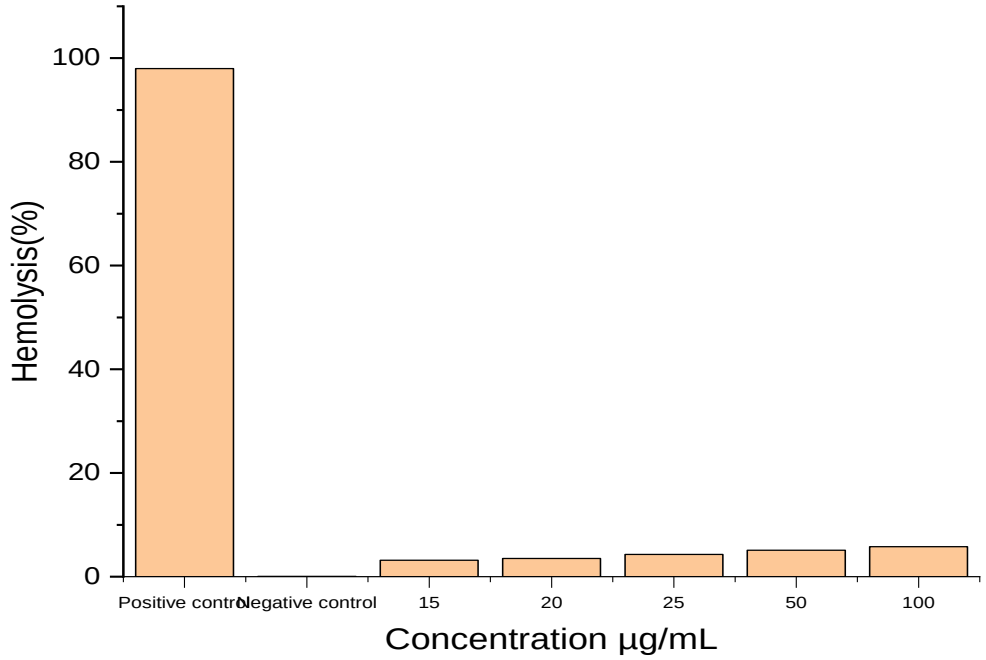

Triton X-100: Positive control
Normal saline: Negative control

Figure (3-25): The percentage of hemolysis induced by AgNPs. Triton X-100 was used as a positive control and normal saline as a negative control.

The mechanism of AgNPs for inducing hemolysis still not revealed. Metallic silver undergoes ionization when came in contact with the body fluids, releasing Ag^{+} ions according to particle surface area response. RBC hemolysis *in vitro* could be induced by low concentrations of Ag^{+} (153).

The metallic NPs ioinzes and release their ions from contact with the blood, which can interact with membrane proteines. However Ag^{+} ion generation is not the only factor for hemolysis; other mechanisms contribute to hemolysis induced by NPs (deformability, adhesiveness, membrane vesiculation, etc.) (107).

The previous study showed that hemolytic activity of green synthesized silver nanoparticles from *Hyphaene thebaica* fruits similar dose-dependent trend was observed in the hemolytic activity of the NPs. Hemolysis was decreased with a decrease gradually in the concentration and reported to be 10.68 % at 12.5 μg mL^{-1} (154). Another study show hemolysis induced by silver nanoparticles was less than 0.4 %, which was well within the acceptable limits of 1 % (155). Also, earlier studies reported by Gajendra *et al.* indicate materials with a hemolysis ratio of less than 5% were regarded as hemocompatible (156).

Conclusions and Future Studies

Conclusions

1. *Dodonaea viscosa* is consided a good source of phytochemical which was responsible for synthesis AgNPs.
2. Phytochemicals of plant are responsible for the reducting and stabilizing of nanoparticle.
3. Silver nanoparticles have good antioxidant activity.
4. The AgNPs synthesized in the green methods have broad activity against cancer cells in a dose-dependent manner with no or little toxicity to normal cells.
5. The synthesized AgNPs have good antibacterial activity, hence we can use them as a drug in bacterial infections after further study.
6. Silver nanoparticles can be used in the medical field, especially in diseases related to thrombosis, as they cause a prolongation of clotting time but after further study.
7. Silver nanoparticles did not cause hemolysis and therefore can be used in pharmaceutical fields.
8. In all the clinical applications experiments, AgNPs was the best effective than *D. viscosa* extract, so the use AgNPs with the adsorbed phytochemicals on their surface is the best choice in clinical application.

Future Studies

1. Studying biosynthesis of another nanoparticles using different medicinal plants.
2. Biosynthesis of silver nanoparticles using microorganisms such as bacteria or fungi.
3. Studying the clinical applications of the synthesized silver nanoparticles *in vivo.*
4. Studying the anti-inflammatory activity of the synthesized silver nanoparticles from *D. viscosa* leaves extract.
5. Studying the catalytic activity of the synthesized silver nanoparticles from *D. viscosa* leaves extract.

References

References

1. Srinivasan P, Sudhakar S, Sengottaiyan A, Subramani P, Sudhakar C, Thiyagarajan KMP. Green synthesis of silver nanoparticles using Cassia auriculata flower extract and its antibacterial activity. 2014.p42-46.
2. Balashanmugam P, Kalaichelvan P. Biogenic synthesis of silver nanoparticles from Dodonaea viscosa Linn. and its effective antibacterial activity. J Sci Trans Environ Technovation. 2014;8:67-71.
3. Jahn W. Chemical aspects of the use of gold clusters in structural biology. Journal of structural biology. 1999;127(2):106-12.
4. Zhang X-F, Liu Z-G, Shen W, Gurunathan S. Silver nanoparticles: synthesis, characterization, properties, applications, and therapeutic approaches. International journal of molecular sciences. 2016;17(9):1534.
5. Khan M, Tareq F, Hossen M, Roki M. Green synthesis and characterization of silver nanoparticles using Coriandrum sativum leaf extract. Journal of Engineering Science and Technology. 2018;13(1):158-66.
6. Parthasarathy G, Saroja M, Venkatachalam M, Gowthaman P, Evanjelene V. Synthesis of nanoparticles from Aloe vera extract review paper. Imperial Journal of Interdisciplinary Research (IJIR) 2016;2:1570-5.
7. Ojha S, Sett A, Bora U. Green synthesis of silver nanoparticles by Ricinus communis var. carmencita leaf extract and its antibacterial study. Advances in Natural Sciences: Nanoscience and Nanotechnology. 2017;8(3):035009.

8. Rani MS, MOHAN RSPK. Dodonaea viscosa Linn.-an overview. Asian Journal of Pharmaceutical Research and Health Care. 2009;1(1).
9. Gilman, Edward F. "Dodonaea viscosa." University of Florida, Cooperative Extension Service, Fact Sheet-181 (1999).
10. Lundgren B, Getahun A, Kaudia A, Chavangi A, Birnie AM, Tengnas B. A Selection of Useful Trees and Shrubs for Kenya-Notes on their Identification, Propagation and Management for use by Agricultural and Pastoral Communities. 1992.
11. Rojas A, Cruz S, Ponce-Monter H, Mata R. Smooth muscle relaxing compounds from Dodonaea viscosa5. Planta medica. 1996;62(02):154-9.
12. Saxena M, Saxena J, Nema R, Singh D, Gupta A. Phytochemistry of medicinal plants. Journal of pharmacognosy and phytochemistry. 2013;1(6).
13. Rao BN. Bioactive phytochemicals in Indian foods and their potential in health promotion and disease prevention. Asia Pacific Journal of clinical nutrition. 2003;12(1).
14. Hamadi SS. Chemical study of Dodonaea viscosa planting in Iraq. Journal of Advances in Chemical Engg., & Biological Sciences. 2017;4:121-5.
15. Egamberdieva D, Mamedov N, Ovidi E, Tiezzi A, Craker L. Phytochemical and pharmacological properties of medicinal plants from Uzbekistan: A review. Journal of Medicinally Active Plants. 2017;5(2):59-75.
16. Hassanpour S, MaheriSis N, Eshratkhah B. Plants and secondary metabolites (Tannins): A Review. International Journal of Forest, Soil and Erosion, 2011, 1 (1).

17. Bajad P, Pardeshi A, Pagore V. Extraction, isolation and quantification of saponin from Dodonaea viscosa JACQ. The Pharma Innovation Journal 2019; 8(5): 41-44.
18. Crozier A, Clifford MN, Ashihara H. Plant secondary metabolites: occurrence, structure and role in the human diet: John Wiley & Sons; 2008.
19. Anulika NP, Ignatius EO, Raymond ES, Osasere O-I, Abiola AH. The chemistry of natural product: Plant secondary metabolites. Int J Technol Enhanc Emerg Eng Res. 2016;4(8):1-9.
20. Hussein RA, El-Anssary AA. Plants secondary metabolites: the key drivers of the pharmacological actions of medicinal plants. Herbal Medicine. 2019;1:13.
21. Carmona ER, Benito N, Plaza T, Recio-Sánchez G. Green synthesis of silver nanoparticles by using leaf extracts from the endemic Buddleja globosa hope. Green Chemistry Letters and Reviews. 2017;10(4):250-6.
22. Thirumurugan D, Cholarajan A, Raja S, Vijayakumar R. An introductory chapter: secondary metabolites. Second metab—sources Appl. 2018:1-21.
23. Hossain MA. Biological and phytochemicals review of Omani medicinal plant Dodonaea viscosa. Journal of King Saud University-Science. 2019;31(4):1089-94.
24. Muqaddas R. Ayesha T. &Farwa N. Historical Origin, Chemical Constituents and Therapeutic Potentials of Sanatha (Dodonaea viscose)–A Brief Review. International Journal of Chemical and Biochemical Sciences. (2018).14:48-54.
25. Al-Snafi AE. A review on Dodonaea viscosa: A potential medicinal plant. IOSR Journal of Pharmacy. 2017;7(2):10-21.

26. Iravani S. Green synthesis of metal nanoparticles using plants. Green Chemistry. 2011;13(10):2638-50.
27. Yadi M, Mostafavi E, Saleh B, Davaran S, Aliyeva I, Khalilov R, et al. Current developments in green synthesis of metallic nanoparticles using plant extracts: a review. Artificial cells, nanomedicine, and biotechnology. 2018;46(sup3):S336-S43.
28. El-Sherbiny IM, Salih E. Green synthesis of metallic nanoparticles using biopolymers and plant extracts. Green Metal Nanoparticles: Synthesis, Characterization and Their Applications. 2018:293-319.
29. Mittal AK, Chisti Y, Banerjee UC. Synthesis of metallic nanoparticles using plant extracts. Biotechnology advances. 2013;31(2):346-56.
30. Parveen K, Banse V, Ledwani L, editors. Green synthesis of nanoparticles: their advantages and disadvantages. AIP conference proceedings; 2016.
31. Khan I, Saeed K, Khan I. Nanoparticles: Properties, applications and toxicities. Arabian journal of chemistry. 2019;12(7):908-31.
32. Iravani S, Korbekandi H, Mirmohammadi SV, Zolfaghari B. Synthesis of silver nanoparticles: chemical, physical and biological methods. Research in pharmaceutical sciences. 2014;9(6):385.
33. Singh A, Gautam PK, Verma A, Singh V, Shivapriya PM, Shivalkar S, et al. Green synthesis of metallic nanoparticles as effective alternatives to treat antibiotics resistant bacterial infections: A review. Biotechnology Reports. 2020;25:e00427.
34. Rajput N. Methods of preparation of nanoparticles-a review. International Journal of Advances in Engineering & Technology. 2015;7(6):1806.
35. Velammal SP, Devi TA, Amaladhas TP. Antioxidant, antimicrobial and cytotoxic activities of silver and gold nanoparticles synthesized

using Plumbago zeylanica bark. Journal of Nanostructure in Chemistry. 2016;6(3):247-60.

36. Klaus T, Joerger R, Olsson E, Granqvist C-G. Silver-based crystalline nanoparticles, microbially fabricated. Proceedings of the National Academy of Sciences. 1999;96(24):13611-4.
37. Du L, Jiang H, Liu X, Wang E. Biosynthesis of gold nanoparticles assisted by Escherichia coli DH5α and its application on direct electrochemistry of hemoglobin. Electrochemistry Communications. 2007;9(5):1165-70.
38. Konishi Y, Tsukiyama T, Tachimi T, Saitoh N, Nomura T, Nagamine S. Microbial deposition of gold nanoparticles by the metal-reducing bacterium Shewanella algae. Electrochimica Acta. 2007;53(1):186-92.
39. Ashok K, Sivakumari K, Rajesh S. Achyranthes aspera mediated green synthesis of silver nanoparticles. Indo American Journal of Pharmaceutical Sciences. 2018;5(1):64-73.
40. Yin Y, Yang X, Hu L, Tan Z, Zhao L, Zhang Z, et al. Superoxide-mediated extracellular biosynthesis of silver nanoparticles by the fungus Fusarium oxysporum. Environmental Science & Technology Letters. 2016;3(4):160-5.
41. Balaji D, Basavaraja S, Deshpande R, Mahesh DB, Prabhakar B, Venkataraman A. Extracellular biosynthesis of functionalized silver nanoparticles by strains of Cladosporium cladosporioides fungus. Colloids and surfaces B: biointerfaces. 2009;68(1):88-92.
42. Basavaraja S, Balaji S, Lagashetty A, Rajasab A, Venkataraman A. Extracellular biosynthesis of silver nanoparticles using the fungus Fusarium semitectum. Materials Research Bulletin. 2008;43(5):1164-70.

43. Kumar B, Smita K, Cumbal L, Debut A. Ficus carica (Fig) fruit mediated green synthesis of silver nanoparticles and its antioxidant activity: a comparison of thermal and ultrasonication approach. BioNanoScience. 2016;6(1):15-21.
44. Bagherzade G, Tavakoli MM, Namaei MH. Green synthesis of silver nanoparticles using aqueous extract of saffron (Crocus sativus L.) wastages and its antibacterial activity against six bacteria. Asian Pacific Journal of Tropical Biomedicine. 2017;7(3):227-33.
45. Roy P, Das B, Mohanty A, Mohapatra S. Green synthesis of silver nanoparticles using Azadirachta indica leaf extract and its antimicrobial study. Applied Nanoscience. 2017;7(8):843-50.
46. Gavamukulya Y, Maina EN, Meroka AM, Madivoli ES, El-Shemy HA, Wamunyokoli F, et al. Green synthesis and characterization of highly stable silver nanoparticles from ethanolic extracts of fruits of Annona muricata. Journal of Inorganic and Organometallic Polymers and Materials. 2020;30(4):1231-42.
47. Singh P, Kim Y-J, Zhang D, Yang D-C. Biological synthesis of nanoparticles from plants and microorganisms. Trends in biotechnology. 2016;34(7):588-99.
48. Rasheed T, Bilal M, Iqbal HM, Li C. Green biosynthesis of silver nanoparticles using leaves extract of Artemisia vulgaris and their potential biomedical applications. Colloids and Surfaces B: Biointerfaces. 2017;158:408-15.
49. Teow S-Y, Wong MM-T, Yap H-Y, Peh S-C, Shameli K. Bactericidal properties of plants-derived metal and metal oxide nanoparticles (NPs). Molecules. 2018;23(6):1366.
50. Gour A, Jain NK. Advances in green synthesis of nanoparticles. Artificial cells, nanomedicine, and biotechnology. 2019;47(1):844-51.

51. Fatima R, Priya M, Indurthi L, Radhakrishnan V, Sudhakaran R. Biosynthesis of silver nanoparticles using red algae Portieria hornemannii and its antibacterial activity against fish pathogens. Microbial Pathogenesis. 2020;138:103780.
52. Singh P, Singh H, Kim YJ, Mathiyalagan R, Wang C, Yang DC. Extracellular synthesis of silver and gold nanoparticles by Sporosarcina koreensis DC4 and their biological applications. Enzyme and Microbial Technology. 2016;86:75-83.
53. Kharissova OV, Dias HR, Kharisov BI, Pérez BO, Pérez VMJ. The greener synthesis of nanoparticles. Trends in biotechnology. 2013;31(4):240-8.
54. Khan MA, Khan T, Nadhman A. Applications of plant terpenoids in the synthesis of colloidal silver nanoparticles. Advances in colloid and interface science. 2016;234:132-41.
55. Chaudhuri SK, Chandela S, Malodia L. Plant Mediated Green Synthesis of Silver Nanoparticles Using Tecomella undulata Leaf Extract and Their Characterization. Nano Biomedicine & Engineering. 2016;8(1).
56. Mahdavi-Ourtakand M, Jafari P, Safaeijavan R. Antibacterial activity of biosynthesized silver nanoparticles from fruit extracts of Bunium persicum Boiss. Int J Bio-Inorg Hybr Nanomater. 2017;6(4):245-51.
57. Moteriya P, Padalia H, Chanda S. Characterization, synergistic antibacterial and free radical scavenging efficacy of silver nanoparticles synthesized using Cassia roxburghii leaf extract. Journal of Genetic Engineering and Biotechnology. 2017;15(2):505-13.
58. Reddy NJ, Vali DN, Rani M, Rani SS. Evaluation of antioxidant, antibacterial and cytotoxic effects of green synthesized silver

nanoparticles by Piper longum fruit. Materials Science and Engineering: C. 2014;34:115-22.

59. Selwal MK, Selwal KK. Biogenic Synthesis of Silver Nanoparticles and Their Applications in Medicine. Fungal Nanotechnology: Springer; 2017. p. 171-87.
60. Ovais M, Khalil AT, Raza A, Khan MA, Ahmad I, Islam NU, ... & Shinwari, Z. K . Green synthesis of silver nanoparticles via plant extracts: beginning a new era in cancer theranostics. Nanomedicine. 2016;12(23):3157-77.
61. Verma P, Maheshwari SK. Applications of Silver nanoparticles in diverse sectors. International Journal of Nano Dimension. 2019;10(1):18-36.
62. Huang H, Lai W, Cui M, Liang L, Lin Y, Fang Q, ... & Xie, L. An evaluation of blood compatibility of silver nanoparticles. Scientific reports. 2016;6(1):1-15.
63. Tripathi D, Modi A, Narayan G, Rai SP. Green and cost effective synthesis of silver nanoparticles from endangered medicinal plant Withania coagulans and their potential biomedical properties. Materials Science and Engineering: C. 2019;100:152-64.
64. Kulkarni N, Muddapur U. Biosynthesis of metal nanoparticles: a review. Journal of Nanotechnology. 2014;2014.
65. Sharma S, Singh L, Singh S. A review on medicinal plants having antioxidant potential. Indian Journal of Research in Pharmacy and Biotechnology. 2013;1(3):404.
66. Gupta SD. Reactive oxygen species and antioxidants in higher plants: CRC press; 2010.

67. Peng C, Wang X, Chen J, Jiao R, Wang L, Li YM, & Chen, Z. Y. Biology of ageing and role of dietary antioxidants. BioMed Research International. 2014;2014.
68. Husain N, Kumar A, Radicals F. Reactive oxygen species and natural antioxidants: a review. Advances in Bioresearch. 2012;3(4):164-75.
69. Xu D-P, Li Y, Meng X, Zhou T, Zhou Y, Zheng J, Zheng J & Li, H. B. Natural antioxidants in foods and medicinal plants: Extraction, assessment and resources. International journal of molecular sciences. 2017;18(1):96.
70. Moussa Z, Judeh ZM, Ahmed SA. Nonenzymatic exogenous and endogenous antioxidants. Free Radical Medicine and Biology: IntechOpen; 2019.
71. Singh G, Babele PK, Shahi SK, Sinha RP, Tyagi MB, Kumar A. Green synthesis of silver nanoparticles using cell extracts of Anabaena doliolum and screening of its antibacterial and antitumor activity. Journal of microbiology and biotechnology. 2014;24(10):1354-67.
72. Yeasmin S, Datta HK, Chaudhuri S, Malik D, Bandyopadhyay A. In-vitro anti-cancer activity of shape controlled silver nanoparticles (AgNPs) in various organ specific cell lines. Journal of Molecular Liquids. 2017;242:757-66.
73. Xu L, Wang Y-Y, Huang J, Chen C-Y, Wang Z-X, Xie H. Silver nanoparticles: Synthesis, medical applications and biosafety. Theranostics. 2020;10(20):8996.
74. Patil RS, Kokate MR, Kolekar SS. Bioinspired synthesis of highly stabilized silver nanoparticles using Ocimum tenuiflorum leaf extract and their antibacterial activity. Spectrochimica Acta Part A: Molecular and Biomolecular Spectroscopy. 2012;91:234-8.

75. Gomathi M, Rajkumar P, Prakasam A, Ravichandran K. Green synthesis of silver nanoparticles using Datura stramonium leaf extract and assessment of their antibacterial activity. Resource-Efficient Technologies. 2017;3(3):280-4.
76. Zhang L, Wu L, Si Y, Shu K. Size-dependent cytotoxicity of silver nanoparticles to Azotobacter vinelandii: Growth inhibition, cell injury, oxidative stress and internalization. PLoS One. 2018;13(12):e0209020.
77. Senthil B, Devasena T, Prakash B, Rajasekar A. Non-cytotoxic effect of green synthesized silver nanoparticles and its antibacterial activity. Journal of Photochemistry and Photobiology B: Biology. 2017;177:1-7.
78. Lateef A, Akande MA, Ojo SA, Folarin BI, Gueguim-Kana EB, Beukes LS. Paper wasp nest-mediated biosynthesis of silver nanoparticles for antimicrobial, catalytic, anticoagulant, and thrombolytic applications. 3 Biotech. 2016;6(2):140.
79. Ness SL, Brooks MB. Clotting times (aPTT and PT). Interpretation of Equine Laboratory Diagnostics. 2017:139-40.
80. Heise K, Hobisch M, Sacarescu L, Maver U, Hobisch J, Reichelt T, & Spirk S. Low-molecular-weight sulfonated chitosan as template for anticoagulant nanoparticles. International journal of nanomedicine. 2018;13:4881.
81. Sowemimo-Coker SO. Red blood cell hemolysis during processing. Transfusion medicine reviews. 2002;16(1):46-60.
82. Effenberger-Neidnicht K, Hartmann M. Mechanisms of hemolysis during sepsis. Inflammation. 2018;41(5):1569-81.
83. Neun BW, Ilinskaya AN, Dobrovolskaia MA. Updated method for in vitro analysis of nanoparticle hemolytic properties. Characterization

of Nanoparticles Intended for Drug Delivery: Springer; 2018. p. 91-102.

84. Chen LQ, Fang L, Ling J, Ding CZ, Kang B, Huang CZ. Nanotoxicity of silver nanoparticles to red blood cells: size dependent adsorption, uptake, and hemolytic activity. Chemical research in toxicology. 2015;28(3):501-9.
85. Dobrovolskaia MA, Clogston JD, Neun BW, Hall JB, Patri AK, McNeil SE. Method for analysis of nanoparticle hemolytic properties in vitro. Nano letters. 2008;8(8):2180-7.
86. Jia Z, Tian C. Quantitative determination of polyethylene glycol with modified Dragendorff reagent method. Desalination. 2009;247(1-3):423-9.
87. Khan AM, Qureshi RA, Ullah F, Gilani SA, Nosheen A, Sahreen S, et al. Phytochemical analysis of selected medicinal plants of Margalla Hills and surroundings. Journal of medicinal plants research. 2011;5(25):6055-60.
88. Uma C, Sekar K. Phytochemical analysis of a folklore medicinal plant Citrullus colocynthis L (bitter apple). Journal of pharmacognosy and Phytochemistry. 2014;2(6).
89. Laheeb S. F. 2020. Green Synthesis of Silver Nanoparticles from Cassia Obtusifolia L. Leaves Extract: Characterization, Antioxidant Activity, and Clinical Application. 2020. (31).
90. Semenya C, Maseko R, Gololo S. Comparative qualitative phytochemical analysis of the different parts of Barleria dinteri (Oberm): A contribution to sustainable use of the plant species. Journal of Pharmacology, Chemistry and Biological Sciences. 2018;6(2):52-9.

91. Yadav R, Khare R, Singhal A. Qualitative phytochemical screening of some selected medicinal plants of shivpuri district (mp). Int J Life Sci Scienti Res. 2017;3(1):844-7.
92. Godghate A, Sawant R, Sutar A. Phytochemical analysis of ethanolic extract of roots of Carrisa carandus Linn. Rasayan Journal of Chemistry. 2012;5(4):456-9.
93. Garcia EJ, Oldoni TLC, Alencar SMd, Reis A, Loguercio AD, Grande RHM. Antioxidant activity by DPPH assay of potential solutions to be applied on bleached teeth. Brazilian dental journal. 2012;23(1):22-7.
94. Pisoschi AM, Negulescu GP. Methods for total antioxidant activity determination: a review. Biochem Anal Biochem. 2011;1(1):106.
95. Kokila T, Ramesh P, Geetha D. Biosynthesis of AgNPs using Carica Papaya peel extract and evaluation of its antioxidant and antimicrobial activities. Ecotoxicology and environmental safety. 2016;134:467-73.
96. Flaih LS, Al-Saadi NH, editors. Green synthesis of silver nanoparticles from Cassia obtusifolia leaves extract: Characterization and antioxidant activity. AIP Conference Proceedings; 2020: AIP Publishing LLC.
97. Prieto P, Pineda M, Aguilar M. Spectrophotometric quantitation of antioxidant capacity through the formation of a phosphomolybdenum complex: specific application to the determination of vitamin E. Analytical biochemistry. 1999;269(2):337-41.
98. Gomaa EZ. Antimicrobial, antioxidant and antitumor activities of silver nanoparticles synthesized by Allium cepa extract: a green approach. Journal of Genetic Engineering and Biotechnology. 2017;15(1):49-57.
99. Félix-Silva J, Souza T, Camara RBBG, Cabral B, Silva-Júnior AA, Rebecchi IMM, et al. In vitro anticoagulant and antioxidant activities

of Jatropha gossypiifolia L.(Euphorbiaceae) leaves aiming therapeutical applications. BMC complementary and alternative medicine. 2014;14(1):405.

100. Gasque KCdS, Al-Ahj LP, Oliveira RC, Magalhães AC. Cell density and solvent are critical parameters affecting formazan evaluation in MTT assay. Brazilian Archives of Biology and Technology. 2014;57(3):381-5.
101. Bethu MS, Netala VR, Domdi L, Tartte V, Janapala VR. Potential anticancer activity of biogenic silver nanoparticles using leaf extract of Rhynchosia suaveolens: an insight into the mechanism. Artificial cells, nanomedicine, and biotechnology. 2018;46(sup1):104-14.
102. Alavi M, Karimi N. Characterization, antibacterial, total antioxidant, scavenging, reducing power and ion chelating activities of green synthesized silver, copper and titanium dioxide nanoparticles using Artemisia haussknechtii leaf extract. Artificial cells, nanomedicine, and biotechnology. 2018;46(8):2066-81.
103. Tripodi A, Caldwell S, Hoffman M, Trotter J, Sanyal A. The prothrombin time test as a measure of bleeding risk and prognosis in liver disease. Alimentary pharmacology & therapeutics. 2007;26(2):141-8.
104. Kim H-S, Jun SH, Koo YK, Cho S, Park Y. Green synthesis and nanotopography of heparin-reduced gold nanoparticles with enhanced anticoagulant activity. Journal of nanoscience and nanotechnology. 2013;13(3):2068-76.
105. Flaih, L. S., &Al-Saadi, N. H. Characterization and clinical application of silver nanoparticles synthesized from *Cassia Obtusifoli*a leaves extract. Plant Archives (2020), 20, 1082-1088.

106. Shah A, Lutfullah G, Ahmad K, Khalil AT, Maaza M. Daphne mucronata-mediated phytosynthesis of silver nanoparticles and their novel biological applications, compatibility and toxicity studies. Green Chemistry Letters and Reviews. 2018;11(3):318-33.
107. Laloy J, Minet V, Alpan L, Mullier F, Beken S, Toussaint O, & Dogné J. M. Impact of silver nanoparticles on haemolysis, platelet function and coagulation. Nanobiomedicine. 2014;1:4.
108. Alshehri AA, Malik MA. Phytomediated Photo-Induced Green Synthesis of Silver Nanoparticles Using Matricaria chamomilla L. and Its Catalytic Activity against Rhodamine B. Biomolecules. 2020;10(12):1604.
109. Fahimirad S, Ajalloueian F, Ghorbanpour M. Synthesis and therapeutic potential of silver nanomaterials derived from plant extracts. Ecotoxicology and environmental safety. 2019;168:260-78.
110. Amini SM. Preparation of antimicrobial metallic nanoparticles with bioactive compounds. Materials Science and Engineering: C. 2019;103:109809.
111. Singh P, Pandit S, Garnæs J, Tunjic S, Mokkapati VR, Sultan A, & Mijakovic I. Green synthesis of gold and silver nanoparticles from Cannabis sativa (industrial hemp) and their capacity for biofilm inhibition. International journal of nanomedicine. 2018;13:3571.
112. Daniel SK, Vinothini G, Subramanian N, Nehru K, Sivakumar M. Biosynthesis of Cu, ZVI, and Ag nanoparticles using Dodonaea viscosa extract for antibacterial activity against human pathogens. Journal of nanoparticle research. 2013;15(1):1319.
113. Saranya K, Divyabharathi U. Gas Chromatography and mass Spectroscopic Analysis of Phytocompounds in *Dodonaea viscosa* leaves extract. Pramana Research Journa. (2019) 9; 26-35.

114. Marinov V, Valcheva-Kuzmanova S. Review on the pharmacological activities of anethole. Scripta scientifica pharmaceutica. 2015;2(2):14-9.
115. Silva-Alves K, Ferreira-da-Silva F, Peixoto-Neves D, Viana-Cardoso K, Moreira-Júnior L, Oquendo M, & Leal-Cardoso J. H. Estragole blocks neuronal excitability by direct inhibition of Na+ channels. Brazilian Journal of Medical and Biological Research. 2013;46(12):1056-63.
116. Abubakar MN, Majinda RR. GC-MS analysis and preliminary antimicrobial activity of Albizia adianthifolia (Schumach) and Pterocarpus angolensis (DC). Medicines. 2016;3(1):3.
117. Arora S, Kumar G. Gas Chromatography-Mass Spectrometry (GC-MS) determination of bioactive constituents from the methanolic and ethyl acetate extract of Cenchrus setigerus Vahl (Poaceae). Antiseptic. 2017;2:0.31.
118. FAYYAD RJ, LEFTA SN, NUAMAN RS, AL-ABBOODI AKA. Exploration the Impact of Morenga Oleifera leaves as anti-bacterial and tumor inhibitor and Phytochemical profiling by GC-Mass analysis. ORIGINAL ARTICLE.2021; (15) 1 p. 343-347.
119. Yasmin S, Nouren S, Bhatti HN, Iqbal DN, Iftikhar S, Majeed J, & Rizvi H. Green synthesis, characterization and photocatalytic applications of silver nanoparticles using Diospyros lotus. Green Processing and Synthesis. 2020;9(1):87-96.
120. Raza MA, Kanwal Z, Rauf A, Sabri AN, Riaz S, Naseem S. Size-and shape-dependent antibacterial studies of silver nanoparticles synthesized by wet chemical routes. Nanomaterials. 2016;6(4):74.
121. Rocchetti G, Lucini L, Chiodelli G, Giuberti G, Montesano D, Masoero F, et al. Impact of boiling on free and bound phenolic profile

and antioxidant activity of commercial gluten-free pasta. Food Research International. 2017;100:69-77.

122. Patil Shriniwas P. Antioxidant, antibacterial and cytotoxic potential of silver nanoparticles synthesized using terpenes rich extract of Lantana camara L. leaves. Biochemistry and biophysics reports. 2017;10:76.
123. Ravichandran V, Vasanthi S, Shalini S, Shah SAA, Tripathy M, Paliwal N. Green synthesis, characterization, antibacterial, antioxidant and photocatalytic activity of Parkia speciosa leaves extract mediated silver nanoparticles. Results in Physics. 2019;15:102565.
124. Revathi, N., and T. S. Dhanaraj. "Synthesis of silver nanoparticles from Dodonaea angustifolia leaf extract and evaluation of its anti-inflammatory activity." *Pramana Res. J.* 9 (2019): 1118-1126.
125. Rashid MU, Bhuiyan MKH, Quayum ME. Synthesis of silver nano particles (Ag-NPs) and their uses for quantitative analysis of vitamin C tablets. Dhaka University Journal of Pharmaceutical Sciences. 2013;12(1):29-33.
126. Rao B, Tang R-C. Green synthesis of silver nanoparticles with antibacterial activities using aqueous Eriobotrya japonica leaf extract. Advances in natural sciences: Nanoscience and nanotechnology. 2017;8(1):015014.
127. Heydari R, Rashidipour M. Green synthesis of silver nanoparticles using extract of oak fruit hull (Jaft): synthesis and in vitro cytotoxic effect on MCF-7 cells. International journal of breast cancer. 2015;2015.
128. Zafar S, Ashraf A, Ashraf MY, Asad F, Perveen S, Z Zafar MA, & Shahzadi A. Preparation of Eco-friendly Antibacterial Silver Nanoparticles from Leaf Extract of Ficus Benjamina. Biomedical Journal. 2018;1:5.

129. Gurunathan S, Jeong J-K, Han JW, Zhang X-F, Park JH, Kim J-H. Multidimensional effects of biologically synthesized silver nanoparticles in Helicobacter pylori, Helicobacter felis, and human lung (L132) and lung carcinoma A549 cells. Nanoscale research letters. 2015;10(1):1-17.
130. Cakić M, Glišić S, Cvetković D, Cvetinov M, Stanojević L, Danilović B, et al. Green synthesis, characterization and antimicrobial activity of silver nanoparticles produced from Fumaria officinalis L. plant extract. Colloid Journal. 2018;80(6):803-13.
131. Kumar B, Smita K, Cumbal L, Debut A. Green synthesis of silver nanoparticles using Andean blackberry fruit extract. Saudi journal of biological sciences. 2017;24(1):45-50.
132. Waseda Y, Matsubara E, Shinoda K. X-ray diffraction crystallography: introduction, examples and solved problems: Springer Science & Business Media; 2011.
133. Priya RS, Geetha D, Ramesh P. Antioxidant activity of chemically synthesized AgNPs and biosynthesized Pongamia pinnata leaf extract mediated AgNPs–A comparative study. Ecotoxicology and environmental safety. 2016;134:308-18.
134. Baghayeri M, Mahdavi B, Hosseinpor-Mohsen Abadi Z, Farhadi S. Green synthesis of silver nanoparticles using water extract of Salvia leriifolia: Antibacterial studies and applications as catalysts in the electrochemical detection of nitrite. Applied Organometallic Chemistry. 2018;32(2):e4057.
135. Annamalai, P., P. Balashanmugam, and P. T. Kalaichelvan. "Biogenic synthesis silver nanoparticles using Peltophorum pterocarpum leaf extracts and its antimicrobial efficacy against selective pathogens." *Int J App Pharm* 10.6 (2018): 112-118.

136. Vivek R, Thangam R, Muthuchelian K, Gunasekaran P, Kaveri K, Kannan S. Green biosynthesis of silver nanoparticles from Annona squamosa leaf extract and its in vitro cytotoxic effect on MCF-7 cells. Process Biochemistry. 2012;47(12):2405-10.
137. Garg D, Shaikh A, Muley A, Marar T. In-vitro antioxidant activity and phytochemical analysis in extracts of Hibiscus rosa-sinensis stem and leaves. Free Radicals and Antioxidants. 2012;2(3):41-6.
138. Otunola GA, Afolayan AJ. In vitro antibacterial, antioxidant and toxicity profile of silver nanoparticles green-synthesized and characterized from aqueous extract of a spice blend formulation. Biotechnology & Biotechnological Equipment. 2018;32(3):724-33.
139. Sudha A, Jeyakanthan J, Srinivasan P. Green synthesis of silver nanoparticles using Lippia nodiflora aerial extract and evaluation of their antioxidant, antibacterial and cytotoxic effects. Resource-Efficient Technologies. 2017;3(4):506-15.
140. Parveen A, Rao S. Cytotoxicity and genotoxicity of biosynthesized gold and silver nanoparticles on human cancer cell lines. Journal of Cluster Science. 2015;26(3):775-88.
141. Lakshmanan G, Sathiyaseelan A, Kalaichelvan P, Murugesan K. Plant-mediated synthesis of silver nanoparticles using fruit extract of Cleome viscosa L.: Assessment of their antibacterial and anticancer activity. Karbala International Journal of Modern Science. 2018;4(1):61-8.
142. Sriranjani R, Srinithya B, Vellingiri V, Brindha P, Anthony SP, Sivasubramanian A, & Muthuraman, M. S. Silver nanoparticle synthesis using Clerodendrum phlomidis leaf extract and preliminary investigation of its antioxidant and anticancer activities. Journal of Molecular Liquids. 2016;220:926-30.

143. Oh KH, Soshnikova V, Markus J, Kim YJ, Lee SC, ingh P, & Yang, D. C. Biosynthesized gold and silver nanoparticles by aqueous fruit extract of Chaenomeles sinensis and screening of their biomedical activities. Artificial cells, nanomedicine, and biotechnology. 2018;46(3):599-606.
144. Wang D, Markus J, Wang C, Kim Y-J, Mathiyalagan R, A Aceituno VC, & Yang D. C. Green synthesis of gold and silver nanoparticles using aqueous extract of Cibotium barometz root. Artificial cells, nanomedicine, and biotechnology. 2017;45(8):1548-55.
145. Mohammed AE, Al-Qahtani A, Al-Mutairi A, Al-Shamri B, Aabed K. Antibacterial and cytotoxic potential of biosynthesized silver nanoparticles by some plant extracts. Nanomaterials. 2018;8(6):382.
146. Pal S, Tak YK, Song JM. Does the antibacterial activity of silver nanoparticles depend on the shape of the nanoparticle? A study of the gram-negative bacterium Escherichia coli. Applied and environmental microbiology. 2007;73(6):1712-20.
147. Salas-Orozco M, Niño-Martínez N, Martínez-Castañón G-A, Méndez FT, Jasso MEC, Ruiz F. Mechanisms of resistance to silver nanoparticles in endodontic bacteria: a literature review. Journal of Nanomaterials. 2019;2019.
148. Al-Dhafri K, Ching CL. Phyto-synthesis of silver nanoparticles and its bioactivity response towards nosocomial bacterial pathogens. Biocatalysis and agricultural biotechnology. 2019;18:101075.
149. Akintayo G, Lateef A, Azeez M, Asafa T, Oladipo I, Badmus J, & Yekeen T, editors. Synthesis, bioactivities and cytogenotoxicity of animal fur-mediated silver nanoparticles. IOP conference series: materials science and engineering; 2020: IOP Publishing.

150. Asghar MA, Yousuf RI, Shoaib MH, Asghar MA. Antibacterial, anticoagulant and cytotoxic evaluation of biocompatible nanocomposite of chitosan loaded green synthesized bioinspired silver nanoparticles. International Journal of Biological Macromolecules. 2020;160:934-43.
151. Azeez MA, Lateef A, Asafa TB, Yekeen TA, Akinboro A, Oladipo IC, et al. Biomedical applications of cocoa bean extract-mediated silver nanoparticles as antimicrobial, larvicidal and anticoagulant agents. Journal of Cluster Science. 2017;28(1):149-64.
152. Lateef A, Folarin BI, Oladejo SM, Akinola PO, Beukes LS, Gueguim-Kana EB. Characterization, antimicrobial, antioxidant, and anticoagulant activities of silver nanoparticles synthesized from Petiveria alliacea L. leaf extract. Preparative Biochemistry and Biotechnology. 2018;48(7):646-52.
153. Hamouda RA, Hussein MH, Abo-Elmagd RA, Bawazir SS. Synthesis and biological characterization of silver nanoparticles derived from the cyanobacterium Oscillatoria limnetica. Scientific reports. 2019;9(1):1-17.
154. Mohamed HEA, Afridi S, Khalil AT, Zia D, Iqbal J, Ullah I, & Maaza M. Biosynthesis of silver nanoparticles from Hyphaene thebaica fruits and their in vitro pharmacognostic potential. Materials Research Express. 2019;6(10):1050c9.
155. Kumar KP, Paul W, Sharma CP. Green synthesis of silver nanoparticles with Zingiber officinale extract and study of its blood compatibility. BioNanoScience. 2012;2(3):144-52.
156. Maity GN, Maity P, Choudhuri I, Sahoo GC, Maity N, Ghosh K, & Mondal S. Green synthesis, characterization, antimicrobial and cytotoxic effect of silver nanoparticles using arabinoxylan isolated

from Kalmegh. International Journal of Biological Macromolecules. 2020;162:1025-34.

الخلاصة

يعتبرالتخليق الحيوي لجسيمات الفضة النانوية (AgNPs) من المستخلصات النباتية احد طرق الكيمياء الخضراء حيث تتميز هذه الطريقة بالسهولة والسرعة و التكلفة المنخفضة. ومن المثير للاهتمام ان جسيمات الفضة النانوية لها دور مهم خاصة في طب النانو. اذ تم في هذه الدراسة تصنيع جسيمات الفضة النانوية من مستخلص اوراق الددونيا (*Dodonaea viscosa*). اذ كان الدليل الاولي لتكوين هذه الجسيمات من خلال تغير اللون.

استخدمت مطيافية GC-mass لتشخيص المكونات الموجودة في المستخلص المائي لاوراق الددونيا و المسؤولة عن اختزال ايونات الفضة الى جسيمات الفضة النانوية. تم توصيف الدقائق النانوية المصنعة باستخدام عدة تقنيات. القياس الطيفي باستخدام الاشعة فوق البنفسجية-المرئية (UV-Visible) اشار الى تكوين جسيمات الفضة النانوية AgNPsعند الطول الموجي 463 نانومتر و طيف الاشعة تحت الحمراء (FT-IR) الذي حدد المجاميع الوظيفية الفعالة التي لديها القدرة على الاختزال الحيوي لأيون الفضة Ag^{+} . استخدمت حيود الاشعة السينية (XRD) لتحديد التركيب البلوري لجسيمات الفضة النانوية كما هو موضح في القمم عند قيم الزاوية 38.1874, 46.2491, 57.54092, و ^{o} 76.8313. التحليل المجهري للقوة الذرية (AFM) بين حجم وخصائص السطح للجسيمات النانوية المصنعة حيويا, واظهر بان الدقائق النانوية تمتلك متوسط حجم قدره 60.22 نانومتر. اخيرا اظهرت صورة الفحص المجهري الالكتروني SEM الشكل الكروي لجسيمات الفضة النانوية كما وان لها متوسط قطر مختلف D1(21.10), D2 (21.39), D3(1.86) نانوميتر.

ان هذه الجسيمات اظهرت فعالية ضد الاورام لخلايا الرئة السرطانية بطريقة تعتمد على الجرعة اذ كان التركيز المثبط لنصف عدد الخلايا (IC_{50}) هو 1.73 مايكروكرام لكل مل . كما و تم اختبار فعالية هذه الجسيمات (AgNPs) ضد انواع مختلفة من البكتريا و كذلك قدرتها كمضادة للاكسدة. جسيمات الفضة النانوية ثبطت نمو البكتريا و الغشاء الحيوي لها مثل البكتريا موجبة الغرام (*Staphylococcus aureus* and *Streptococcus pneumonia*) و البكتريا سالبة الغرام (*E. coli* and *Pseudomonas aeruginosa*). كما و اظهرت جسيمات الفضة النانوية نشاطا مضادا للاكسدة و يمكن استخدامها ضد الاضرار التي تنتجها الجذور الحرة.

بينت نتائج التطبيقات السريرية ان جسيمات الفضة النانوية المصنعة و مستخلص اوراق الددونيا المائي لها القدرة على اطالة وقت تخثر الدم عن طريق زيادة زمن التخثر و زمن التخثر الجزئي المنشط كما و كان لجسيمات الفضة النانوية تاثير منخفض جدا لحدوث انحلال الدم لكريات الدم الحمراء عند استخدام الدم البشري.

جمهورية العراق
وزارة التعليم العالي والبحث العلمي
جامعة كربلاء/ كلية العلوم
قسم الكيمياء

التخليق الحيوي ، التوصيف ، الفعالية المضادة للاكسدة ، والتطبيقات السريرية لجسيمات الفضة النانوية المصنعة من مستخلص أوراق الدودونيا

رسالة مقدمة الى مجلس كلية العلوم – جامعة كربلاء
كجزء من استكمال متطلبات نيل درجة الماجستير في الكيمياء الحياتية

من قبل

زينب فيصل حبيب الموسوي

بكالوريوس علوم في الكيمياء/ جامعة كربلاء (2017)

بأشراف

أ.د. نرجس هادي السعدي

1443ه **2021م**